UNIVERSITY OF SOUTHAMPTON

Faculty of Engineering and Applied Science

Department of Electronics and Computer Science

Southampton S017 1BJ

Genetic Algorithm Assisted CDMA Multiuser Detection

by

Kai Yen

B.Eng.

A Doctoral Thesis submitted in partial fulfilment of the requirements for the award of Doctor of Philosophy at the University of Southampton

March 2001

SUPERVISOR: Professor Lajos Hanzo

Dipl Ing, MSc, PhD, SMIEEE

Chair of Telecommunications

Department of Electronics and Computer Science

University of Southampton

Southampton SO17 1BJ

United Kingdom.

UNIVERSITY OF SOUTHAMPTON

ABSTRACT

Faculty of Engineering and Applied Science
Department of Electronics and Computer Science

Doctor of Philosophy

Genetic Algorithm Assisted CDMA Multiuser Detection

by Kai Yen

This dissertation explores the application of Genetic Algorithms (GAs) assisted multiuser detection in the context of Code Division Multiple Access (CDMA). The optimum multiuser detector proposed by Verdu [1] entails searching for a particular K-bit sequence that optimises the correlation metric, where K is the number of users. Hence, it has a computational complexity that is exponentially proportional to the number of users and its implementation becomes impractical, when there is a high number of users. GAs have been successfully applied to solve complex optimisation problems in many fields. Hence in this dissertation, we will investigate the feasibility of employing GAs in solving the optimum multiuser detection problem. We commence by determining a set of GA configurations that are capable of offering a near-optimum performance at the cost of a reduced computational complexity, compared to the optimum multiuser detector receiving over a simple AWGN channel. Our study showed that certain GA parameters substantially influence the overall performance of the detector. More importantly, we will show that the optimum performance can be achieved up to a certain SNR value at a complexity less than half of that required by the optimum multiuser detector. The employment of the GA-assisted multiuser detector is then extend to an asynchronous CDMA system. Antenna diversity based on the Pareto optimality approach can further improve the achievable performance.

The proposed GA-assisted multiuser detector is then extended further, so that Channel Impulse Response (CIR) estimation can also be performed jointly by the same GA without incurring any additional computational complexity and without requiring training symbols. Hence the joint GA-assisted channel estimator and symbol detector is capable of offering a higher throughput and a shorter detection delay, than that of explicitly trained CDMA multiuser detectors. Simulation results showed that the GA-assisted channel estimator is capable of achieving a Mean Squared Error (MSE) as low as 0.001. The joint GA-assisted multiuser CIR estimator and symbol detector exhibits an error floor, which is similar to that exhibited

by other multiuser detectors in conjunction with imperfect CIR estimation.

Acknowledgements

First of all, I would like to thank the Centre for Wireless Communications (CWC), Singapore for putting their faith in me and my abilities by awarding me the scholarship that allowed me to pursue the reserach leading to completing my PhD. Without their financial support, this would not have been possible. Secondly, I would like to thank Professor Raymond Steele for introducing to me this wonderful communication research group at the University of Southampton and especially to my supervisor Professor Lajos Hanzo, for his willingness to accept me as his student. Over the past three years or so, his enthusiasm in searching for new ideas in mobile communications has always inspired and motivated me to reach new heights, which I never dreamed I would accomplish. He is, without a doubt, the best supervisor any PhD student can ever get, and I am one of the more fortunate ones. I could have never reached new heights alone, without the help and support of all my colleagues in the communications group. There are simply too many to mention here and all of them should be given equal credit. So I just want to say a big thank you to all of them. I would also like to thank my family and friends in Singapore for the invaluable encouragement they have provided, while I was thousands of miles away. Lastly, as the saying goes, behind every successful man, there is a woman. That woman is none other than Choon Woei. No word can describe my appreciation for her unlimited understanding and support, be it here in the UK or in Singapore, throughout my entire course. Thank you.

List of Publications

1. K. Yen, L. L. Yang and L. Hanzo, "Residual Number System Assisted CDMA - A New System Concept," *Proceedings of ACTS Mobile Communication Summit'99, Sorrento, Italy June 1999*, pp. 177–182.
2. K. Yen and L. Hanzo "Third-Generation Wireless Systems," *Mobile Radio Communications 2nd ed.*, Raymond Steele and Lajos Hanzo, editors, John Wiley and Sons, 1999, pp. 897–963.
3. K. Yen and L. Hanzo, "Hybrid Genetic Algorithm Based Multi-user Detection Schemes for Synchronous CDMA System," *Proceedings of the IEEE Vehicular Technology Conference (VTC) 1999, Tokyo, Japan, May 2000*, pp. 1400–1404.
4. K. Yen and L. Hanzo, "Genetic Algorithm Assisted Joint Multiuser symbol Detection and Fading Channel Estimation for Synchronous CDMA Systems," Accepted for publication in IEEE Journal on Selected Areas in Communications.
5. L. L. Yang, K. Yen, M. Dillinger and L. Hanzo, "Performance of RS Coded DS-CDMA using Noncoherent M-ary Orthogonal Modulation over Multipath Fading Channels," *Proceedings of PIMRC'2000, London, UK, September 2000*, pp. 584–588.
6. L. L. Yang, K. Yen and L. Hanzo, "A Reed-Solomon Coded DS-CDMA System using Noncoherent M-ary Orthogonal Modulation over Multipath Fading Channels," To appear in IEEE Journal on Selected Areas in Communications, November 2000.
7. K. Yen and L. Hanzo, "Antenna-Diversity-Assisted Genetic Algorithm-Based Multiuser Detection Schemes for Synchronous CDMA Systems," To appear in

the Proceedings of the IEEE Vehicular Technology Conference (VTC) 2001, Spring conference.

8. K. Yen and L. Hanzo, "Genetic Algorithm Assisted Multiuser Detection in Asynchronous CDMA Communications," To appear in the IEEE Communications Conference (ICC) 2001.
9. K. Yen and L. Hanzo, "Antenna-Diversity-Assisted Genetic Algorithm-Based Multiuser Detection Schemes for Synchronous CDMA Systems," Submitted to IEEE Transactions on Communications in February 2000. First revision September 2000.
10. K. Yen and L. Hanzo, "Genetic Algorithm Assisted Multiuser Detection in Asynchronous CDMA Communications," Submitted to IEEE Transactions on Communications in September 2000.

Contents

CHAPTER 1

Introduction

In this introductory chapter, a brief discussion of Code Division Multiple Access (CDMA) together with its advantages and disadvantages over other multiple access techniques is presented in Section 1.1. An overview of the organisation of this dissertation is then given in Section 1.2. Finally, a brief discourse on global optimisation is provided in Section 1.3.

1.1 Code Division Multiple Access

Spread Spectrum (SS) communications systems have been in existence for decades, although up until the last decade or so, most of these systems have been designed for military applications. In the late 1980s, spread spectrum communications gained increasing interest in the commercial sector for use in cellular wireless communications.

CDMA [2–6] implemented in conjunction with Direct-Sequence Spread-Spectrum (DS-SS) modulation constitutes an attractive multiuser scheme that allows users to transmit at the same carrier frequency in an uncoordinated manner. CDMA was already employed in some second generation (2G) systems, such as the Interim Standard-95 (IS-95) scheme [6] and it has proved to be a success since making its debut in the United States in 1995. CDMA has been known to provide the best user capacity in a cellular environment amongst all the known access schemes, such

as Frequency Division Multiple Access (FDMA) and Time Division Multiple Access (TDMA). Unlike the more traditional FDMA or TDMA, CDMA is capable of mitigating the effects of the hostile mobile propagation channel through RAKE multipath diversity combining [7]. Furthermore, it simplifies frequency planning due to its potentially achievable near-unity frequency reuse. In addition, being a wideband system, it can coexist with other narrowband microwave systems, which corrupt the CDMA signal's spectrum in a fraction of its total frequency band. This eases the problem of frequency management, while allowing a smooth evolution from narrowband systems to wideband systems.

Thanks to these advantages, it is not surprising to see that a majority of the proposals submitted to the International Telecommunication Union (ITU) in June 1998 as candidates for the third generation (3G) mobile radio systems were based on the Wideband-CDMA (W-CDMA) concept [5], since its advantageous properties satisfy most of the requirements for 3G mobile radio systems.

However, it is well known that the CDMA system capacity is limited by the multiuser interference generated by other users in the traffic cell, who use the same carrier frequency, but different user signature sequences or spreading codes, in order to transmit the signals. Because of the practical difficulty in designing a sufficiently large set of orthogonal signature sequences for asynchronous transmission conditions, the uncoordinated signal transmission from the multiplicity users creates Multiple Access Interference (MAI). If not controlled, the MAI arising from the asynchronous transmissions of the mobile stations can seriously deteriorate the quality of reception at the base station. Note that the MAI is negligible in FDMA systems or TDMA systems, since the users' signals are orthogonal in terms of either frequency or time, respectively. Numerous methods have been proposed for reducing the amount of MAI present in the received signal such as power control [8], the optimisation of signature sequences [9] and sectorised antennas [10]. Nevertheless, these techniques have their limitations in combating the effects of MAI, in conjunction with the conventional single-user detector. The poor performance of the conventional single-user detector in a multiple-access environment is not due to problems inherent in CDMA, but rather due to problems associated with the detector's structure, since in this case the MAI is treated as noise.

The optimal CDMA multiuser detector [1] based on the Maximum-Likelihood (ML) detection rule performs an exhaustive search of all the possible combinations of the users' transmitted bit sequences and then selects the most likely combination as the detected bit sequence. Since an exhaustive search is conducted, the computational complexity of the detector grows exponentially with the number of users.

Since a CDMA system could potentially have a large number of users, the optimum ML multiuser detector is impractical to implement. This complexity constraint led to numerous so-called suboptimal multiuser detection [11] proposals. A rudimentary classification of the more popular suboptimal multiuser detectors is illustrated in Figure 1.1 [12]. Amongst others, notable members of the adaptive multiuser detectors family are the decorrelating detector [13–16], the Minimum Mean Squared Error (MMSE) detector [17] and the Extended Kalman Filter (EKF)-based detector [18]. Joint detection schemes have been typically used for detecting data transmitted in burst mode. The family of joint detectors is comprised of the Zero-Forcing Block Linear Equalizer (ZF-BLE) [19], the MMSE-BLE [20], the ZF-Block Decision Feedback Equalizer (ZF-BDFE) [21] and the MMSE-BDFE [21]. A more detailed account of these JD schemes can be found for example in [12,22]. In contrast to joint detectors, which aim for detecting the information of all users simultaneously, iterative multiuser detectors attempt to detect the users' bits in a number of consecutive stages. As the number of stages is increased, the BEP will improved. However, increasing the number of stages will lead to an increased detection complexity. Hence, these detectors offer a trade-off between complexity and performance. Examples of these detectors include the Successive Interference Cancellation (SIC) detector [23], the Parallel Interference Cancellation (PIC) detector [24] and a hybrid version of the SIC and PIC [25]. There is another class of multiuser detectors based on a tree-search algorithm of the M- or T-type [26–28]. These detectors are capable of achieving the optimum performance attained by Verdu's ML detector up to a certain Signal-to-Noise Ratio (SNR) value at a complexity lower than that of Verdu's optimum multiuser detector. In this dissertation, we will also show that the multiuser detector based on Genetic Algorithms (GAs), which can be considered as an iterative multiuser detector, is also capable of achieving the optimum performance at a reduced complexity. Let us now review the organisation of the dissertation.

1.2 Organisation of the Thesis

In this thesis, we will focus our attention on multiuser detection techniques based on an efficient optimisation procedure known as GAs. The outline of the thesis is as follows :

- **Chapter 2 :** In this dissertation, we assume that the reader is familiar with the basic CDMA principles. Hence we will not delve into the basic concepts of CDMA here. Instead, we will commence our discourse by giving an overview of GAs, since the concepts of GAs is not widely known in the mobile

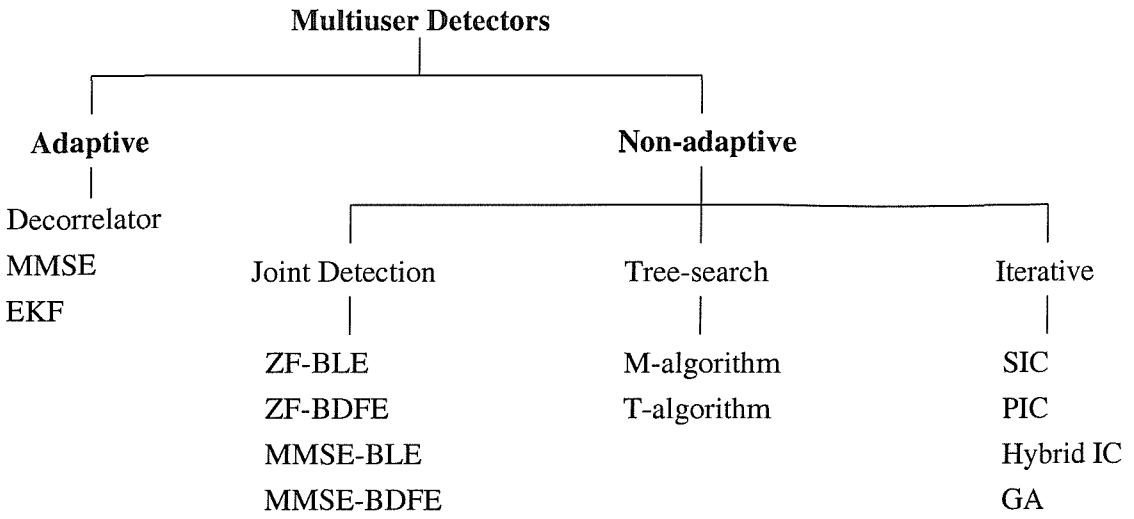

MMSE : Minimum Mean-square Error
EKF : Extended Kalman Filter
ZF-BLE : Zero-forcing Block Linear Equalizer
MMSE-BLE : Minumum Mean-square Error Block Linear Equalizer
ZF-BDFE : Zero-forcing Block Decision Feedback Equalizer
MMSE-BDFE : Minimum Mean-square Error Block Decision Feedback Equaliser
SIC : Successive Interference Cancellation
PIC : Parallel Interference Cancellation
IC : Interference Cancellation
GA : Genetic Algorithms

Figure 1.1: Classification of CDMA multiuser detectors [12].

communications community. We will present the basic functions of a GA in optimising an objective function, with the aid of a flowchart as well as an example. An insight into why a GA constitutes an efficient function optimiser is also given in the context of the schemata and the schema theorem [29]. Some of the more advanced GA processes are also highlighted here, in order to improve the efficiency of our search for the optimum solution. Finally, a survey of the GA-based CDMA mutiuser detection schemes found in the current literature is conducted.

- **Chapter 3 :** In this chapter, we will invoke the GA-assisted multiuser detector in a symbol-synchronous CDMA system over a simple AWGN channel as well as over a single-path Rayleigh fading channel. While this system model is not practical, it can provide us with a better insight into how certain GA operations and parameters behave in the context of our specific application, without considering the effects of the multipath interference and the asynchronism amongst the users. We will first define the objective function for our optimisation by deriving the correlation metric for the optimum multiuser

detector. As mentioned above, the complexity of the optimum multiuser detector is exponential to the number of users and hence it is impractical to implement. Hence we will apply GAs in optimising the correlation metric, while achieving a reduction in the associated complexity. Through a series of experiments, we will attempt to find the particular GA configuration that is capable of offering a near-optimum bit error probability (BEP) performance at a reduced computational complexity, compared to that of the optimum multiuser detector. Upon determining the GA configuration that we will be adopting for our GA-assisted multiuser detection scheme, we will then investigate its BEP performance in an AWGN channel as well as in a single-path Rayleigh fading channel.

- **Chapter 4 :** In Chapter 3, we have assumed that the Channel Impulse Response (CIR) coefficients are perfectly known by the receiver, which allowed us to detect the users' transmitted bits coherently. In practice, these coefficients must be estimated either blindly or with the aid of pilot symbols. By exploiting the capabilities of the GAs in dealing with both binary and floating point variables, we proposed a joint GA-assisted multiuser channel estimation and symbol detection technique in this chapter. Unlike in traditional systems, where the CIR estimation and symbol detection are usually performed by separate but inter-linked algorithms, such as the Kalman filter used for channel estimation [18] and the decorrelator for symbol detection [30], our proposed technique is capable of performing both the channel estimation and symbol detection concurrently using the same GAs. The achievable MSE of the estimated CIR coefficients as well as the BEP performance of our proposed joint GA-assisted multiuser CIR estimator and symbol detector are then evaluated using computer simulations.
- **Chapter 5 :** In order to obtain a BEP performance improvement, in this chapter we evaluated the performance of the GA-assisted multiuser detector in conjunction with antenna diversity. More specifically, we investigated the BEP performance of the GA-assisted multiuser detector using two different diversity selection strategies. According to the first strategy, the so-called mating pool is created by selecting the K-bit GA individuals based on the combined figure of merits of the diversity antennas. On the other hand, we can exploit the population-based optimisation approach of the GAs and invoke the so-called Pareto optimality [31], in order to aid our search. According to this strategy, the mating pool is comprised of all non-dominated individuals. The BEP performance of the antenna diversity aided GA-assisted multiuser

detector based on these two stragtegies is evaluated and compared for various fading scenarios.

- **Chapter 6 :** The model that we have adopted in Chapters 3-5 is based on a symbol-synchronous CDMA system and multiuser detection is performed at the centralised base station. Unless strict timing control is employed, it is almost impossible to maintain a symbol-synchronous transmission among the users. Hence in Chapter 6, we will propose a GA-assisted multiuser detector for an asynchronous transmission environment. The correlation metric over a finite observation window is derived. The effects of the so-called edge bits, which placed a limitation on the BEP performance, must be taken into account when detection is considered over a finite observation window. In our proposed technique, we can reduce the effects of the edge bits by attempting to estimate the tentative decisions concerning these edge bits, while at the same time detecting the desired bits using the same GA. The BEP performance of our proposed scheme is then compared with that of a similar GA-assisted multiuser detector, where the edge bits are estimated using the conventional single-user matched filter.

The novel contributions of this dissertation are listed below :

- A feasibility study of employing GAs in the context of CDMA multiuser detection was given in Chapter 3 for transmissions over a symbol-synchronous AWGN system. Based on the results obtained in Section 3.5, we arrived at the conclusion that different GA schemes and their associated parameters have a significant impact on the BEP performance. If these GA schemes and their parameters are carefully chosen, a fast convergence can be accomplished in addition to a reliable search.
- A novel GA-assisted joint multiuser CIR estimation and data detection technique was proposed for employment in a symbol-synchronous CDMA system based on the ML decision rule [32]. Our results showed that as a channel estimator, the GA was capable of tracking the amplitude and phase variations of the complex fading channel envelope, while achieving a channel gain estimation MSE as low as 10^{-3} in a noiseless channel. The proposed symbol detector was capable of attaining a near-optimum BER performance at low ξ_k/N_0 values using perfect channel estimates under the conditions of equal received bit energy for all users, while maintaining a computational complexity significantly lower, than that of a ML optimum multiuser detector. Upon exploiting its capabilities as a channel estimator and symbol detector, the proposed joint channel estimator and symbol detector can achieve a BER as

low as 2×10^{-3} at an ξ_k/N_0 value of 30 dB in a 10-user CDMA environment without the assistance of channel coding or diversity. However, an error floor was observed beyond $\xi_k/N_0 = 30$ dB due to the imperfect channel estimation employed. Furthermore, since the channel estimation and symbol detection are performed simultaneously, no pilot symbols or decision feedback are necessary, which results in a higher effective throughput and shorter detection time, than that of explicitly trained CDMA multiuser detectors.

- A GA-assisted CDMA multiuser detector was developed using dual antenna diversity techniques [33]. Two diversity selection strategies were highlighted for the GAs. In our first solution the mating pool was formed based on the combination of the statistics derived from the diversity antennas and we had a fixed mating pool size. According to our second strategy, the mating pool was formed based on the Pareto optimality approach, whereby the diversity antennas' statistics were treated independently, in order to select the non-dominated individuals to form the mating pool. Hence, the mating pool size was not fixed. We have shown that GAs employing the latter strategy always exhibit a lower BER compared to those employing the former strategy. We have also shown that the BER performance can be improved by increasing the population size.
- We formulated the correlation metric of an asynchronous CDMA system in a multipath channel based on a truncated window size. GAs were then invoked in order to improve the bit error probability of the edge bits and at the same time to detect the desired bits within the truncated observation window. By improving the reliability of the edge bits, simulation results showed that the GA-based multiuser detector can achieve a near-optimal desired bit detection performance at the cost of a lower number of correlation metric evaluations compared to Verdu's optimum multiuser detector using a 'brute-force' approach. Furthermore, both the edge bits and the desired bits are detected by the same GAs, resulting in potential complexity savings [34].

1.3 Function Optimisation

Optimisation [35, 36] may be defined as the process of finding a set of decision variables that results in attaining the maximum or minimum value of a function. This function is typically known as the *objective function.* In mathematical terms,

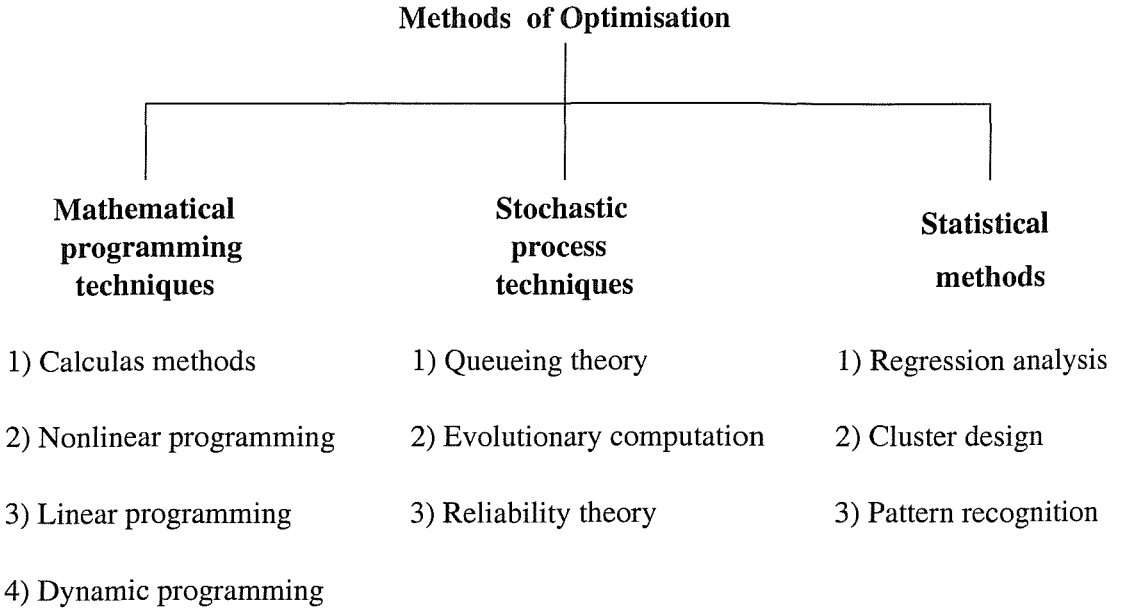

Figure 1.2: Classification of various optimisation techniques [35].

the optimisation problem can be formulated as [35] :

$$\text{Find } \boldsymbol{X} = [x_1, \ldots, x_n] \text{ which maximises/minimises } \Lambda(\boldsymbol{X}), \tag{1.1}$$

where $\boldsymbol{X}$ is an n-dimensional vector consisting of n number of decision variables and $\Lambda(\boldsymbol{X})$ is the objective function. In the context of *global* optimisation, the criterion is to find a vector $\boldsymbol{X}^*$ such that $f(\boldsymbol{X}^*) \geq f(\boldsymbol{X})$ for all legitimate $\boldsymbol{X}$ [36].

In the context of Multiuser Detection (MUD) for example we aim for finding the most likely n-bit vector of the n users supported during the bit-interval considered, which minimises the associated BEP. There is no single best method available for solving all optimisation problems efficiently. Hence a number of optimisation methods have been developed for solving different types of optimisation problems and these methods can be classified according to three different categories, as shown in Figure 1.2.

Mathematical programming techniques are useful only, if the objective function is analytically tractable. On the other hand, statistical methods involve analysing the experimental data and then constructing empirical models, in order to obtain the statistically most accurate representation of the physical situation. In the context of optimum multiuser detection, we will see in our further discourse that the objective function is not analytically tractable. However the function varies versus time, and hence it is infeasible to obtain an accurate time-invariant model that is applicable at all times. Hence, the most efficient way of solving the optimisation problem in multiuser detection is with the aid of stochastic optimisation techniques

or guided random search methods, such as the family of GAs. Let us now commence our introduction to GAs.

CHAPTER 2

Genetic Algorithms Overview

> "I have called this principle, by which each slight variation, if useful, is preserved, by the term of Natural Selection." *Charles Darwin, On the Origin of Species [37]*

Darwin's theory of evolution by natural selection, or survival of the fittest, has fascinated many scientists. In particular, the idea that the concept of evolution could be used as an optimisation tool for engineering problems was conceived by a group of independent scientists [29,38–40] in the 1960s and during the 1970s. Their pioneering ideas eventually led to the creation of a new discipline in engineering, known as *Evolutionary Computation* [36]. The concept behind evolutionary computation was to evolve a population of candidate solutions to a given problem, using operators stimulated by natural genetic variations and natural selection.

The implementations of evolutionary algorithms can be classified into three strongly related, but independently developed methodologies :

- *Evolutionary Strategies* (ESs) [38,39]
- *Evolutionary Programming* (EP) [40]
- *Genetic Algorithms* [29].

Although the conceptual framework in mimicking the process of natural evolution with the aid of these methods is similar, each of these methods implements the associated algorithms in a different manner.

In this dissertation, we are only concerned with the family of GAs and their application as an optimisation tool in the context of multiuser detection in CDMA. Hence, only the concepts of GAs [29, 31, 41, 42] will be highlighted in our further discourse. We will commence with an introduction to GAs in Section 2.1, following the excellent monograph by Goldberg [31]. Following this, we will show how a GA operates as an optimisation tool in practice with the aid of an example in Section 2.2. We will then proceed to highlight why GAs are efficient optimisation tools by identifying the resemblance between human search traits and the GA in Section 2.3. The derivation of the fundamental theorem of GAs is also included in this section. The various elements that constitute a GA are then highlighted in Section 2.4. A survey of GA-assisted CDMA multiuser detection schemes found in the current literature is presented in Section 2.5. Finally, Section 2.6 concludes this chapter. It should be stressed here that the GAs we will be describing in this chapter constitute only a small portion of the entire GA literature. Furthermore, the GAs that are employed for solving our optimisation problem are modified, in order to suit our applications and hence the GAs are slightly different from those commonly found in the GA literature. The interested readers might like to consult references [29, 31, 41] for a more detailed discourse on GAs.

2.1 An Introduction to Genetic Algorithms

[29, 31, 41, 43, 44]

The origins of GAs [29, 31, 41, 43, 44] can be traced back to the 1960s, when Holland [29] and his students undertook the task of studying the phenomenon of adaptation, as it occurs in nature and then imported these adaptive mechanisms into artificial systems. The results of these studies were published in the seminal monograph by Holland [29] in 1975. Since then, the level of interest in GAs has been growing rapidly and has attracted the attention of numerous scientists, including Goldberg [31], Mühlenbein [45] and Grefenstette [46], just to mention a few.

Although GAs have been used in countless applications, such as machine learning and modelling adaptive processes, by far the largest application of GAs is in the domain of function optimisation. In contrast to traditional search methods, such as the method of steepest descent, GAs can be invoked in robust global search and

optimisation procedures that do not require the knowledge of the objective function's derivatives or any gradient-related information concerning the search space. Hence, non-differentiable functions as well as functions with multiple local optima represent classes of problems, where GAs can be efficiently applied [43].

The basic approach of a GA employed for optimising a specific problem defined by an objective function is simple. The flowchart of a GA is shown in Figure 2.1. Firstly, an initial population consisting of P number of so-called *individuals* is created in the 'Initialisation' block, where P is known as the population size. Each individual represents a legitimate solution to the given optimisation problem. An individual can be considered as a vector consisting of the decision variables to be optimised, as shown in Figure 2.2. Here, we will regard the leftmost decision variable in an l-length vector as the 1st decision variable, while the rightmost decision variable is referred to as the lth decision variable. Traditionally, the individuals in a GA population take the form of binary bit vectors. Hence if the decision variables to be optimised are not binary in nature, they have to be discretised and encoded to a bit vector, analogously to analogue-to-digital conversion. The representation of the decision variables as an individual will be highlighted further in Section 2.4.1. This initial population of individuals is usually generated randomly, although it does not necessarily have to be random specifically. If explicit *a priori* knowledge concerning the optimum vector is available, then this knowledge can also be used to generate the individuals of the initial population, in order to bias and expedite the search.

Associated with each individual in the population there is a figure of merit, or more commonly known in GA parlance as the *fitness* value. The fitness value is evaluated by substituting the candidate solution represented by the individual under consideration into the objective function, as indicated by the 'Evaluation' block of Figure 2.1. Individuals having the T number of highest fitness values are then placed in a so-called *mating pool*[1], where $2 \leq T \leq P$. Using a kind of natural selection scheme together with the genetically-inspired operators of *crossover* and *mutation*, the individuals in the mating pool are then evolved to a new population, as depicted in Figure 2.3. Based solely on the fitness values of these individuals in the current mating pool, the *selection* process [47] chooses those individuals in the mating pool that will be allowed to reproduce. These individuals chosen

[1]Note that the definition of mating pool here is different from that found in the GA literature [31, 44]. Here the mating pool consists of T individuals associated with the highest fitness values in the current population, whereas in [31,44] the mating pool is, where the selected parents of the previous population are placed. We adopted our definition in this dissertation, in order to aid our description of GAs, which are modified to suit our specific application.

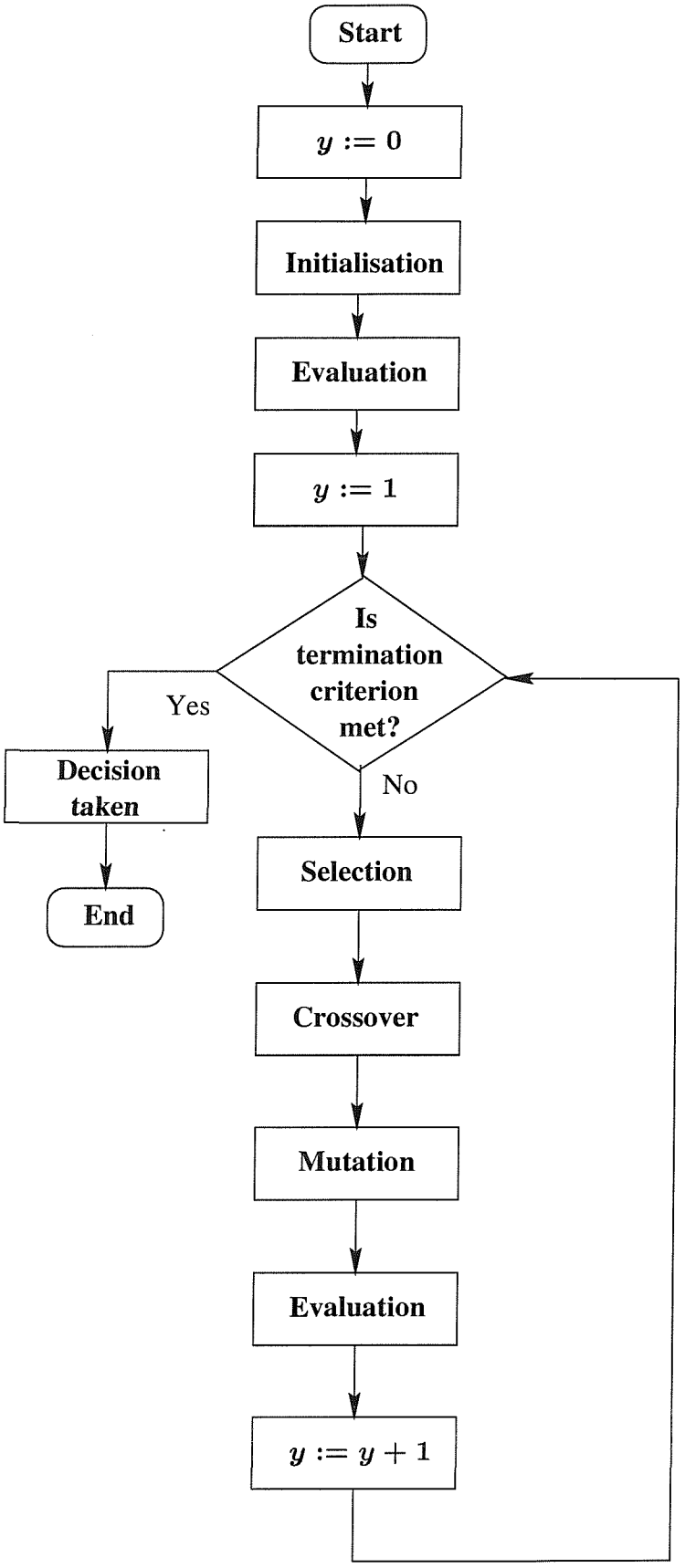

Figure 2.1: A flowchart depicting the structure of a generic genetic algorithm used for function optimisation.

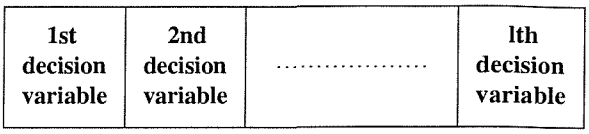

Figure 2.2: A typical l-length individual.

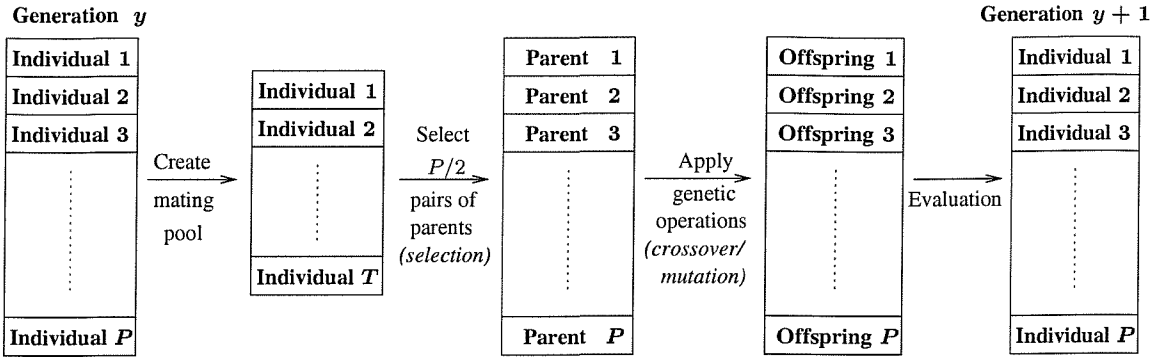

Figure 2.3: An example of a GA operation during a single cycle or generation.

from the mating pool, referred to as *parents* in Figure 2.3, are then used by the crossover and mutation operations, in order to generate new individuals, which will form the new population for the next iteration. The selection process is invoked for improving the average fitness value of the population by giving individuals of higher fitness values a higher probability to be reproduced in the new population. Hence it focuses the search on the promising regions in the search space, which might contain the optimum solution. Numerous selection schemes have been proposed in the GA literature. Some of the more common selection methods will be highlighted in Section 2.4.2. However, the selection process does not alter the individuals. If the optimum solution is to be found, new individuals must be generated. The task of generating new individuals, using the individuals chosen by the selection process is accomplished by the crossover operation.

The *crossover* [41] operation is a process in which arbitrary decision variables are exchanged between a pair of selected parents, mimicking the biological recombination process between two single-chromosome organisms. Hence, the crossover operation creates two new individuals, known as *offspring* in GA parlance, as portrayed in Figure 2.3, which have a high probability of having better fitness values than their parents. In order to generate P number of new offspring by approximately 'combining' the bitstreams constituting the parents, $P/2$ number of crossover operations are required for combining the P parents. A new pair of parents is selected from the mating pool for each crossover operation. The newly created offspring will form the basis of the new population.

During the *mutation* [41] operation, each decision variable in the offspring is

perturbed, with a probability of p_m, by either a predetermined or a random value. This allows new areas in the search space to be explored. The mutation probability of a decision variable is usually very small, in the region of 0.1-0.01 [31]. However, the mutation operation is necessary in a GA, in order to prevent the phenomenon of so-called *premature convergence*. Premature convergence refers to the loss of population diversity before the optimum solution has been found.

Each cycle of selection, crossover, mutation and evaluation constitutes a so-called *generation* in the execution of a GA, as depicted in Figure 2.3. This cycle will continue until some termination criterion is met, as shown in Figure 2.1. Generally, if this cycle is executed for many generations, the population will eventually converge on a set of individuals, in which the individual that corresponds to the highest fitness value is deemed to be the optimum or near-optimum solution.

GAs are not guaranteed to find the optimal solution [31] and their efficiency is determined predominantly by the population size P, i.e. the number of individuals in a population. Hence, the size of the population in a GA is a major factor in determining the accuracy of convergence [48]. As the population size increases, the GA has a better chance of finding the global optimum solution, but the computational cost also increases as a function of the population size. Apart from the population size, a GA's performance will also depend substantially on other factors, such as the choice of the selection method, the type of genetic operations employed, the parameter settings, for example the value of T and p_m, as well as the particular iteration termination criterion. We will be highlighting the effects of each of these factors in our further discourse. Let us now consider an example of how GAs search for the optimum solution during a single generation, as exemplified by Figure 2.3.

2.2 Genetic Algorithms at Work

Consider an optimisation problem, where the objective function is given by[2] :

$$\Lambda(\boldsymbol{b}) = 2\boldsymbol{by} - \boldsymbol{bRb}^T. \tag{2.1}$$

[2]Notice that the objective function of Equation (2.1) is identical to the correlation metric $\Omega(\boldsymbol{b})$ of Equation (3.23) for the optimum multiuser detection in CDMA [1], which will be shown in Chapter 3.

	Individuals					Fitness f_i	Mapped fitness $f_i' = f_i + 10$	Selection probability $p_i = f_i' / \sum_j^T f_j'$
A_1	1	1	1	-1	1	9.06	19.06	0.3985
A_2	1	1	-1	-1	-1	-1.056	8.944	0.1870
A_3	-1	1	-1	-1	-1	-6.368	3.632	0.07594
A_4	1	-1	-1	1	1	6.192	16.192	0.3385
							$\sum_j^P f_j' = 47.828$	

Table 2.1: An example of the initial population consisting of $P = 4$ individuals, where the associated fitness values are evaluated according to the objective function given by Equation (2.1).

Assuming that the following information is available :

$$\boldsymbol{y} = \begin{bmatrix} 1.328 \\ -2.183 \\ 0.044 \\ -2.856 \\ 2.485 \end{bmatrix}; \quad \boldsymbol{R} = \begin{bmatrix} 1 & 0.1 & 0.2 & 0.3 & 0.4 \\ 0.1 & 1 & 0.4 & 0.2 & 0.3 \\ 0.2 & 0.4 & 1 & 0.5 & 0.1 \\ 0.3 & 0.2 & 0.5 & 1 & 0.6 \\ 0.4 & 0.3 & 0.1 & 0.6 & 1 \end{bmatrix},$$

the goal of this optimisation process is to find the decision variable vector $\boldsymbol{b}$, which consists of $l = 5$ antipodal bits, that maximises the objective function of Equation (2.1).

Since the candidate solutions in this case are in the form of vectors consisting of $l = 5$ antipodal bits, no conversion of the individuals to this format is required. GAs commence their search by generating an initial population of individuals at random. For this example, we adopted a population of size $P = 4$. Each bit of the $l = 5$ bits of an individual can be constructed by tossing an unbiased coin. These randomly generated individuals and their associated fitness values are shown in Table 2.1. For simplicity, we will assume that the mating pool size is equal to the population size, i.e. $T = P$. In this case, all the individuals of Table 2.1 will be given a chance to reproduce. The next step of the GA is the selection of parents, in order to create new offspring. A common selection method used in GAs is the so-called *fitness-proportionate selection* [31], in which the probability of selection p_i of the ith individual is equal to its fitness value f_i divided by the total fitness value of the mating pool. This method requires the fitness values to be positive for all combinations of $\boldsymbol{b}$ because a negative fitness value would yield a negative probability of selection. According to our objective function of Equation (2.1), this requirement is not met, since certain combinations of $\boldsymbol{b}$ exhibit negative fitness values, as shown in Table 2.1. Hence a mapping function must be invoked, in order

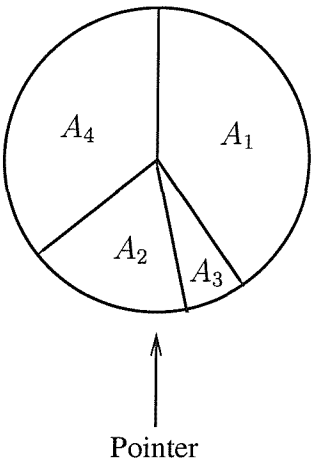

Individual	Probability of Selection
A_1	0.3985
A_2	0.1870
A_3	0.07594
A_4	0.3385

Figure 2.4: An implementation of the fitness-proportionate selection scheme using a roulette wheel, whereby each individual of Table 2.1 is allocated a slice of the wheel proportional in area to the individual's probability of selection.

to ensure that the fitness values for all combinations of $\boldsymbol{b}$ become positive. A simple mapping function is to add a constant positive value to the fitness values of all the individuals, as indicated in Table 2.1. In this example, we arbitrarily invoked a constant shift of 10, which will ensure that all fitness values become positive. Summing the mapped fitness values f_i' over all four individuals, we obtained a total mapped fitness value of 47.828 and an average mapped fitness value of 11.957 for the initial population of Table 2.1. The probability of selection p_i for each individual is calculated in proportion to their individual fitnesses and the values are as listed in Table 2.1. We can see that individuals having higher fitness values are allocated a higher probability of selection. Note that the probability of selection p_i of an individual is defined with respect to the average fitness of the current population. Hence, the probability of selection of the same individual would be different in a different population.

A simple method of implementing the fitness-proportionate selection scheme is the so-called *roulette wheel sampling* [29], whereby each individual is allocated a slice of a circular roulette wheel proportional in area to the individual's probability of selection. An example of a roulette wheel is shown in Figure 2.4 for the population of Table 2.1. When the roulette wheel is spun and the pointer comes to standstill on one of the wedge-shaped slices, the corresponding individual will be selected as a parent. Each spin of the roulette wheel yields a new parent. Hence we can see here that by using this implementation, individuals with higher probability of selection have a higher chance of being selected as parents.

Once a pair of parents is selected, the crossover operation is then applied to this pair of parents, as depicted in Figure 2.3. A number of variants of the

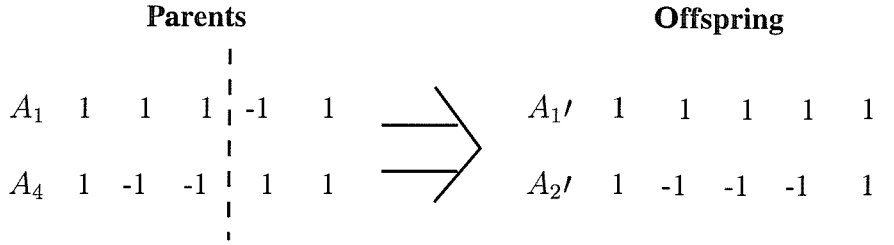

a) Single-point crossover operation between individuals A_1 and A_4

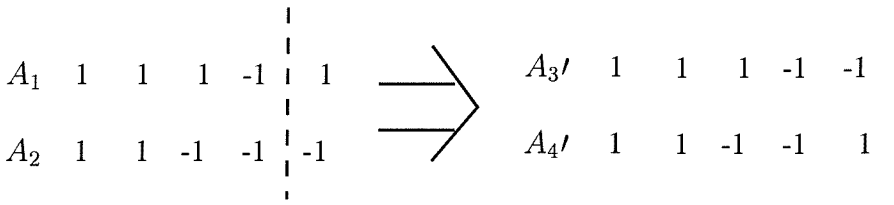

b) Single-point crossover operation between individuals A_1 and A_2

Figure 2.5: Examples of the single-point crossover operation between the pairs of selected individuals of Table 2.1, where the vertical dashed line represents the crossover point.

crossover operations were proposed and the simplest form is the so-called *single-point crossover* [31]. In a single-point crossover operation, a so-called *crossover point* x is arbitrarily selected between the range $[1, l-1]$, where l is the length of the individual. Two offspring are created by swapping all decision variables beyond this crossover point between the parents, i.e. from the $(x+1)$st decision variable to the lth decision variable. For example, let us assume that the individuals A_1 and A_4 were selected as parents from our initial population of Table 2.1. The resulting crossover between these two parents, as illustrated in Figure 2.5a with the crossover point indicated by the vertical dashed line, yields two new offspring, A_1' and A_2'. The crossover operation is then repeated for another newly selected pair of individuals, for example individuals A_1 and A_2 of Table 2.1, with a newly generated crossover point, in order to create two more new offspring namely A_3' and A_4', as shown in Figure 2.5b. These two pairs of newly created offspring with their associated fitness values shown in Table 2.2, will form the new population for the next generation. ¿From Table 2.2, we can clearly see that both the maximum and the average mapped fitness values have improved during the transition to the new population over that of the previous population of Table 2.1. The average mapped fitness value of the population has improved from 11.957 to 16.186 during the lifetime of a generation. Similarly, the maximum mapped fitness value has increased from 19.06 to 27.616 during the same generation. Note that the fitness values of Table 2.2 are calculated before the mutation operation is invoked. The conventional

	Individuals					Fitness f_i	Mapped fitness $f_i' = f_i + 10$
A_1'	1	1	1	1	1	-2.364	8.364
A_2'	1	-1	-1	-1	1	17.616	27.616
A_3'	1	1	1	-1	-1	-0.88	9.88
A_4'	1	1	-1	-1	1	8.884	18.884
							$\sum_j^P f_j' = 64.744$

Table 2.2: An example of the new population created by the single-point crossover operation between pairs of selected individuals of Table 2.1, as shown in Figure 2.5. Their associated fitness values are evaluated according to the objective function given by Equation (2.1).

procedure [31], however, would be to perform the mutation operation on the offspring before their fitness values are evaluated, as depicted in Figure 2.1. On the other hand, as mentioned in the previous section, the probability of mutation is fairly small. Hence, on average the mutation operation will not affect the average fitness value of the population significantly, even though the maximum fitness value may be different due to the probability that offspring A_2' may be mutated. Despite the fact that the mutation of individuals may occasionally cause the loss of important information learnt from the previous generation, there are instances when the mutation operation is useful. Considering Table 2.2, we note that due to the bias of the selection process, the leftmost bit of all the offspring that is produced is a logical '1'. Further crossover operations between any pairs of these offspring in the subsequent generation will be unable to change the state of the leftmost bit. On the other hand, it is possible that the leftmost bit of the optimum solution is in fact a logical '0' represented by '-1'. Hence in this case, with the aid of crossovers alone, we will be unable to find the optimum solution. This effect is more significant during the latter stages of the GA, when the individuals in the population begin to resemble each other more closely due to the effects of selection and crossover. Although the probability is small, the mutation operation ensures that new information is injected and hence provides an opportunity to sample the unexplored regions of the search space. In order to prevent the individuals in the population becoming self-similar too rapidly, potentially resulting in a premature convergence, it is important to maintain a high diversity of individuals in the population, especially during the initial phase of a search.

With the aid of this example, we have shown that by granting the individuals associated with high fitness values a higher probability of reproduction, a process reminiscent of the natural selection theory was realised. Then, by using the simple

probabilistic operations of crossover and mutation in the context of these individuals, new individuals are produced, which in general will have higher fitness values than their parents. Yet, this example brings forth even more questions than answers. How can it be possible that better solutions may be found by simply exchanging decision variables between two individuals in a random manner? What will ensure that the average fitness value of the population will be improved, even after a single generation? We will attempt to provide the answers to these questions in the next section.

2.3 Why do GA work?

From our brief conceptual introduction of the family of GAs given in Section 2.1, it may appear still somewhat farfetched that simple GA operations such as the selection of individuals based purely on their associated fitness values, on the partial random exchange of decision variables between individuals and on the random perturbation of a few decision variables lends itself to solving even the most complex optimisation problems. Even with the aid of our example in Section 2.2, it is still non-trivial as to why GAs can be efficiently used to search for the optimum solution. In this section, we will attempt to further augment the key concepts of GAs.

The fundamental concept of GAs can be readily justified by first observing the way humans perform a search for the optimum solution based purely on human intuition, given a set of candidate solutions. This approach is plausible, since the notion of GAs is in effect based on natural adaptation.

2.3.1 Optimisation from a Human's Perspective

Let us consider again the optimisation example highlighted in Section 2.2. Upon observing the four individuals given in Table 2.1, we will notice certain similarities in specific segments of the individuals. Furthermore, certain bit sequences are associated with a high fitness value. For example, observe that the three individuals A_1, A_2 and A_4, which have a higher fitness value compared to individual A_3, have a common decision variable, since their leftmost bit is a logical '1'. Hence, it is highly probable that the optimum solution contains a logical '1' in its leftmost bit position. We also noticed that the individuals ending with a logical '1' seem to be associated with high fitness values. This fact is gleaned by comparing individuals A_1 and A_4 against the individuals A_2 and A_3. Hence, it is also highly probable that the optimum solution contains a logical '1' at its rightmost bit position. However, at this stage, we are uncertain about the value of the middle three bits, since

these three bits of the two fittest individuals A_1 and A_4 differ from each other. In order to resolve this dilemma, we may exchange some decision variables between these two individuals that are associated with a high fitness value, with the hope that the resulting individual will have an even higher fitness value. This course of action is analogous to our behaviour of exchanging and combining good ideas from different sources. For example techniques from the field of GAs and CDMA multiuser detection may be amalgamated, with the hope that a more likely solution can be found for the transmitted CDMA signals. Hence, in order to continue our search for the optimum solution, we will generate four new individuals (offspring) using the information that is available to us at this moment as a guide. We may then end up with a new population that resembles that shown in Table 2.2.

In summary, what we have followed this course of action in order to seek similarities among individuals in the population and then sought a causal relationship between these similarities while aiming for high fitness values [31]. The idea is that it is these similarities that confer high fitness values on the individuals. In our next optimisation step we attempt to amalgamate these similarities in the hope of creating a new individual that will exhibit an even higher fitness value. This is accomplished in GAs by the selection and crossover mechanisms, which bestow them with their ability to converge.

There will come a time when no more information can be gleaned from the individuals in a population, when all the individuals in the population become similar. In order acertain that the individual associated with the maxmimum fitness value in this population is the optimum solution, we will attempt to change the state of certain bits and then check the associated effects on the fitness through a series of trial-and-error steps. In other words, we safeguard our tentative solution against premature convergence. This is executed in GAs with the aid of the mutation operation. However, in order to refrain from changing the state of the bits of an individual aggressively, the mutation operation in GAs is usually carried out with a low probability. Again, this is analogous to our behaviour, when combining the ideas of GAs and CDMA multiuser detection. After combining these two ideas, we tend to modify the resulting solution, in order to gauge, whether the solution can be improved further. This will usually involve a series of trial-and-error steps.

So far, we have compared the approach of GAs with certain human search traits and have identified the resemblance between the way humans and GAs perform a search in their quest for the optimum solution. Let us now highlight the theoretical aspects of the optimisation from a GA's perspective.

2.3.2 Optimisation from a GA's Perspective

We have seen from the previous section that we can search for the optimum solution more effectively, if we exploit important similarities amongst highly fit individuals. Hence the focus here is no longer on individuals alone, but rather on their similarities. Holland [29] introduced the notion of a so-called *schema* (plural, *schemata*), in order to explain how GAs search for regions of high fitness. A schema H is a similarity template, defined over the alphabet $\{0, 1, *\}$, where 0 and 1 are referred to as *defined bits*, while $*$ denotes a *don't care* symbol. The *order* of a schema $o(H)$ is determined by the number of defined bits in that schema. By contrast, the *defining length* of a schema $\delta(H)$ is the distance between its leftmost and rightmost defined bits, including only one end of the interval in the distance calculation. An individual is said to be an *instance* of a particular schema, if at every position in that schema, a 1 matches a 1 in the individual, a 0 matches a 0, or a $*$ matches either. Using our example in Section 2.2, by replacing the logical '-1' with a logical '0', individuals A_1 and A_4 of the initial population of Table 2.1 are instances of the schema 1***1, while the individuals A_2 and A_3 are instances of the schema *1000. These two schemata have an order of 2 and 4, respectively, and have a defining length of 4 and 3, respectively. Hence we see that the definition of schemata provides us with a better representation of the similarities amongst the individuals in a population and simplifies the analysis of the GAs.

From a different perspective, schemata can be considered to represent hyperplanes in the search space [44]. Perhaps the best way of visualising schemata as hyperplanes is to consider an $l = 3$-dimensional search space, where each candidate solution contains 3 bits, as shown in Figure 2.6 [31]. In this case, the search space takes the form of a cube, where the corners of the cube represent the legitimate individuals, which constitute schemata of order 3. The edges of the cube are schemata of order 2, as illustrated in Figure 2.6, while the planes of the cube are schemata of order 1. The whole space is represented by the schema of order 0.

From Figure 2.6, we can readily see that each individual representing a candidate solution of length l is the intersection of 2^l schemata. Hence, a population of size P will contain between 2^l – when all the individuals in the population are identical – and $P \times 2^l$ schemata, where $P \times 2^l$ cannot exceed 3^l. The explicit fitness value of an individual evaluated from the objective function implicitly gives valuable information concerning the average fitness value of the 2^l different schemata of which the individual concerned is an instance. Hence the explicit fitness evaluation of a population of P individuals, at a given generation, also implies an implicit evaluation of the estimated average fitness value of a significantly higher number

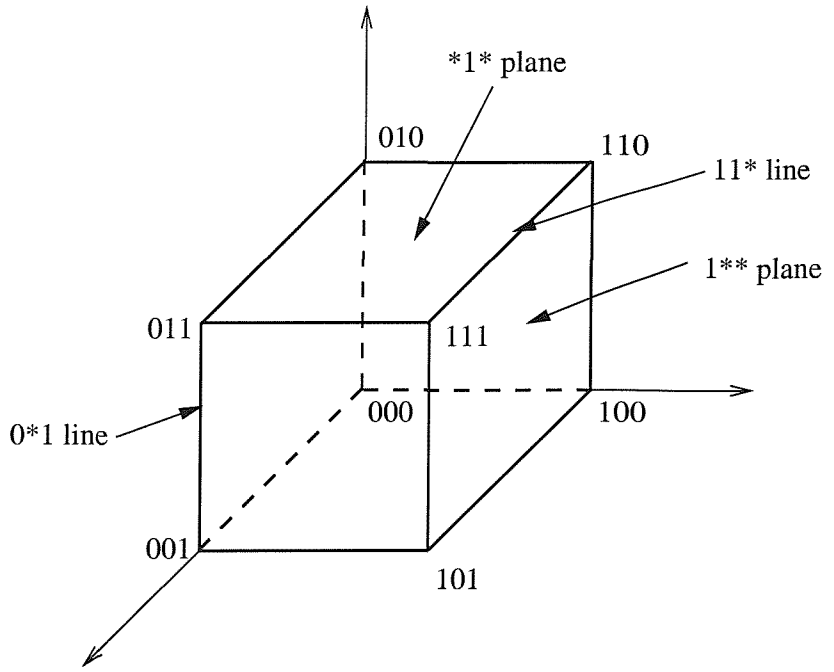

Figure 2.6: Visualisation of schemata as hyperplanes in the l=3-dimensional search space [31].

of schemata. This simultaneous evaluation of a high number of schemata in a population of P individuals is referred to as *implicit parallelism* [29, 44]. It should be stressed here that the implicit average fitness value of a schema evaluated in this case is only an estimation, since the instances evaluated in a finite-size population constitute only a small sample of all possible instances. For example, consider the schema 1**** of length $l = 5$. In order to obtain its actual average fitness value, we have to evaluate the fitness of 16 different individuals, i.e. that of all $l = 5$-bit individuals that contain a logical '1' in the leftmost bit. However, in a practical GA, the population size invoked will be typically less than 16, when searching for a 5-bit optimum solution.

Having demonstrated that a high number of schemata is present in a given population and their estimated average fitness values are implicitly estimated by the GAs, we will now consider the growth-rate and decaying-rate of these schemata in response to selection, crossover and mutation.

Effects of Selection on the Schemata

Let us assume that there are $m(H, y)$ number of instances corresponding to the schema H present in a population of size P at generation y. The estimated average fitness value of the schema H, considering its $m(H, y)$ number of instances at generation y is denoted as $f(H, y)$. Following our example given in Section 2.2, the probability of selection p_i as a parent for an individual A_i is equal to its fitness value

f_i divided by the total fitness value of the population[3], i.e. $p_i = f_i / \sum_j^P f_j$. Hence the expected number of offspring associated with individual A_i in the next generation $y+1$, ignoring the effects of crossover and mutation, is equal to $A_i \times P \times p_i$ or $A_i \times f_i/\bar{f}$, where $\bar{f} = (\sum_j^P f_j)/P$ is the average fitness value of the population. Similarly, we can express the expected growth rate of the schema H in terms of its estimated average fitness value $f(H, y)$ and the population's average fitness value $\bar{f}$ as [31] :

$$m(H, y+1) = m(H, y)\frac{f(H, y)}{\bar{f}}, \tag{2.2}$$

where $m(H, y+1)$ is the expected number of instances of the schema H in the next generation $y+1$. According to Equation (2.2), due to the effects of the selection process alone, the number of schemata having average fitness values above the population's average fitness value is expected to increase in the next generation. At the same time, the number of schemata having average fitness values lower than the population's average fitness value are expected to decrease. Furthermore, when the population is evolving over many generations, the estimate of a schema's average fitness should, in principle, become more and more accurate, since the GA is sampling more and more instances of that schema.

Effects of Crossover on the Schemata

In order to observe the effects of crossover on the schemata, let us first consider the following two schemata of length $l = 5$ [43] :

$$\begin{aligned} H_1 &= 11***\\ H_2 &= 1***1. \end{aligned}$$

Note that the individual A_1 of Table 2.1 is an instance of the schemata H_1 and H_2 and they have a defining length $\delta(H)$ of 1 and 4, respectively. We assume that the single-point crossover operation is invoked, as highlighted in Section 2.2. Recall that the crossover point is randomly generated in the range $[1, l-1]$, inclusively. Hence we can readily see that the probability that the defined bits of schema H_1 will be separated during the crossover operation is only $1/(l-1)$. Specifically this will happen if the crossover point is located at position 1. On the other hand, the probability that the defined bits of schema H_2 will be separated during the crossover operation is $(l-1)/(l-1) = 1$. In other words, schema H_2 will be 'destroyed' by the crossover operation, regardless of where the crossover point is located. Based

[3]Again, here we assumed that the mating pool size T is equal to the population size P.

on this observation, we can see that the probability $p_s(H)$ that a schema H will survive during the crossover operation is dependent on its defining length $\delta(H)$. If the generated crossover point is beyond the defining length of a schema, this schema will remain intact. However, we should also note that even if the crossover point is within the defining length of a schema, there is still a finite probability that the schema will survive. This will happen, if both the parents selected for the crossover are instances of that schema. Hence, we can express a lower bound of $p_s(H)$ as [31] :

$$p_s(H) \geq 1 - \frac{\delta(H)}{l-1}. \tag{2.3}$$

Now if we combine the effects of both the selection and crossover on the schema H, we can expect the number of instances of that schema in the next generation $y+1$ to be [31] :

$$m(H, y+1) \geq m(H, y) \cdot \frac{f(H, y)}{\bar{f}} \left[1 - \frac{\delta(H)}{l-1}\right]. \tag{2.4}$$

According to Equation (2.4), schemata having above-average fitness values and short defining lengths are expected to increase their number of instances in the subsequent generation. Let us next consider the effects of mutation on the schemata.

Effects of Mutation on the Schemata

It was mentioned in Section 2.1 that mutation is the random alteration of each bit with a probability of p_m. Hence, in order for a schema H to survive, all its associated defined bits must themselves survive. Recall that the order of a schema $o(H)$ is defined by the number of defined bits it contains. Therefore, the probability that a schema H of order $o(H)$ will survive during the mutation operation is $(1-p_m)^{o(H)}$. In short, the probability of survival under the effects of mutation is higher for lower-order schemata.

Now we can formulate the expected growth-rate of the schemata by combining the effects of selection, crossover and mutation, which is given as [31] :

$$m(H, y+1) \geq m(H, y) \cdot \frac{f(H, y)}{\bar{f}} \left[1 - \frac{\delta(H)}{l-1}\right] (1-p_m)^{o(H)}. \tag{2.5}$$

Equation (2.5), as formulated by Holland [29], is known as the *Schema Theorem* [29, 31], which is the fundamental theorem behind the concepts of GAs. The schema theorem formulated in the context of Equation (2.5) states that short, low-order schemata having an above-average fitness will increase in their number of

instances in the subsequent generation. These schemata are known in GA parlance as *building blocks* and the assumption that this is indeed the nature of the process behind GAs is known as the *building block hypothesis* [41]. According to the above-mentioned building block hypothesis, the GA initially biases its search towards higher fitness values in certain low-order schemata and converges on this part of the search space. During its further operations it gradually biases its search towards higher-order schemata by combining information from low-order schemata with the aid of crossovers and eventually converges on a small region of the search space that exhibits a high fitness value [44].

However, Holland's schema theorem has its critiques. As seen in Equation (2.5), the schema theorem only makes predictions concerning the expected number of instances of schemata from one generation to the next. Unfortunately it does not provide predictions about the quality of the solution that the GA can deliver over many generations, or about the speed at which the GA will converge, or indeed provide an exact picture of the GAs' behaviour. Hence intensive research has been carried out in order to provide a more exact mathematical analysis concerning the behaviour of GAs [49–51]. However, the portrayal of this analysis are beyond the scope of this dissertation. Nevertheless, the schema theorem of Equation (2.5) provides a fundamental stepping stone towards a better understanding of why GAs work. In the next section, we will highlight the various elements of GAs in more details.

2.4 Elements of Genetic Algorithms

2.4.1 Representation

Representation refers to the way candidate solutions are represented by individuals. Traditionally, as defined by Holland [29], the individuals are represented in the form of bit vectors, in which each vector is comprised of a combination of zeros and ones. The strong preference for using binary representations of solutions in GAs was justified by Holland [29] according to the schema theory, as highlighted in Section 2.3. It is claimed [31] that GAs are well suited to handle pseudo-Boolean and combinatorial optimisation problems. For optimisation problems involving nonbinary or real-valued decision variables, these decision variables have to be quantised and encoded into binary-valued bit vectors, in order to perform the genetic operations. Similarly, these bit vectors must be converted back to their original real-valued form, in order to evaluate their associated fitness values from the objective function.

Binary Encoding

There are several potential encoding schemes for mapping nonbinary decision variables to binary-valued bit vectors. The so-called *binary encoding* [41] is the simplest and most commonly used encoding scheme. Encoding of nonbinary integers is straightforward. For example, 4 and 12 can be represented as 100 and 1100, respectively. For real-valued decision variables, the number of bits invoked will determine the resolution of the encoding. Suppose a real-valued decision variable x, where $a \leq x \leq b$, is to be encoded to an n-bit vector. Firstly we can convert x to a nonbinary integer y according to [52] :

$$y = \left\lfloor \frac{b-a}{2^n} \times x \right\rfloor . \tag{2.6}$$

We can then encode the integer y according to any nonbinary integer encoding. Binary encoding has the drawback that in some cases all the bits must be changed in order to increase a number by 1. For example, the bit pattern 011 translates to 3 in decimal, but 4 is represented by 100. This can make it implementationally difficult for an individual that is close to an optimum solution to move even closer to the optimum with the aid of the crossover and mutation operation [44].

Gray Encoding

In order to overcome this drawback, a different encoding scheme, namely *Gray coding* [41] was proposed. Gray codes have the property that incrementing or decrementing any integer number by 1 always involves only a one-bit change. The mapping function from the binary coded n-bit vector to a Gray coded n-bit vector is given by [52] :

$$g_k = \begin{cases} b_1 & \text{if } k = 1 \\ b_{k-1} \oplus b_k & \text{if } k > 1 \end{cases} , \tag{2.7}$$

where g_k and b_k are the kth Gray code bit and binary code bit, respectively, for $k = 1, \ldots, n$ and $\oplus$ denotes a modulo 2 addition. The conversion from Gray coding to binary coding is given by [52] :

$$b_k = \sum_{i=1}^{k} g_i, \tag{2.8}$$

where the summation is based on the modulo-addition. In practice, Gray-coded representations are often more successful for real-valued parameter function optimisation applications, than binary-coded representations.

The issue of the representation of nonbinary or real-valued decision variables in terms of bit vectors is still open to debate. If real-valued decision variables are represented in their original form, the search space is continuous and will have an infinite number of search points. Coding these decision variables into bit vectors discretises the search space and reduces its size. On the other hand, analoguously to the analogue-to-digital conversion process in digital systems, this conversion results in a *quantisation error*, where the accuracy of the decision variables is determined by the number of bits used to represent the real-valued decision variables. Furthermore, an additional complexity and delay is incurred, since the real-valued decision variables have to be binary encoded and decoded for each generation, in order to perform the required genetic operations and to evaluate their corresponding fitness values, respectively. Moreover, comparisons [52, 53] have shown that GAs representing the real-valued decision variables in their original form, using *real-valued coding* exhibit a better performance, than those converting the decision variables to bit vectors. Hence in this treatise we will be using the real-valued representation of the decision variables, as it will be highlighted in Chapter 4. Let us now review the range of selection schemes in the next section.

2.4.2 Selection

There are numerous ways, in which a new population can be created from the previous population. However, regardless of what method is used, it is imperative that individuals having higher fitness values in a given mating pool must be given a better chance of reproducing offspring in the subsequent generation, than the lower-fitness individuals in the same mating pool. Otherwise the GA will be unable to take advantage of the presence of high-quality individuals in the population and to efficiently search for the optimum solution. The task of choosing these individuals for reproduction is performed by the selection process [47]. The type of selection scheme used predetermines the convergence characteristics of the GA. A strongly selective scheme implies that suboptimal, but highly fit individuals will dominate the population, reducing the diversity needed for further change and progress and hence may lead to premature convergence, without exploring the entire search space. On the other hand, a weakly selective scheme will result in a slower convergence rate due to the presence of poor quality, low-fitness individuals. Numerous selection schemes have been proposed in the GA literature. We will highlight some of the more commonly used selection regimes below. Here we will assume that the selection process is invoked in the mating pool, which contains T number of individuals associated with the highest fitness values in a given population.

Fitness-proportionate Selection

In *fitness-proportionate* selection, as invoked in our example in Section 2.2, the probability of selection p_i of the ith individual is defined as :

$$p_i = \frac{f_i}{\sum_j^T f_j}, \tag{2.9}$$

where f_i is the fitness value associated with the ith individual. However, the fitness-proportionate selection scheme has several deficiencies. Based on Equation (2.9), we can see that if there is only a small percentage of individuals with relatively high fitness values in a mating pool, then these individuals will be assigned with a high probability of selection compared to the other individuals in the mating pool. Hence the offspring produced in this case are fairly similar in the subsequent generation. This may lead to a premature convergence, since the search space has not been sufficiently well explored. This phenomenon typically occurs during the early stages of a GA's operation, when the initial population is randomly generated and the fitness distribution of the mating pool happens to be non-uniform at the beginning. Hence a small number of individuals have a tendency of dominating the selection process.

Furthermore, if the fitness value distribution of the mating pool is fairly uniform, i.e. the fitness value of each individual is fairly close to one another, then all the individuals in the mating pool will have an approximately equal probability of selection. Hence all solutions will have a similar chance of being assigned to the mating pool and hence producing offspring.

Sigma Scaling

The *sigma scaling* selection scheme [41,54] was proposed in order to render the GA less susceptible to premature convergence. Under this scheme, the probability of selection of the ith individual is a function of several variables, namely that of its fitness value, the mating pool mean fitness and the mating pool fitness' standard deviation, as given by [41] :

$$p_i = \begin{cases} \frac{1}{T}\left(1 + \frac{f_i - \bar{f}}{2\sigma}\right) & \text{if } \sigma \neq 0 \\ \frac{1}{T} & \text{if } \sigma = 0, \end{cases} \tag{2.10}$$

where f_i is the fitness value of the ith individual, $\bar{f}$ is the mean fitness of the mating pool and σ is the standard deviation of the mating pool's fitness values. According to Equation (2.10), it is possible that the value of p_i is negative. In

the context of maximisation, p_i will be set to a small value (eg. $0.1/T$ in [54]) since a negative p_i calculated from Equation (2.10) implies that the corresponding individual has a fitness value significantly lower than the population's average fitness value. As specified by Equation (2.10), we can see that if the standard deviation of the mating pool's fitness values is high, individuals having high fitness values will not be assigned a significantly higher probability of selection in comparison to the individuals having lower fitness values. Hence the individuals having lower fitness values are given a fair chance of reproducing. On the other hand, if the individuals in the mating pool are similar, resulting in a low standard deviation, then the individuals exhibiting higher fitness values will be assigned a higher probability of selection.

Linear Ranking Selection

The *linear ranking* selection scheme [55] is an alternative method of preventing premature convergence. According to this method, the individuals in the mating pool are ranked according to their associated fitness values, such that the rank T is assigned to the individual associated with the highest fitness value in the mating pool, while the rank 1 is assigned to the individual exhibiting the lowest fitness value in the mating pool. Similarly, the remaining individuals in the mating pool are ranked accordingly. The ith individual will then be assigned its probability of selection p_i, based on its specific ranking $rank_i$ in the mating pool, as given by [56]:

$$p_i = \frac{1}{T}\left[\eta^- + \left(\eta^+ - \eta^-\right)\frac{rank_i - 1}{T - 1}\right], \tag{2.11}$$

where $\frac{\eta^-}{T}$ is the probability of selection assigned to the individual associated with the lowest fitness value and $\frac{\eta^+}{T}$ the probability of selection assigned to the individual having the highest fitness value. If the mating pool size T always remains the same from generation to generation, the conditions $\eta^+ = 2 - \eta^-$ and $\eta^- \geq 0$ must be fulfiled.

Hence in this selection scheme, we can see that each individual's probability of selection is determined by its rank in the mating pool and it is independent of the fitness value distribution of the mating pool. However, this scheme suffers from a slow convergence rate since the probability of selection of an individual is determined regardless of its relative fitness value in the mating pool.

Tournament Selection

According to the *tournament selection* scheme [57], t number of individuals are chosen randomly from the mating pool, where $t < T$ is referred to as the *tournament size*. The individual associated with the highest fitness value out of these t preferred individuals will be selected as a parent. This process is repeated for another t set of individuals, in order to form a pair of parents for the crossover operation.

Again, the probability of selection of each individual is independent of the fitness distribution of the mating pool according to the tournament selection scheme.

Incest Prevention

Before we commence our detailed discussions it should be pointed out here that incest prevention is not a selection scheme. However, it is directly related to how the mating pool was formed and hence affects the calculation of the individuals' selection probability. Therefore we introduce incest prevention in this selection-related section. According to the previously discussed selection regimes it is possible that two identical individuals are selected. The offspring resulting from the crossover operation between these two so-called *incest* individuals will also be identical. While this will ensure that some individuals will be transferred from one generation to the next generation, this method does not promote diversity and may also lead to premature convergence [41].

Hence an alternative technique, known as *incest prevention* has been proposed [58], which only allows different individuals to be selected for the crossover operation. This technique will ensure that sufficient diversity is maintained from generation to generation and the likelihood of a premature convergence is reduced. As alluded earlier, an alternative way of mitigating the premature convergence problem is invoking scaling. In our application, we will invoke the above-mentioned incest prevention scheme by ensuring that all individuals in the mating pool are dissimilar. Unfortunately, by favouring dissimilarity, the high-merit individuals, which are fairly similar to the best individual may be discarded during this process. Hence there is a clear trade-off between the advantageous nature of diversity and favouring high-merit individuals.

We will compare the performance of each of the above-mentioned selection schemes in the context of GAs in Chapter 3. More importantly, we will study the effects of the mating pool size T and that of incest prevention on the performance of GAs. Let us now consider the family of crossover operations.

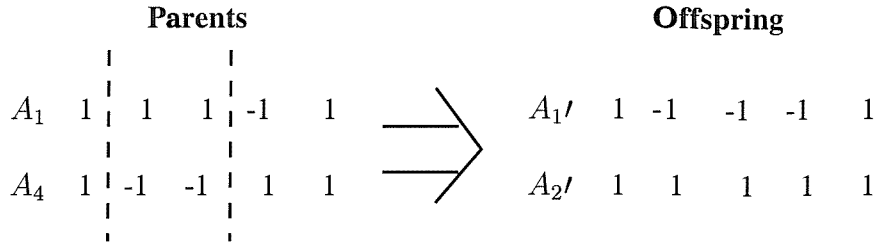

Figure 2.7: Example of the double-point crossover operation between the individuals A_1 and A_4 of Table 2.1, where the vertical dashed lines represent the crossover points, in order to produce the offspring A_1' and A_2'.

2.4.3 Crossover

Single-point Crossover

The simplest form of a crossover operation is the *single-point crossover*, which we have highlighted in our example in Section 2.2. The single-point crossover was also used by Holland [29] in deriving the schema theorem of Equation (2.5). However, the single-point crossover has several shortcomings. Firstly, as we have observed in Equation (2.3), single-point crossover may destroy schemata, and the higher the defining lengths of schemata, the higher the probability of destroying them. However, the probability of destroying schemata is lower for a single-point crossover mask, than for multi-point crossover masks. In other words, schemata that can be created or destroyed by the single-point crossover depend strongly on the location of the bits in the individual. Secondly, a single-point crossover cannot combine all possible schemata [41]. For example, instances of schemata 1***1 and **11* cannot be combined for forming an instance of 1*111. In order to mitigate these shortcomings, two other crossover operations were introduced in GAs, namely the double-point crossover [41] and the uniform crossover [59]. These two operations will be highlighted below.

Double-point Crossover

A *double-point crossover* [41] operation uses two randomly chosen crossover points. Decision variables that fall between these crossover points are then exchanged between the parents. Figure 2.7 illustrates an example of the double-point crossover between individuals A_1 and A_4 of Table 2.1. Double-point crossover is less likely to destroy schemata having a high defining length and can combine more schemata, than the single-point crossover [41]. However, there are still certain schemata that the double-point crossover cannot combine.

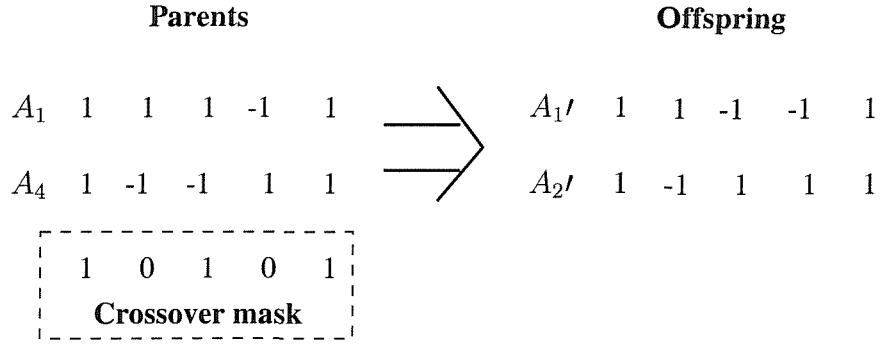

Figure 2.8: Example of the uniform crossover operation between the individuals A_1 and A_4 of Table 2.1 with the aid of a crossover mask, in order to produce the offspring A_1' and A_2'.

Uniform Crossover

In a *uniform crossover* operation [59], a so-called *crossover mask* is invoked instead of the crossover point. The crossover mask is a vector consisting of randomly generated 1s and 0s of equal probability, having a length equal to that of the individuals. Bits are exchanged between the selected pair of parents at locations corresponding to a 1 in the crossover mask. An illustration of the uniform crossover operation is shown in Figure 2.8. While it was shown in [60] that the uniform crossover operation has a higher probability of destroying a schema, it is also capable of creating new schemata.

Intensive research efforts have been invested in quantifying and comparing the usefulness of these crossover operations. However, the results did not give a definitive guidance on when to use a specific type of crossover operation, since their effectiveness is very much dependent on the problem in which they are used. Hence the general consensus is that various crossovers have to be tested and possibly modified, in order to determine what type of crossover operation is most suitable for solving the problem at hand. Let us next consider the potential mutation operations proposed in the literature [41].

2.4.4 Mutation

The various selection methods and crossover operations we have highlighted so far are applicable to binary or real-valued, individuals. In other words, the procedures in carrying out these selection and crossover operations are the same, regardless of how the legitimate solutions are mapped to individuals. However, the mutation operation will be different for a binary-coded individual and a real-valued individual. Recall from Section 2.4.1 that a binary-coded individual consists of bit decision variables, while a real-valued individual consists of real-valued decision variables. After

the production of the offspring with the aid of the crossover operation, each decision variable of the offspring will be mutated with a probability of p_m. The mutation operation is invoked, in order to ensure that sufficient diversity is maintained in the population so as to protect it against premature convergence. Numerous studies have been carried out, in order to determine the optimum value of p_m. A high probability of mutation may prevent the survival of schemata of high fitness values and hence may lead to suboptimal solutions. On the other hand, a low probability of mutation may result in premature convergence to suboptimum solutions due to the lack of diversity in the population. Schaffer *et al.* [61] suggested that the value of p_m should lie in the range of $[0.005, 0.01]$, Grefenstette [62] recommended the choice of $p_m \approx 0.01$, while Bäck [63] claimed that $p_m = 1/l$, where l is the length of the individual, is the most useful choice for unimodal functions. Adaptive mutation rates that change during the search process have also been proposed by Bäck [64]. We will be evaluating the effects of the value of p_m in the context of our specific optimisation problem in Chapter 3. Let us now highlight the effects of the mutation operation on a binary decision variable, which will be followed by a discourse on the mutation of a real-valued decision variable.

Mutation of binary decision variables

There are only two possible values for each binary decision variable hosted by an individual. Hence, when mutation is invoked for a particular bit, the value of the bit is toggled to the other possible value. For example, a bit of logical '1' is changed to a logical '0' and vice versa.

Mutation of real-valued decision variables

The mutation of real-valued decision variables [52] is slightly more complicated, since each decision variable can assume an infinite number of possible values. Due to the associated granularity of representing the individuals, it is impossible to obtain the exact value that conforms to the optimum solution. Hence we can only strive for achieving a value that is as close to the optimum value as possible.

When a decision variable x is picked for mutation, the direction of mutation is chosen randomly with equal probability. Then a real-valued *mutation size* Δ is randomly generated, whose value ranges between $[0, \Delta_{max}]$, where Δ_{max} is the maximum mutation range. This value is usually pre-determined, in order to ensure that the value of x after mutation does not exceed the maximum and minimum limits specified by the problem. The value of x is then increased or decreased accordingly by a magnitude prescribed by the mutation size as $x = x \pm \Delta$. The

mutation operation on real-valued decision variables will be further elaborated on in Section 4.3.3.

2.4.5 Elitism

We have mentioned in Section 2.3 that the crossover and mutation operations are capable of destroying a schema. This also implies that an individual associated with a high fitness value may be lost from one generation to the next. A good example of this scenario can be found by considering Table 2.1 and Table 2.2, which characterise the population before and after the crossover operation was invoked, respectively. Notice that the individual A_1 of Table 2.1, which has a corresponding fitness value of 9.06 did not appear in the new population of Table 2.2. While the individual A_1 will never qualify as the optimum solution, since the individual A'_2 was found to have an even higher fitness value, it should be given a chance to be exploited further, since it has the second highest fitness value so far.

Hence, in order to ensure that high-merit individuals are not lost from one generation to the next, the best or a few of the best individuals are included into the forthcoming generation, replacing the worst offspring of the new population. This technique is known as *elitism* [41]. Alternatively, the population can be simply extended by the additionally included best individual [31].

2.4.6 Termination Criterion

The exact structure of the search space is often unknown in optimisation problems. Hence in search algorithms, with the exception of an exhaustive search, it is typically infeasible to ensure that the optimum solution can be found. There are numerous ways of determining the termination criterion for GAs. The GA-assisted search can be terminated, if there are no further improvements in the maximum fitness value after several consecutive generations. In this case, the time required for the GA to reach a decision is uncertain. On the other hand, if the structure of the search space is time-invariant, then it is possible to set a threshold, such that the GA-assisted search is terminated, once the fitness value of an individual is found to exceed this threshold. Unfortunately neither of these termination criteria can be applied to GA-assisted CDMA multiuser detection, since typically a fixed implementational complexity is required and also the search space is time-variant due to the noise and fading imposed by the transmission channel. Hence in our application, we will terminate the GA-assisted search at the Yth generation and the individual associated with the highest fitness value at this point will be the detected solution.

Hence the value of Y must be carefully determined, in order to ensure that a high-probability solution is obtained. Furthermore, by specifying the exact number of generations, the computational complexity of the GA can be determined. In this case, the upper bound limit on the number of objective function evaluations is equivalent to $P \times Y$. This figure is derived by assuming that we calculate the fitness values of all the individuals in the population at every generation. If we can store the fitness values associated to each different individual in memory, then if identical individuals are created in the subsequent generations, their associated fitness values can be directly accessed from memory and do not need to be calculated again. This will lead to a significant reduction in the computational complexity.

2.5 Survey of Genetic Algorithm-Assisted CDMA Multiuser Detection

Despite establishing itself as a useful optimisation tool in numerous scientific as well as non-scientific applications, the employment of GAs in the area of mobile communications, especially at the physical layer, has been extremely scarce. There were only a handful of proposals in the current literature that invoked GAs in CDMA multiuser detection. Below we shall give a brief review of these proposals by outlining the GA configurations invoked.

The earliest notion of a GA-based CDMA multiuser detection scheme was suggested by Juntti, *et al.* [65] in 1997. In their contribution, the performance of the GA-based multiuser detector was studied by computer simulations based on a synchronous 20-user CDMA system. Random signature sequences with a spreading factor of 31 were used. The interfering users were assumed to have a power 3 dB higher than the desired user. It was not explicitly stated in the contribution as to which selection scheme was invoked nor the probability of mutation and the population size. The single-point crossover operation was used. Three different approaches of generating the initial population of individuals were simulated, which are as follows :

1. All the individuals of the initial population were randomly generated.
2. Some individuals of the initial population were randomly generated, while the remaining individuals were based on the hard decisions made at the output of the conventional matched filter detector.
3. Some individuals of the initial population were randomly generated, some were based on the hard decisions made by the conventional matched filter

detector, while the remaining individuals were based on the hard decisions made by the decorrelating detector.

A performance comparison was made between these three different approaches. While no results were explicitly shown, it was concluded that at high signal-to-noise ratios (SNRs), the bit error probability (BEP) associated with the first approach exhibited a residual value. On the other hand, if the initial population contains some good guesses of the likely solution, as provided by the hard decisions at the output of the matched filter or the decorrelating detector, then the performance of the GA-based multiuser detector is close to that of the single-user system. Hence, it was concluded that using GAs alone cannot provide a robust multiuser detection performance or a high near-far resistance.

In the following year, a GA-based multiuser detection scheme was proposed by Wang, *et al.* [66] for an asynchronous CDMA system communicating over an AWGN channel. The users' bits were detected sequentially in conjunction with a modified Viterbi algorithm. A so-called *window mapping* technique was invoked, in order to ensure that all legitimate solutions have positive fitness values. The fitness-proportionate selection scheme and the uniform crossover operation were used. Furthermore, the elitism strategy was employed for ensuring that some of the best individuals from the previous population are copied into the new population. As we have mentioned in Section 2.1, the population size and the rate of convergence, and therefore the computational complexity, is proportional to the size of the search space. Hence, in order to reduce the size of the search space, Wang, *et al.* used a threshold value for estimating the BEP based on its corresponding matched filter output. If the matched filter output is above the threshold value, then the corresponding bit can be directly determined based on the hard decision provided by its matched filter output. Consequently, this bit will not be involved in the GA optimisation. The performance of the GA-based multiuser detector was also compared against that of the decorrelating detector and the MMSE detector when supporting 20 users. The signature sequences were based on 31-chip Gold codes. A population size of 20 was used in the simulations and the GA was terminated after 6 generations. The probability of mutation was not explicitly stated. It was shown that the performance of the GA-based multiuser detector is very close to that of the MMSE detector and compares favourably with that of the decorrelating detector.

More recently, Ergün, *et al.* [67,68] proposed a hybrid approach that employs a GA and a Multi Stage Detector (MSD) for the multiuser detection, in order to mitigate the irreducible error floor imposed by conventional MSD detectors due to the high bit error rate typically associated with the first detection stage of suboptimal

methods, where these first-stage errors typically propagate through the subsequent stages. Three specific implementations were evaluated :

1. The GA was used for detection. The computational complexity per bit is $O(PY)$, where P and Y denote the population size and the number of generations, respectively.
2. The GA was used as the first stage of the MSD in order to provide a good initial point for the successive stages of the MSD. The computational complexity per bit is $O(K^2)$, where K is the number of users. This approach will be referred to using the acronym C-GA/MSD.
3. The MSD was embedded into the GA as a genetic operator in order to improve further the fitness of the population at each generation. The computational complexity per bit is $O(K^2) + PY \cdot O(K)$. This approach will be referred to using the acronym E-GA/MSD.

Again, the window mapping function was invoked, in order to ensure that the fitness values for all legitimate solutions are positive. The fitness-proportionate selection scheme was employed with a mating pool size of $T = P$, where P is the population size. A single-point crossover and the elitism strategy were also used. The probability of mutation was set to a value of 0.05. Simulations were performed for a 10-user CDMA system over an AWGN channel and Gold codes with a spreading factor of 15 were used as the signature sequences. Performance results were shown for both synchronous and asynchronous scenarios. In the synchronous case, the results showed that the E-GA/MSD converges to the optimum performance at an SNR of about 6dB after 7 generations for a population size of $P = 30$. On the other hand, the GA and C-GA/MSD techniques attained the optimum performance only after 50 generations. This leads to an excessive computational complexity. Furthermore, the E-GA/MSD approach is capable of achieving a near-optimal performance for all near-far ratios. In an asynchronous transmission scenario using a very short packet size of 4, it was shown that neither the GA nor the C-GA/MSD approaches attained the optimum performance, even after 50 generations for a population size of $P = 50$ at the SNR of 6 dB. On the other hand, the E-GA/MSD approach was capable of attaining the optimal performance after about 10 generations.

A summary of the GA configuration utilised in these proposals is listed in Table 2.3. Based on the limited number of proposals found in the literature, the general conclusion [65,67,68] was that multiuser detection based on GAs alone was not attractive due to its slow convergence, even when a high population size was invoked, and hence a high computational complexity was invested. In order to increase its convergence rate, it was proposed that other forms of detection ought

	Juntti, *et al.* [65]	Wang, *et al.* [66]	Ergün, *et al.* [67,68]
Selection method	Not specified	Fitness-proportionate	Fitness-proportionate
Crossover operation	Single-point	Uniform	Single-point
Mutation operation	Standard binary mutation		
Elitism	No	Yes	Yes
Incest prevention	No	No	No
Population size P	Not specified	20 for $K = 20$	30 for $K = 10$
Mating pool size T	Not specified	P	P
Probability of mutation p_m	Not specified	Small	0.05

Table 2.3: A summary of the configuration of the GA used in References [65–68] for the application in CDMA multiuser detection.

to be used in conjunction with the GA [67, 68]. The size of the search space was reduced by the proposition in [66]. Nevertheless, more research must be carried out, in order to establish the feasibility of GA-assisted multiuser detection schemes, which is the objective of this treatise. There was a different GA-assisted multiuser detection scheme that has been proposed recently by Abedi [69, 70], in which the optimum filter coefficients at the detector was acquired by the GA, in order to detect the users' transmitted bits. Due to its contrasting approach, this method will not be compared against our proposed GA-assisted scheme.

2.6 Chapter Summary and Conclusions

In this chapter we have presented a terse overview of GAs. Specifically, we introduced the terminologies and procedures of GAs in Section 2.1. We then proceeded with an example in Section 2.2, which demonstrated how a GA operates in practice. Section 2.3 augmented the rationale of using GAs by first identifying the resemblance between the way humans and GAs performed a search for the optimum solution. These discussions were followed by the derivation of the schema theorem, which is the fundamental theorem of GAs. Following that, we reviewed some of the more commonly used GA-based operations, such as selection schemes, crossover and mutation operations as well as implementation strategies in Section 2.4. Last but not least, a survey of the GA-based multiuser detection schemes found in the literature was conducted in Section 2.5.

GAs have been successfully applied in many function optimisation problems, as justified by the countless references found in the GA literature. It is this potential of the GAs in solving complex optimisation problems that provided the motivation for this dissertation.

Lastly, it should be stressed here that no GA configuration exists that is universally applicable to the solution of every optimisation problem. As seen in Section 2.4, there are many ways of implementing a GA, using different combinations of selection schemes, crossovers and mutation operations. There is no definite theoretical justification as to which combination gives the optimum performance, since different combinations work best for different problems. The best way of identifying the specific combination of operations that is most suitable for the problem at hand is to critically appraise and adapt these combinations on the problem. On this note, let us proceed with the applcation of GAs in the context of CDMA multiuser detection.

CHAPTER 3

Genetic Algorithm-Assisted Multiuser Detection for Synchronous CDMA Systems

3.1 Introduction

In this chapter, we will apply a GA-assisted scheme as a suboptimal multiuser detection technique in bit-synchronous CDMA systems over single-path Rayleigh fading channels. This provides a simple model for investigating the feasibility of applying GAs in CDMA multiuser detection as well as for determining the GA's configuration, in order to obtain a satisfactory performance. Based on the results obtained in this chapter, the GA-assisted CDMA multiuser detector will then be subsequently extended to an asynchronous system model incorporating multipath Rayleigh fading channels in Chapter 6.

This chapter is organised as follows. We will first highlight our system model used in this chapter in Section 3.2. The notations defined here will also be used in the subsequent chapters. An equivalent discrete-time system model is also highlighted in Section 3.3. We will then derive the optimum multiuser detector based on the Maximum Likelihood (ML) criterion for the system model adopted in this

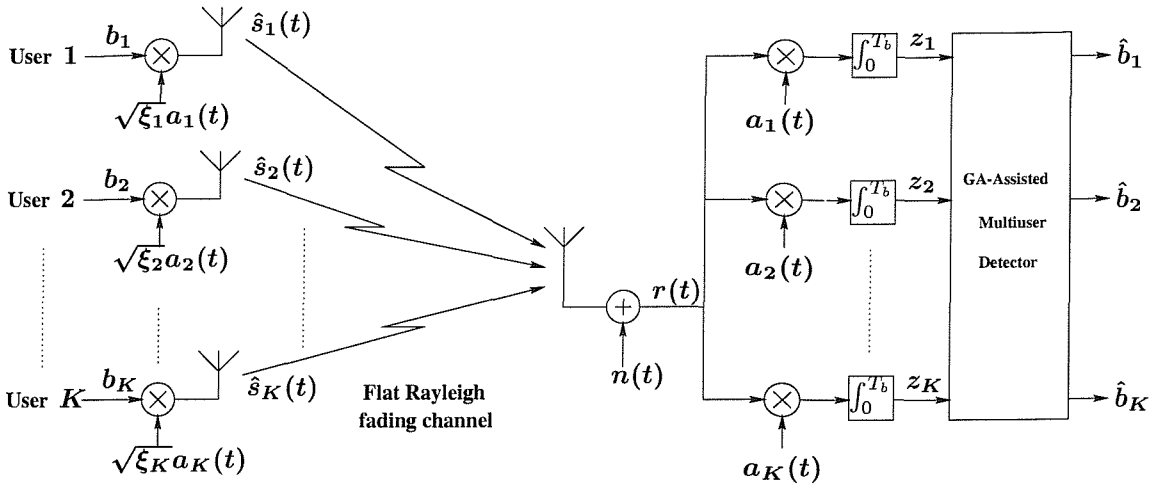

Figure 3.1: Block diagram of the K-user synchronous CDMA system model in a flat Rayleigh fading channel.

chapter in Section 3.4, which can be seen to have a computational complexity exponentially proportional to the number of users. GA-assisted multiuser detectors are then developed through a series of experiments, in order to find the GA configuration that is best suited for our application and the results will be shown in Section 3.5. Finally, using this GA configuration, the BEP performance of the GA-assisted multiuser detector based on our system model is assessed by simulations in Section 3.6. The summary of this chapter is given in Section 3.7. Before we commence our in-depth discourse, a few observations are made regarding our mathematical notations used in this dissertation. Vectors and matrices are represented in boldface, while $(\cdot)^T$ and $(\cdot)^*$ denote the transpose matrix and the conjugate matrix of $(\cdot)$, respectively. Hermitian matrices, defined as the complex conjugate transpose of the matrices, are denoted as $(\cdot)^H$. Furthermore, diag$(\cdot)$ represents a diagonal matrix, where the diagonal elements correspond to the vector $(\cdot)$. A summary of the mathematical notations used in this dissertation can be found in Appendix B.

3.2 Synchronous CDMA System Model

We consider a bit-synchronous CDMA system as illustrated in Figure 3.1, where K users simultaneously transmit data packets of equal length to a single receiver. In this dissertation we will adopt the Binary Phase Shift Keying (BPSK) modulation technique for all the transmissions. The transmitted signal of the kth user can be expressed in an equivalent lowpass representation as :

$$\hat{s}_k(t) = \sqrt{\xi_k} \sum_{m=0}^{M-1} b_k^{(m)} a_k(t - mT_b), \quad \forall k = 1, \ldots, K \tag{3.1}$$

where ξ_k is the kth user's signal energy per bit, $b_k^{(m)} \in \{+1, -1\}$ denotes the mth data bit of the kth user, $a_k(t)$ is the kth user's signature sequence, T_b is the data bit duration and M is the number of data bits transmitted in a packet. When considering a synchronous system experiencing no multipath interference, it is sufficient to observe the signal over a single bit duration T_b, since there is no interference inflicted by symbols outside this duration. Hence without loss of generality, we can omit the superscript (m) from all our equations in this chapter.

The kth user's signature sequence $a_k(t)$ may be written as :

$$a_k(t) = \sum_{h=0}^{N_c-1} a_k^{(h)} \Gamma_{T_c}(t - hT_c), \quad 0 \leq t < T_b, \quad \forall k = 1, \ldots, K \tag{3.2}$$

where T_c is the chip duration, $a_k^{(h)} \in \{+1, -1\}$ denotes the hth chip, N_c is the spreading factor, which refers to the number of chips per data bit duration T_b such that $N_c = T_b/T_c$ and $\Gamma_{T_c}(t)$ is the chip pulse shape. In practical applications, $\Gamma_\tau(t)$ has a bandlimited waveform, such as a raised cosine Nyquist pulse. However, for the sake of simplicity in our analysis and simulation, we will assume that $\Gamma_\tau(t)$ is a rectangular pulse throughout this dissertation, which is defined as :

$$\Gamma_\tau(t) = \begin{cases} 1, & 0 \leq t < \tau \\ 0, & \text{otherwise.} \end{cases} \tag{3.3}$$

Without loss of generality, we assume that the signature sequence $a_k(t)$ of all K users has unit energy, as given by :

$$\int_0^{T_b} a_k^2(t)dt = 1, \quad \forall k = 1, \ldots, K. \tag{3.4}$$

Each user's signal $\hat{s}_k(t)$ is assumed to propagate over a single-path frequency-nonselective slowly Rayleigh fading channel, as shown in Figure 3.1 and the fading of each path is statistically independent for all users. The complex lowpass channel impulse response (CIR) for the link between the kth user's transmitter and the receiver, as shown in Figure 3.1, can be written as :

$$h_k(t) = \alpha_k(t) e^{j\phi_k(t)} \delta(t), \quad \forall k = 1, \ldots, K \tag{3.5}$$

where the amplitude $\alpha_k(t)$ is a Rayleigh distributed random variable and the phase $\phi_k(t)$ is uniformly distributed between $[0, 2\pi)$.

Hence, when the kth user's spread spectrum signal $\hat{s}_k(t)$ given by Equation (3.1) propagates through a slowly Rayleigh fading channel having an impulse response

given by Equation (3.5), the resulting output signal $\hat{s}_k(t)$ over a single bit duration can be written as :

$$\hat{s}_k(t) = \sqrt{\xi_k}\alpha_k b_k a_k(t) e^{j\phi_k}, \quad \forall k = 1, \ldots, K \tag{3.6}$$

Upon combining Equation (3.6) for all K users, the received signal at the receiver, which is denoted by $r(t)$ in Figure 3.1, can be written as :

$$r(t) = \sum_{k=1}^{K} \hat{s}_k(t) + n(t), \tag{3.7}$$

where $n(t)$ is the zero-mean complex Additive White Gaussian Noise (AWGN) with independent real and imaginary components, each having a double-sided power spectral density of $\sigma^2 = N_0/2$ W/Hz.

At the receiver, the output of a bank of filters matched to the corresponding set of the users' signature sequences is sampled at the end of the bit interval. The output of the lth user's matched filter, denoted as z_l in Figure 3.1, can be written as :

$$\begin{aligned} z_l &= \int_0^{T_b} r(t) a_l(t) dt \\ &= \int_0^{T_b} \sum_{k=1}^{K} \sqrt{\xi_k}\alpha_k b_k a_k(t) e^{j\phi_k} a_l(t) dt + \int_0^{T_b} n(t) a_l(t) dt \\ &= \underbrace{\sqrt{\xi_l}\alpha_l b_l e^{j\phi_l}}_{\text{Desired signal}} + \underbrace{\sum_{\substack{k=1 \\ k\neq l}}^{K} \sqrt{\xi_k}\alpha_k b_k \rho_{lk} e^{j\phi_k}}_{\text{Multiple Access Interference}} + \underbrace{n_l}_{\text{Noise}}, \end{aligned} \tag{3.8}$$

where ρ_{lk} is the cross-correlation of the lth user's and the kth user's signature sequence, as given by :

$$\rho_{lk} = \int_0^{T_b} a_l(t) a_k(t) dt, \tag{3.9}$$

and

$$n_l = \int_0^{T_b} n(t) a_l(t) dt. \tag{3.10}$$

As seen in Equation (3.8), apart from the Gaussian noise n_l, the desired signal is interfered by signals transmitted by the other users. This interference due to the other users' signals is also known as Multiple Access Interference (MAI).

Assuming that the receiver has perfect knowledge of the lth user's CIR coefficients $\alpha_l e^{j\phi_l}$, the detected bit $\hat{b}_{l,MF}$ of the lth user based on the conventional coherent single-user detector will be given by the sign of the matched filter output

in Equation (3.8) as :

$$\hat{b}_{l,MF} = \text{sgn}\left[\Re\left(z_l \alpha_l e^{-j\phi_l}\right)\right]. \tag{3.11}$$

Multiplication by $\alpha_l e^{-j\phi_l}$ is necessary for coherent detection, because the phase rotation introduced by the channel has to be removed. By approximating the MAI as a Gaussian distributed random variable by virtue of the central limit theorem [71–73], the Bit Error Probability (BEP) of the desired user can be shown to be given by [22] :

$$P_l = \frac{1}{2}\left(1 - \sqrt{\frac{\xi_l}{N_0/2 + \sum_k \xi_k \rho_{lk}}}\right). \tag{3.12}$$

Hence from Equation (3.12), we can see that unless the signature sequences of the interfering users are orthogonal to that of the desired user, yielding $\rho_{lk} = 0$ for $k = 1, \ldots, K, k \neq l$, the BEP performance of the desired user will be inferior to that achieved in a single-user environment in conjunction with a single-user matched filter. Furthermore, since the BEP performance will deteriorate in conjunction with an increasing number of users, the conventional single-user detector is highly vulnerable to near-far effects [74].

3.3 Discrete-Time Synchronous CDMA Model

For our application, it is more convenient to express the associated signals in matrix and vectorial format. Invoking Equation (3.6) describing the transmitted signal of each user, the sum of the transmitted signals of all users can be expressed in vector notation as :

$$\begin{aligned} s(t) &= \sum_{k=1}^{K} \hat{s}_k(t) \\ &= \boldsymbol{a}\boldsymbol{C}\boldsymbol{\xi}\boldsymbol{b}, \end{aligned} \tag{3.13}$$

where

$$\begin{aligned} \boldsymbol{a} &= [a_1(t), \ldots, a_K(t)] \\ \boldsymbol{C} &= \text{diag}\left[\alpha_1 e^{j\phi_1}, \ldots, \alpha_K e^{j\phi_K}\right] \\ \boldsymbol{\xi} &= \text{diag}\left[\sqrt{\xi_1}, \ldots, \sqrt{\xi_K}\right] \\ \boldsymbol{b} &= [b_1, \ldots, b_K]^T. \end{aligned} \tag{3.14}$$

Hence the received signal of Equation (3.7) can be written as :

$$r(t) = s(t) + n(t). \tag{3.15}$$

Based on Equations (3.13) and (3.15), the output vector $\boldsymbol{Z}$ of the bank of matched filters portrayed in Figure 3.1 can be formulated as :

$$\begin{aligned} \boldsymbol{Z} &= [z_1, \ldots, z_K]^T \\ &= \boldsymbol{RC\xi b} + \boldsymbol{n}, \end{aligned} \tag{3.16}$$

where

$$\boldsymbol{R} = \begin{bmatrix} 1 & \rho_{12} & \cdots & \rho_{1K} \\ \rho_{21} & 1 & \cdots & \rho_{2K} \\ \vdots & \vdots & \vdots & \vdots \\ \rho_{K1} & \rho_{K2} & \cdots & 1 \end{bmatrix} \tag{3.17}$$

is the $K \times K$ dimensional user signature sequence cross-correlation matrix having elements given by Equation (3.9) and

$$\boldsymbol{n} = [n_1, \ldots, n_K]^T$$

is a zero-mean Gaussian noise vector with a covariance matrix $\boldsymbol{R}_n = 0.5N_0\boldsymbol{R}$. Based on this discrete-time model, we will next derive the optimum multiuser detector based on the maximum likelihood criterion for the synchronous CDMA system considered [1].

3.4 Optimum Multiuser Detector for Synchronous CDMA Systems

In this section we will derive the joint optimum decision rule for a K-user CDMA system based on the synchronous system model highlighted in Section 3.2. Specifically, we want to maximise the probability of jointly correct decisions of the K users supported by the system based on the received signal $r(t)$ of Equation (3.15).

¿From Equation (3.14) we note that there are $m = 2^K$ possible combinations of $\boldsymbol{b}$. We shall denote the ith combination as $\boldsymbol{b}_i$ and the combined transmit signal of all users in Equation (3.13) corresponding to the ith combination as $\boldsymbol{b}_i \leftrightarrow s_i(t)$.

Based on the above notations, we can express the joint maximum *a posteriori* probability (MAP) criterion as [75] :

$$\hat{\boldsymbol{b}} = \arg\left\{\max_{\boldsymbol{b}_i}\left[P\left(s_i(t)|r(t)\right)\right]\right\}, \tag{3.18}$$

where $\hat{\boldsymbol{b}}$ denotes the detected bit combination. According to Equation (3.18), the MAP criterion refers to finding the specific transmitted bit sequence $\boldsymbol{b}_i$ that exhibits the highest probability of being transmitted given the received signal $r(t)$.

Using Bayes' rule, the *a posteriori* probability expression of Equation (3.18) can be written as [75] :

$$P\left(s_i(t)|r(t)\right) = \frac{p\left(r(t)|s_i(t)\right)P(s_i(t))}{p(r(t))}, \tag{3.19}$$

where $p\left(r(t)|s_i(t)\right)$ is the conditional joint probability density function (pdf) of the received signal $r(t)$ in Equation (3.15), $P(s_i(t))$ is the *a priori* probability of the signal containing the ith bit combination and $p(r(t))$ is the pdf of the received signal. Since the transmitted data bits of the K users are independent, the *a priori* probability $P(s_i(t)) = 1/2^K$ is equal for all $m = 2^K$ bit combinations. Furthermore, the received signal pdf $p(r(t))$ is independent of which of the $m = 2^K$ bit combinations is transmitted. Consequently, the decision rule based on finding the signal that maximises $P\left(s_i(t)|r(t)\right)$ is equivalent to finding the signal that maximises $p(r(t)|s_i(t))$. This decision criterion, which is based on the maximum of $p(r(t)|s_i(t))$ is termed as the Maximum Likelihood (ML) criterion and $p(r(t)|s_i(t))$ is referred to as a *likelihood function* [75]. Hence, in contrast to the MAP criterion of Equation (3.18), the ML criterion evaluates the probability of the received signal $r(t)$ given the transmitted signal $s_i(t)$.

According to Equation (3.7), the received signal $r(t)$ is a Gaussian distributed random variable having a mean equal to that of $s(t)$ given by Equation (3.13). Hence, it can be shown that the likelihood function $p(r(t)|s_i(t))$ is given by [22] :

$$\begin{aligned} p(\boldsymbol{Z}|\boldsymbol{s}) &= \exp\left(-\frac{1}{2\sigma^2}\int_0^{T_b}\left|r(t)-s(t)\right|^2 dt\right) \\ &= \exp\left(-\frac{1}{2\sigma^2}\int_0^{T_b}\left|r(t)-\sum_{k=1}^{K}\sqrt{\xi_k}\alpha_k b_k a_k(t)e^{j\phi_k}\right|^2 dt\right). \end{aligned} \tag{3.20}$$

Taking the natural logarithm of the likelihood function of Equation (3.20), the resulting so-called *Log-Likelihood Function* (LLF) can be written as :

$$\begin{aligned}\ln p(\boldsymbol{Z}|\boldsymbol{s}) &= -\frac{1}{2\sigma^2}\left\{\int_0^{T_b}|r(t)|^2\,dt+\int_0^{T_b}\left|\sum_{k=1}^{K}\sqrt{\xi_k}\alpha_k b_k a_k(t)e^{j\phi_k}\right|^2 dt\right.\\ &\quad\left.-2\Re\left[\int_0^{T_b} r(t)\sum_{k=1}^{K}\sqrt{\xi_k}\alpha_k b_k a_k(t)e^{-j\phi_k}dt\right]\right\}. \qquad (3.21)\end{aligned}$$

The term $|r(t)|^2$ is common to all decision metrics, and hence it can be ignored during the optimisation. Similarly, the constant term $1/2\sigma^2$ will not influence the maximisation. Thus we can express the log-likelihood function of Equation (3.21) in the form of a correlation metric as [75] :

$$\begin{aligned}\Omega(\boldsymbol{b}) &= 2\Re\left[\int_0^{T_b} r(t)\sum_{k=1}^{K}\sqrt{\xi_k}\alpha_k b_k a_k(t)e^{-j\phi_k}dt\right]-\int_0^{T_b}\left|\sum_{k=1}^{K}\sqrt{\xi_k}\alpha_k b_k a_k(t)e^{j\phi_k}\right|^2 dt\\ &= 2\Re\left[\sum_{k=1}^{K}\sqrt{\xi_k}\alpha_k b_k e^{-j\phi_k}z_k\right]-\sum_{l=1}^{K}\sum_{k=1}^{K}\sqrt{\xi_l\xi_k}b_l b_k\alpha_l\alpha_k e^{j\phi_l}e^{-j\phi_k}\rho_{lk}, \qquad (3.22)\end{aligned}$$

where z_k and ρ_{lk} are given by Equation (3.8) and Equation (3.9), respectively. Employing our discrete-time model highlighted in Section 3.3, the correlation metric of Equation (3.22) can be expressed in vector notation as [22] :

$$\Omega(\boldsymbol{b}) = 2\Re\left[\boldsymbol{b}^T\boldsymbol{\xi}\boldsymbol{C}^*\boldsymbol{Z}\right]-\boldsymbol{b}^T\boldsymbol{\xi}\boldsymbol{C}\boldsymbol{R}\boldsymbol{C}^*\boldsymbol{\xi}\boldsymbol{b}. \qquad (3.23)$$

Hence the decision rule for the Verdu's optimum CDMA multiuser detection scheme [1] based on the maximum likelihood criterion is to choose the specific bit combination $\boldsymbol{b}$, which maximises the correlation metric of Equation (3.23). Hence,

$$\hat{\boldsymbol{b}} = \arg\left\{\max_{\boldsymbol{b}}\left[\Omega(\boldsymbol{b})\right]\right\}. \qquad (3.24)$$

In recent years Minimum Bit Error Rate (MBER) multiuser detection [76] has emerged as a new research direction and the research of MBER GA-based MUDs may constitute a promising future research area. The maximisation of Equation (3.23) is a combinatorial optimisation problem, which requires an exhaustive search for each of the $m = 2^K$ combination of $\boldsymbol{b}$, in order to find the one that maximises the correlation metric of Equation (3.23). Explicitly, since there are $m = 2^K$ possible combinations of $\boldsymbol{b}$, the optimum multiuser detection has a complexity that grows exponentially with the number of users K.

We have mentioned in Chapter 2 that GAs have been known to solve combinatorial optimisation problems efficiently in many other applications [31]. Hence, in this dissertation, we will investigate the feasibility of invoking GAs in dealing with the CDMA multiuser detection optimisation problem as governed by Equation (3.23).

3.5 Experimental Results

As we have mentioned in Section 2.1 of Chapter 2, a GA's performance is dependent on numerous factors, such as the population size P, the choice of the selection method, the genetic operation employed, the specific parameter settings as well as the particular termination criterion used. In this section, we will attempt to find an appropriate GA setup and parameter configurations that are best suited for our optimisation problem.

Our objective function is defined by the correlation metric of Equation (3.23). Here, the legitimate solutions are the $m = 2^K$ possible combinations of the K-bit vector $\boldsymbol{b}$. Hence, each individual will take the form of a K-bit vector corresponding to the K users' bits during a single bit interval. We will denote the pth individual here as $\tilde{\boldsymbol{b}}_p(y) = \left[\tilde{b}_{p,1}(y), \ldots, \tilde{b}_{p,K}(y)\right]$, where y denotes the yth generation. Our goal is to find the specific individual that corresponds to the highest fitness value. However, we note that the fitness values corresponding to certain combinations of $\boldsymbol{b}$ evaluated from the correlation metric of Equation (3.23) will be negative. However, we have mentioned in Section 2.4.2 that some selection schemes can only operate with the aid of positive fitness values. Hence, in order to ensure that the fitness values are positive for all combinations of $\boldsymbol{b}$, we modify the correlation metric of Equation (3.23) according to [65] :

$$\exp\left\{\Omega\left(\boldsymbol{b}\right)\right\} = \exp\left\{2\Re\left[\boldsymbol{b}^T\boldsymbol{\xi}\boldsymbol{C}^*\boldsymbol{Z}\right] - \boldsymbol{b}^T\boldsymbol{\xi}\boldsymbol{C}\boldsymbol{R}\boldsymbol{C}^*\boldsymbol{\xi}\boldsymbol{b}\right\}. \tag{3.25}$$

The reason for invoking an exponential mapping function is to put more emphasis on the high-merit individuals such that they will be assigned a much higher selection probability as compared to the low-merit individuals. This will ensure a faster convergence rate, but runs the risk of a premature convergence. Increasing the mutation rate can alleviate this problem, as we shall see in Section 3.5.3.

Our performance metric is the average Bit Error Probability (BEP) evaluated over the course of several generations. In the context of CDMA multiuser detection the three most important criteria to be satisfied by an efficient detection scheme are its BEP performance, its detection time as well as its computational complexity.

Parameter	Value
Spreading factor N_c	31
Modulation mode	BPSK
Number of CDMA users, K	10 (20 for Figure 3.4)
SNR per bit ξ_k/N_0	9 dB for $k = 1, \ldots, K$

Table 3.1: Simulation parameters for the experiments of Figures 3.2-3.9.

The detection time of the GA is governed by the number of generations Y required, in order to obtain a reliable decision. We also mentioned in Section 2.4.6 that the computational complexity of the GA, in the context of the total number of objective function evaluations, is related to $P \times Y$. On the other hand, it is well-known that the convergence accuracy of the GA is mainly determined by the population size P, as alluded to in Section 2.1. Hence, in this section the purpose of our study is to find GA configurations that achieve a satisfactory BEP performance at the expense of an acceptable computational complexity within a reasonable time. Since our GA-assisted multiuser detector is based on optimising the modified correlation metric of Equation (3.25), the computational complexity is deemed to be acceptable, if there is a significant amount of reduction in comparison to the optimum multiuser detector, which requires $m = 2^K$ objective function evaluations, in order to reach a decision, as highlighted in Section 3.4. In order to evaluate the average BEP performance of the GA-assisted multiuser detectors, randomly generated signature sequences will be used in our simulations. The simulation parameters used for our investigations in this section are presented in Table 3.1 and the following assumptions are stipulated :

- We will assume that perfect power control is invoked by all users such that, on average, their signals arrive at the receiver with the same power.
- Initially only the AWGN channel is invoked, such that $\alpha_k = 1.0$ and $\phi_k = 0$ for $k = 1, \ldots, K$, i.e. there is no fading.

3.5.1 Simulation Algorithm

Due to the random nature of the GAs, several random seeds have to be utilised in our simulation program, in order to obtain a reliable average BEP result. Specifically, for a particular SNR value, our simulation program will repeatedly transmit a random set of bits at a given channel condition and then detect the received bits using the proposed GA-assisted detection scheme. The detected bits are then checked against the transmitted bits, until a certain criterion is satisfied. Specifically, simulations were conducted until 100-1000 detection errors were found. Hence

Setup/Parameter	Method/Value
Individual initialisation method	Random
Selection method	Fitness-Proportionate
Crossover operation	Single-point
Mutation operation	Standard binary mutation
Elitism	No
Incest Prevention	No
Population size P	Given in Figure 3.2
Mating pool size T	Population size P
Probability of mutation p_m	0.01

Table 3.2: Configuration of the GA used to obtain the results of Figure 3.2. Explicit description of the fitness-proportionate selection scheme and the single-point crossover operation can be found in Section 2.4.2 and Section 2.4.3, respectively.

assuming for example that the BEP is about 10^{-3} and the stop-criterion is set to finding 100 detection errors, $100/10^{-3} = 100,000$ bits would have to be transmitted and hence the simulation program would have to be run $k/10^{-3} = 100,000$ number of times for detecting all the bits of the k users. Each time the simulation program is activated, a new set of user bits and signature sequences are generated and the bits are transmitted over an independently generated dispersive or non-dispersive Rayleigh-fading channel, adding independent AWGN components. At the detector, the seeds required for generating the random processes of the GAs during the initialisation, crossover and mutation processes would be different from those used during the transmission of the previous bits, again, with each process having an independent seed. As a result, the various random processes are independent from each other and if the simulation program is activated a sufficiently high number of times, a reliable average BEP performance is obtained.

3.5.2 Effects of the Population Size

Let us commence our experiments by investigating the effects of the population size P on the convergence rate of the GA. Since at this moment we have no knowledge of which configuration of the GA is best suited for our optimisation problem, we shall adopt the most commonly used GA configuration found in the literature for our initial simulations. This configuration is tabulated in Table 3.2, which follows the flowchart of Figure 2.1. Basically, the individuals, which represent the candidate solutions of $\boldsymbol{b}$, are randomly created during the initialisation phase of the GA. Upon evaluating their associated fitness values based on the modified objective function of Equation (3.25), pairs of individuals found in the mating pool are selected for

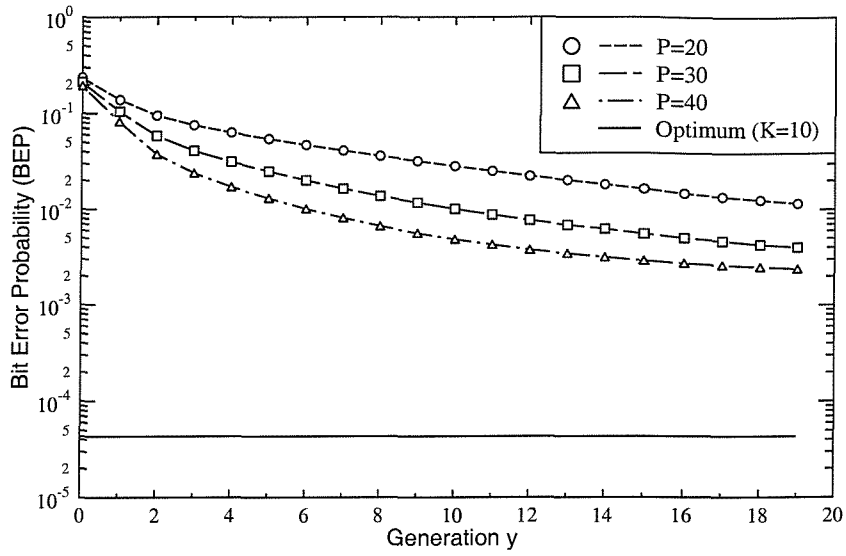

Figure 3.2: The bit error probability performance with respect to the number of generations of the GA-assisted multiuser detector for various population sizes and $K = 10$ users. The configuration of the GA used to obtain these results is tabulated in Table 3.2, while the simulation parameters are listed in Table 3.1.

crossover and mutation operations, in order to produce offspring. The associated fitness values of these offspring are then evaluated and these offspring will form the new population of the next generation. The processes of selection, crossover, mutation and evaluation are repeated for a total of $Y - 1$ generations[1]. Based on this configuration, the BEP performance of the GA-assisted multiuser detector was evaluated and the results, which showed the achievable BEP at the end of each generation are displayed in Figure 3.2. Note that the BEP at each generation, with the exception of the 0th generation, is derived by identifying the offspring associated with the highest fitness value amongst all the offspring created at that generation. The BEP at the 0th generation is derived by identifying the specific individual that exhibits the highest fitness value after the random initialisation. It is seen from the figure that the BEP performance of the GA-assisted multiuser detector improved with increasing the population size. However, the computational cost also increases as a function of the population size, as highlighted in Section 2.4.6. In order to maintain a moderate computational complexity, we shall adopt a fixed population size of $P = 30$ for all our simulations in this section. Upon closer inspection of Figure 3.2, we will notice that the BEP performance of the GA-assisted

[1]The 0th generation only consists of initialisation and evaluation.

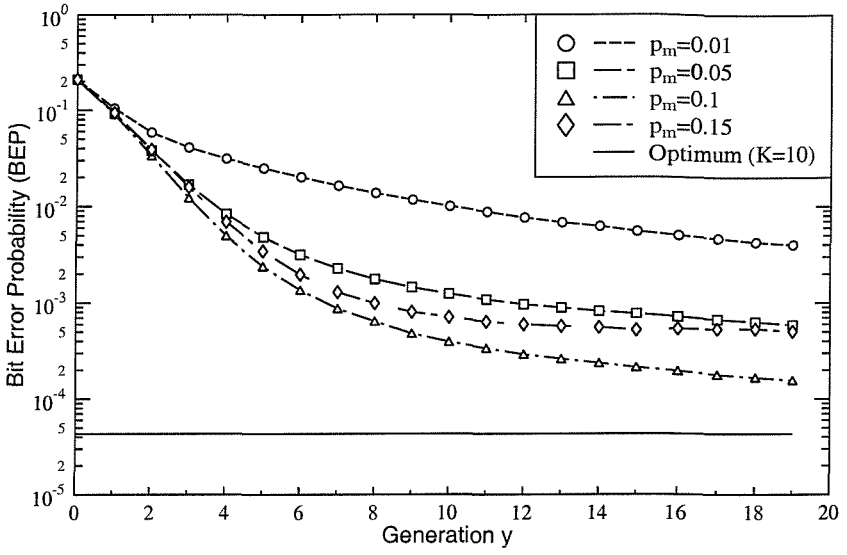

Figure 3.3: The bit error probability performance with respect to the number of generations of the GA-assisted multiuser detector for various probability of mutation values p_m and for $K = 10$ users. The configuration of the GA is specified in Table 3.3, while the simulation parameters are listed in Table 3.1.

multiuser detector based on the configuration of Table 3.2 is far from promising. Furthermore, the convergence rate of the GA is very slow. Let us now study whether the performance can be improved by varying some of the GA parameters and the GA configuration, commencing with the probability of mutation.

3.5.3 Effects of the Probability of Mutation

As we have mentioned in Section 2.4.4, the rate of mutation plays an important role in determining the quality of convergence of a GA. A high probability of mutation p_m may disrupt schemata of potentially high fitness values and hence may lead to suboptimal solutions, while a low probability of mutation may result in premature convergence due to the lack of diversity in the population. This assertion is supported by Figure 3.3, which shows the achievable BEP performance of the GA-assisted multiuser detector over $Y = 20$ generations for various values of p_m. The configuration of the GA implemented for this simulation study is listed in Table 3.3, which is similar to the one given in Table 3.2 of Section 3.5.2. Considering the results shown in Figure 3.3, we will immediately notice that the BEP performance has improved significantly over the rather poor results obtained in the previous section for $p_m > 0.01$. Furthermore, according to Figure 3.3, $p_m = 0.1$

Setup/Parameter	Method/Value
Individual initialisation method	Random
Selection method	Fitness-Proportionate
Crossover operation	Single-point
Mutation operation	Standard binary mutation
Elitism	No
Incest Prevention	No
Population size P	30
Mating pool size T	Population size P
Probability of mutation p_m	Given in Figure 3.3 and Figure 3.4.

Table 3.3: Configuration of the GA used to obtain the results of Figures 3.3 and 3.4. Explicit description of the fitness-proportionate selection scheme and the single-point crossover operation can be found in Section 2.4.2 and Section 2.4.3, respectively.

appears to give the best performance. All the other values of p_m have a slower convergence rate, leading to solutions far from the optimal one. Although this contradicts the conventional recommendation that the value of p_m should be in the region of 0.01-0.001, a high p_m value was found advantageous in our case because, since we have mentioned previously that our exponential mapping scheme favours the high-merit individuals, which can lead to premature convergence due to a lack of diversity. Hence a high p_m value can provide this diversity. On the other hand, excessive mutation can also lead to a slow convergence because of the birth of too many low-merit individuals. Hence according to Figure 3.3, the scheme associated with $p_m = 0.15$ does not converge as fast as that using $p_m = 0.1$. Furthermore, the value of p_m is very much dependent on the length of the individual, as exemplified in Figure 3.4 for $K = 20$ users. Here, each individual will consist of a $K = 20$-bit multi-user vector to be optimised. In this case, $p_m = 0.07$ gives the best performance[2]. Since our simulations performed in this dissertation are based on a CDMA system supporting $K = 10 - 20$ users, we will adopt a probability of mutation $p_m = 0.1$ for all our subsequent simulations, since this value was shown in Figures 3.3 and 3.4 to give a good BEP performance for this user population range. However, further investigations concerning the suitable value of p_m must be performed for a higher number of users. Let us now consider, whether we can further improve the achievable BEP performance by using different crossover operations.

[2]The poor BEP shown in Figure 3.4 is due to the inadequate population size in handling a sizeable search space for $K = 20$.

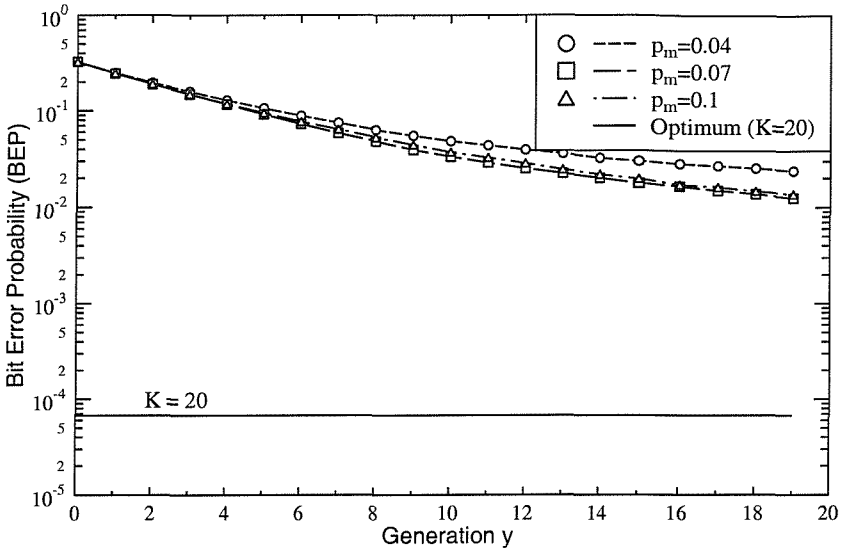

Figure 3.4: The bit error probability performance with respect to the number of generations of the GA-assisted multiuser detector for various probability of mutation values p_m and for $K = 20$ users. The configuration of the GA is specified in Table 3.3, while the simulation parameters are listed in Table 3.1.

3.5.4 Effects of the Choice of Crossover Operation

In this section, we will investigate, whether the choice of the crossover operation will have an effect on the convergence rate of the GA. Three types of crossover operations are investigated, namely the single-point crossover, the double-point crossover and the uniform crossover, which were highlighted in Section 2.4.3. The configuration of the GA is characterised by Table 3.4 and the associated results are shown in Figure 3.5. Judging from the results displayed in Figure 3.5, there is no significant performance disparity amongst the different crossover operations. Nonetheless, the GA employing the uniform crossover can be seen to exhibit a slightly faster convergence rate, than that using the single-point and double-point crossover. This may be due to the fact that for the uniform crossover operation, every bit of the individual has an equal probability of being exchanged, unlike in the single-point crossover or the double-point crossover, where the leftmost and the rightmost bits have a lower probability of being exchanged. Hence, we shall be adopting the uniform crossover operation for all our subsequent simulations.

Setup/Parameter	Method/Value
Individual initialisation method	Random
Selection method	Fitness-Proportionate
Crossover operation	Given in Figure 3.5
Mutation operation	Standard binary mutation
Elitism	No
Incest Prevention	No
Population size P	30
Mating pool size T	Population size P
Probability of mutation p_m	0.1

Table 3.4: Configuration of the GA used to obtain the results of Figure 3.5. Explicit description of the fitness-proportionate selection scheme and the various crossover operations can be found in Section 2.4.2 and Section 2.4.3, respectively.

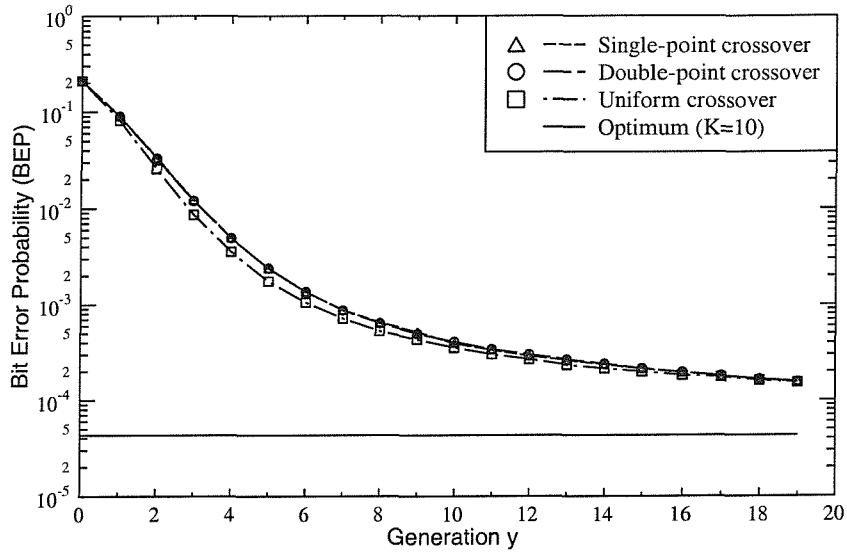

Figure 3.5: The bit error probability performance with respect to the number of generations of the GA-assisted multiuser detector employing the single-point crossover, double-point crossover and the uniform crossover for $K = 10$ users. The configuration of the GA is specified in Table 3.4, while the simulation parameters are listed in Table 3.1.

3.5.5 Effects of Incest Prevention and Elitism

Let us now investigate the effects of invoking the incest prevention and the elitism strategy, as featured in Section 2.4. In the case of the incest prevention strategy, we will ensure that the individuals in the mating pool are not identical. Hence, the mating pool size $T \leq P$ will not be fixed, because it depends on the number of non-identical individuals in the population. As for the elitism strategy, we will only replace the offspring having the lowest fitness value in the new population with the individual corresponding to the highest fitness value in the old population. The configuration of the GA for this investigation is specified by Table 3.5 and the associated results are shown in Figure 3.6. A welcome improvement that can be gleaned from Figure 3.6 is that the GA-assisted multiuser detector has finally managed to achieve the optimum performance for $K = 10$, based on the configuration of Table 3.5 in conjunction with the incest prevention and elitism strategies. Furthermore, we can see that the optimum performance is attained only, if both strategies are invoked. This can be explained as follows. Firstly, the incest prevention strategy will always ensure that a high diversity of individuals is maintained in the population, since only non-identical individuals are allowed to mate. Hence, the offspring that are produced by the crossover and mutation operations will have a high probability that they are not identical to their parents. This will ensure that new areas in the search space will be explored, which is always a good trait from an optimisation point of view. On the other hand, this will also obliterate the parents associated with high fitness values, since the offspring will constitute the new population. This is undesirable especially, if the parent is actually the optimum solution. Hence the elitism strategy can be invoked in order to counteract this effect. Since in our optimisation problem we are interested in finding only one specific individual that gives the highest fitness value and not a set of likely individuals, the elitism strategy is required to keep track of the individual having the highest fitness value found during the course of evolution. Hence by combining these two strategies, a fast convergence rate and a good performance can be achieved. Now that we know that the GA-assisted multiuser detector is capable of attaining the optimum performance within 20 generations, as shown in Figure 3.6, let us now consider, whether the detector is capable of achieving this level of performance at a faster convergence rate by invoking various selection schemes.

Setup/Parameter	Method/Value
Individual initialisation method	Random
Selection method	Fitness-Proportionate
Crossover operation	Uniform
Mutation operation	Standard binary mutation
Elitism	Given in Figure 3.6
Incest Prevention	Given in Figure 3.6
Population size P	30
Mating pool size T	– Population size P if incest prevention is not invoked – $\leq P$ if incest prevention is invoked
Probability of mutation p_m	0.1

Table 3.5: Configuration of the GA used to obtain the results of Figure 3.6. Explicit description of the fitness-proportionate selection scheme and the incest prevention strategy can be found in Section 2.4.2 while the uniform crossover operation and the elitism strategy can be found in Section 2.4.3 and Section 2.4.5, respectively.

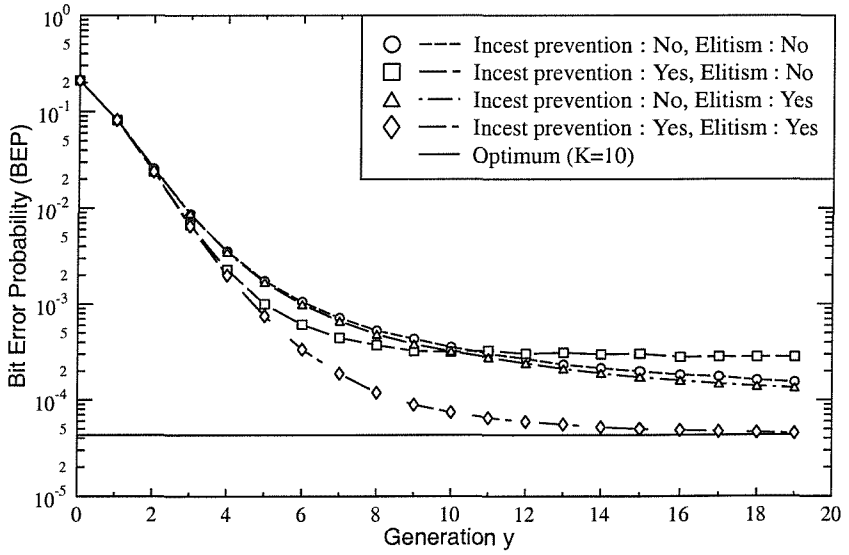

Figure 3.6: The bit error probability performance with respect to the number of generations of the GA-assisted multiuser detector employing the incest prevention strategy and/or elitism strategy, as featured in Section 2.4. The configuration of the GA is specified in Table 3.5, while the simulation parameters are listed in Table 3.1 for $K = 10$ users.

Setup/Parameter	Method/Value
Individual initialisation method	Random
Selection method	Given in Figure 3.7
Crossover operation	Uniform crossover
Mutation operation	Standard binary mutation
Elitism	Yes
Incest Prevention	Yes
Population size P	30
Mating pool size T	$T \leq P$ depending on the total number of non-identical individuals
Probability of mutation p_m	0.1

Table 3.6: Configuration of the GA used to obtain the results of Figure 3.7. Explicit description of the various selection schemes and the uniform crossover operation can be found in Section 2.4.2 and Section 2.4.3, respectively.

3.5.6 Effects of the Choice of Selection Schemes

In this section, we will attempt to identify the specific selection scheme for our GA-assisted multiuser detector that is capable of offering a fast convergence rate, while maintaining the same level of BEP performance that was attained in Figure 3.6. The selection schemes that were reviewed in Section 2.4.2, namely the fitness-proportionate selection, the sigma scaling selection, the linear ranking selection and the tournament selection, will be investigated. The configuration of the GA is listed in Table 3.6. For the linear ranking selection scheme, we set η^+ and η^- in Equation (2.11) to 1.9 and 0.1, respectively so as to place a higher emphasis on the individuals exhibiting higher fitness values. As for the tournament selection scheme, $t = 5$ individuals are selected from the population randomly with equal probability and the individual that corresponds to the highest fitness value within this group of t individuals will be chosen as a parent. Finally, for sigma scaling selection, if the probabability of selection p_i corresponding to the ith individual is a negative value when calculated according to Equation (2.10), then we will set this p_i value to 0.0 and discard the associated individual from the selection process. The BEP results are shown in Figure 3.7.

As we can see, GAs utilising the fitness-proportionate selection scheme gave the best performance. On the other hand, GAs using either the sigma scaling selection scheme or the linear ranking selection scheme exhibited a slow convergence rate. A plausible explanation is due to the fact that the mating pool size T spanned over all non-identical individuals. Hence the fitness value variance of the mating pool was high. As a result, individuals having high fitness values are not given sufficient

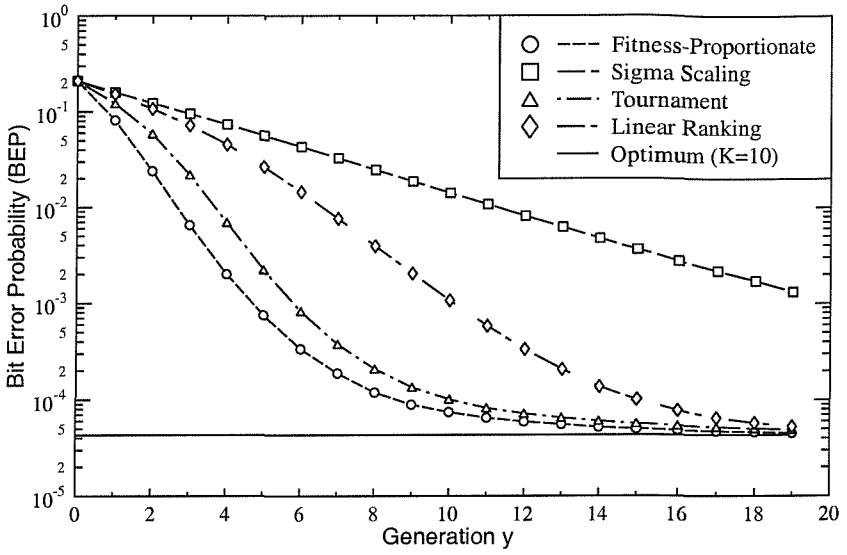

Figure 3.7: The bit error probability performance with respect to the number of generations of the GA-assisted multiuser detector employing various selection schemes. The configuration of the GA is specified in Table 3.6, while the simulation parameters are listed in Table 3.1 for $K = 10$ users.

priority to be selected as a parent in the case of the sigma scaling selection. Similarly, because of the linearity of Equation (2.11), the higher-rank individuals are not assigned with a high probability of selection. Another interesting point to note from Figure 3.7 is that the linear ranking selection scheme, which is independent of the type of mapping function used to ensure that all fitness values are positive, has a slower convergence rate than that of the fitness-proportionate selection scheme. This is due to the fact that insufficient emphasis is placed on the high-merit individuals, if the individuals in the population are ranked. Hence our decision of invoking an exponential mapping function is a plausible one, if fast convergence is of prime importance.

A feasible way of overcoming the slow convergence of the sigma scaling and linear ranking based selection schemes is to reduce the size T of the mating pool, such that we have $T \ll P$. This implies that only the $T \ll P$ number of non-identical individuals that are associated with the highest fitness values in the current population will be placed in the mating pool. If the number of non-identical individuals in the population happens to be less than T, then the value of T is set to be equivalent to the number of available non-identical individuals, in order to prevent incest mating. We set $T = 10$ and when using the GA configuration given by Table 3.7, the corresponding simulation results are shown in Figure 3.8. Now we can see that

Setup/Parameter	Method/Value
Individual initialisation method	Random
Selection method	Given in Figure 3.8
Crossover operation	Uniform crossover
Mutation operation	Standard binary mutation
Elitism	Yes
Incest Prevention	Yes
Population size P	30
Mating pool size T	$T \leq 10$ depending on the number of non-identical individuals
Probability of mutation p_m	0.1

Table 3.7: Configuration of the GA used to obtain the results of Figure 3.8. Explicit description of the various selection schemes and the uniform crossover operation can be found in Section 2.4.2 and Section 2.4.3, respectively.

the achievable BEP performance of the GAs employing either the sigma scaling selection scheme or the linear ranking selection scheme has improved significantly. In particular, the GA-assited MUD employing the sigma scaling selection scheme has an almost identical performance to that using the fitness-proportionate selection scheme. From these results we conclude that the mating pool size T plays a significant part in determining the convergence rate of the GA using a particular type of selection scheme. More specifically, for the sigma scaling selection and the linear ranking selection the value of T must be set appropriately. We also have to determine the best value of t for the tournament selection scheme. On the other hand, the results obtained in Figure 3.8 for the fitness-proportionate selection scheme are similar to those shown in Figure 3.7, where no specific mating pool size T constraint was imposed, using T equal to the number of non-identical individuals in the population during the particular generation. Furthermore, the fitness-proportionate selection scheme does not involve any external parameters for it to work and judging from Figure 3.7 and Figure 3.8, GAs utilising the fitness-proportionate selection scheme gave the best performance from the range of selection schemes considered. Hence, in order to reduce the number of parameters to be optimised for the GAs to perform reliably, we will only consider the fitness-proportionate selection scheme hereafter. In most cases, the mating pool size T will also be set according to the number of non-identical individuals in the population. However, as we will see in our further discourse, there are certain situations, where a specific value of T must be set, in particular, when the population contains many non-identical individuals.

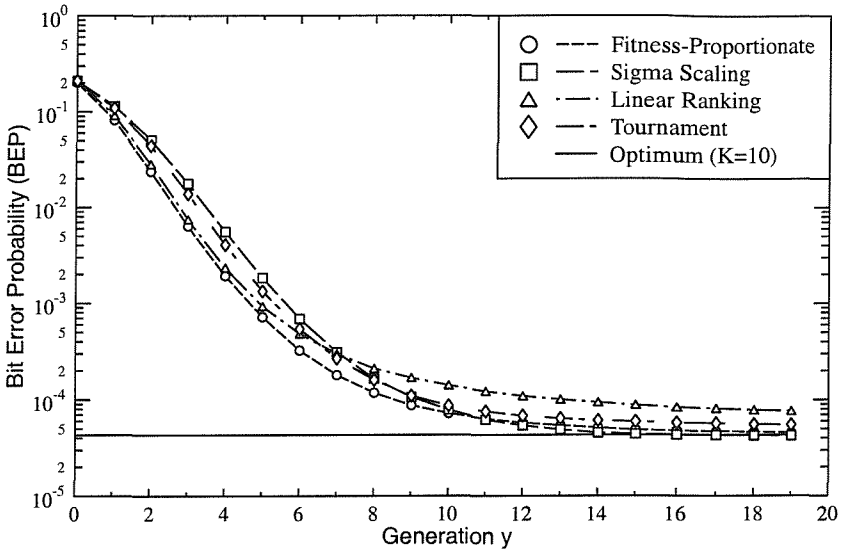

Figure 3.8: The bit error probability performance with respect to the number of generations of the GA-assisted multiuser detector employing various selection schemes. The configuration of the GA is specified in Table 3.7, while the simulation parameters are listed in Table 3.1.

3.5.7 Effects of a Biased Generated Population

In Section 2.1, we mentioned that instead of randomly creating the initial population of individuals at the commencement of a GA-assisted search, we can invoke any useful information that is available to aid us in creating the initial population of individuals, in order to aid our search at the beginning. In our case, we can use the hard decisions offered by the matched filter outputs $\boldsymbol{Z}$ of Equation (3.16), in order to aid our search. We shall denote these hard decisions here as :

$$\hat{\boldsymbol{b}}_{MF} = \left[\hat{b}_{1,MF}, \hat{b}_{2,MF}, \ldots, \hat{b}_{K,MF}\right] \tag{3.26}$$

where $\hat{b}_{k,MF}$ for $k = 1, \ldots, K$ is given by Equation (3.11). Two methods of biasing are proposed for our investigations. Firstly, we will assign the hard decisions of Equation (3.26) to only one individual. The remaining $P - 1$ individuals will be randomly generated. This will ensure that a high diversity of individuals are present in the population at the beginning. We shall refer to this method as M1. For our second method, we will assign a different randomly 'mutated' version of the hard decision vector $\hat{\boldsymbol{b}}_{MF}$ of Equation (3.26) to each of the individuals in the initial population. We shall adopt the same probability of mutation as p_m. In this way, the individuals in the initial population will be almost identical. Note that we

Setup/Parameter	Method/Value
Individual initialisation method	Given in Figure 3.9
Selection method	Fitness-proportionate
Crossover operation	Uniform crossover
Mutation operation	Standard binary mutation
Elitism	Yes
Incest Prevention	Yes
Population size P	30
Mating pool size T	$T \leq P$ depending on the number of non-identical individuals
Probability of mutation p_m	0.1

Table 3.8: Configuration of the GA used to obtain the results of Figure 3.9. Explicit description of the fitness-proportionate selection scheme and the uniform crossover operation can be found in Section 2.4.2 and Section 2.4.3, respectively.

cannot assign the same hard decision vector $\hat{\boldsymbol{b}}_{MF}$ to all the individuals, since incest prevention is invoked, which will not allow identical individuals to mate. We shall refer to this method as M2. Using the GA configuration listed in Table 3.8, the simulation results are shown in Figure 3.9. As the figure suggests, method M2 gives a better performance in terms of a faster convergence rate due to a good initial population of individuals. This fact conforms to the results obtained in [65]. Hence we shall adopt method M2 of initialising the initial population.

Based on the results gathered from our simulations, the final GA configuration that we will be utilising for most of our simulations in this dissertation, unless specified otherwise in the associated plots, is given in Table 3.9. The associated flowchart is depicted in Figure 3.10. Further useful information can be gleaned by comparing our GA configuration to the previously proposed GA-assisted multiuser detectors [65–68] in the literature, as given by Table 2.3. Notice that a low probability of mutation p_m as well as no incest prevention strategy were invoked in these proposals [65–68]. On the other hand, according to our results summarised in Section 3.5.3 and Section 3.5.5, the effects of the value of p_m and those of the incest prevention strategy can have a significant impact on the convergence rate and hence also on the BEP performance of the GA-assisted multiuser detector. As shown in Figure 3.9, our proposed GA-assisted multiuser detector is capable of reaching a near-optimal BEP performance within $Y = 10$ generations with the aid of a population size of $P = 30$ for $K = 10$ users over an AWGN channel at an SNR of 9 dB. This constitutes a total of $P \times Y = 300$ number of correlation metric evaluations according to Equation (3.25). In fact, as we have mentioned in

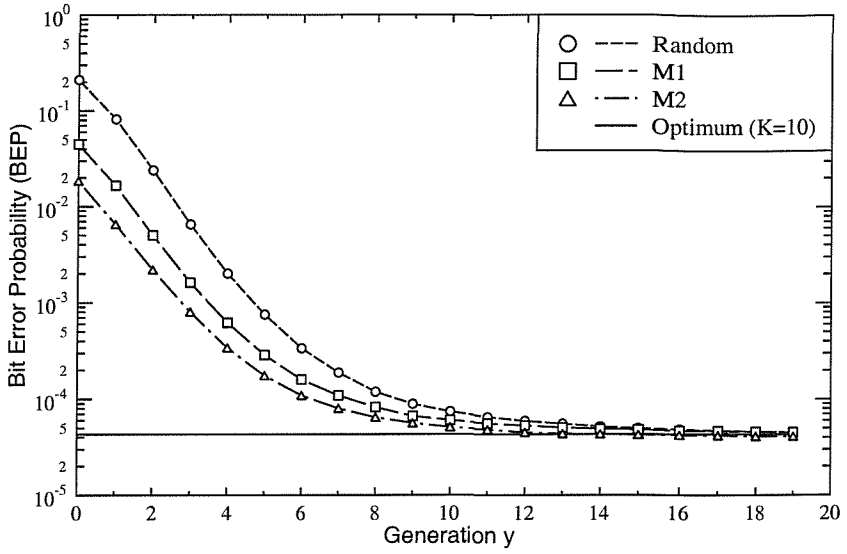

Figure 3.9: The bit error probability performance with respect to the number of generations of the GA-assisted multiuser detector employing different methods of initialising the individuals at the beginning. The configuration of the GA is specified in Table 3.8, while the simulation parameters are listed in Table 3.1 for $K = 10$ users.

Section 2.4.6, this number was derived based on the fact that the fitness value is calculated for every individual in the population at every generation. However in reality, certain individuals will reappear over the course of the evolution. Hence, the fitness values of these individuals need not be recalculated, if they are stored in memory. Based on our simulations for $P = 30$, $Y = 10$ and $K = 10$, we found that the average number of unique K-bit combinations that were evaluated by the GA for a single bit interval was ≈ 89. Comparing this number to that of the optimum multiuser detector, which requires $2^{10} = 1024$ correlation metric evaluations for every $\boldsymbol{b}$ combination, our proposed GA-assisted multiuser detector is capable of attaining a significantly reduced computational complexity and yet delivering a near-optimum BEP performance up to a specific SNR value. Hence the implementation of our proposed GA-assisted multiuser detector is feasible in practical terms and offers an alternative to the implementation of the optimum multiuser detector.

Finally, it should be stressed that we have only explored a fraction of the numerous possible configurations of GAs, a fact noted at the beginning of Chapter 2. Furthermore, the settings of certain parameters were not investigated extensively, such as the probability of mutation p_m, the ideal mutation pool size T and the

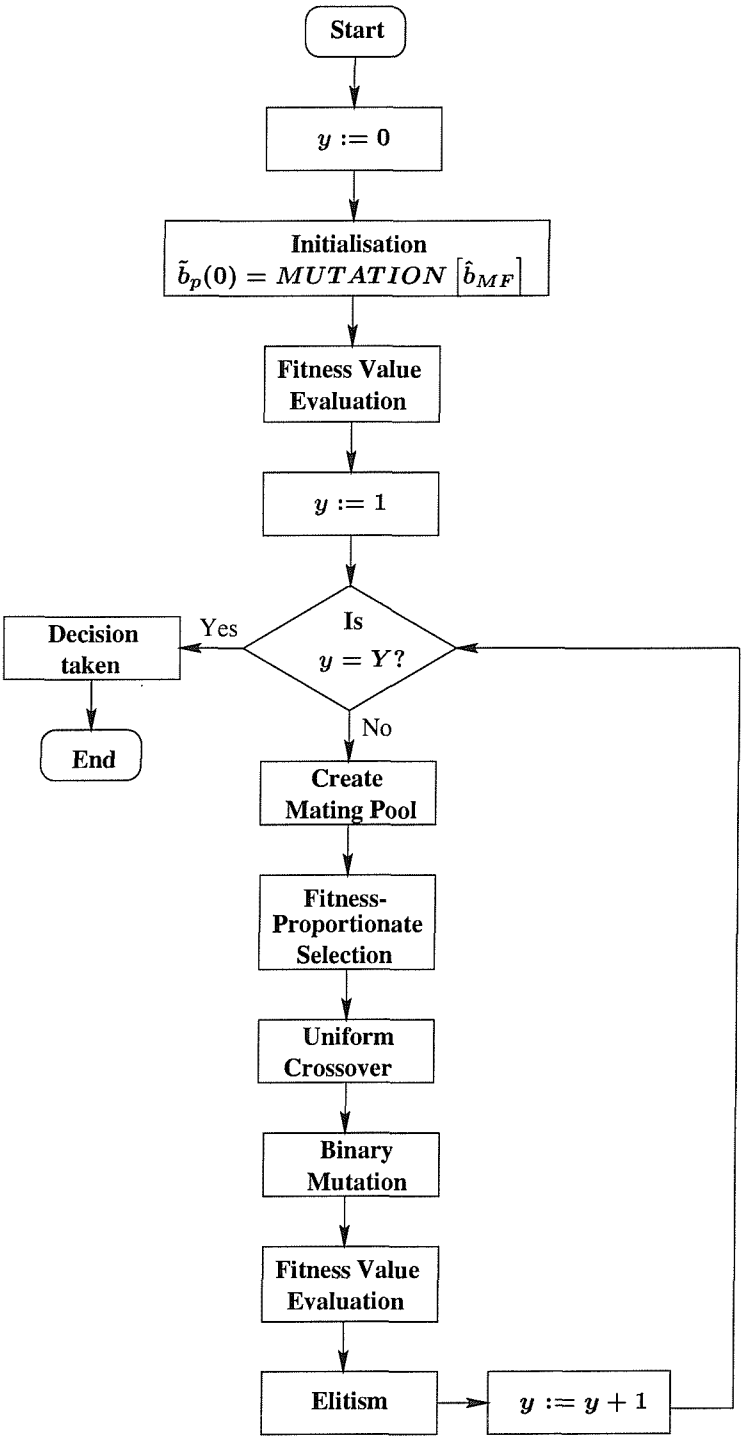

Figure 3.10: A flowchart depicting the structure of the genetic algorithm adopted for our GA-assisted multiuser detection technique, which is a specific version of Figure 2.1.

Setup/Parameter	Method/Value
Individual initialisation method	Mutation of $\hat{\boldsymbol{b}}_{MF}$ of Equation (3.26)
Selection method	Fitness-proportionate
Crossover operation	Uniform crossover
Mutation operation	Standard binary mutation
Elitism	Yes
Incest Prevention	Yes
Population size P	30
Mating pool size T	$T \leq P$ depending on the number of non-identical individuals
Probability of mutation p_m	0.1
Termination generation Y	10

Table 3.9: Configuration of the GA that will be used in this disseration hereafter, unless otherwise specified.

population size P. These values will depend very much on the number of users K and the desired quality of detection. There are also many variants of GAs that have not been studied or indeed even highlighted in this dissertation. Hence we made no claims about the optimality of the GAs used in this dissertation for the application in CDMA multiuser detection. Hence it is possible that different GA variants, which were not covered in this dissertation, or a different set of parameters may give an even better performance. However, we will show with the aid of the following simulation results of this chapter as well as in subsequent chapters that the GA configuration of Table 3.9 together with the set of GA parameters that we have adopted is capable of offering a satisfactory trade-off between computational complexity, detection delay and an acceptable BEP performance. Using the GA configuration of Table 3.9, let us now consider the BEP performance of the GA-assisted CDMA multiuser detector in both an AWGN channel as well as in a non-dispersive Rayleigh fading channel.

3.6 Simulation Results

3.6.1 AWGN Channel

All the results in this section were based on evaluating the BEP performance of a bit-synchronous K-user CDMA system over an AWGN channel. The signature sequences were randomly generated 31-chip per bit sequences and the transmit bit energy ξ_k was assumed to be equal for all users.

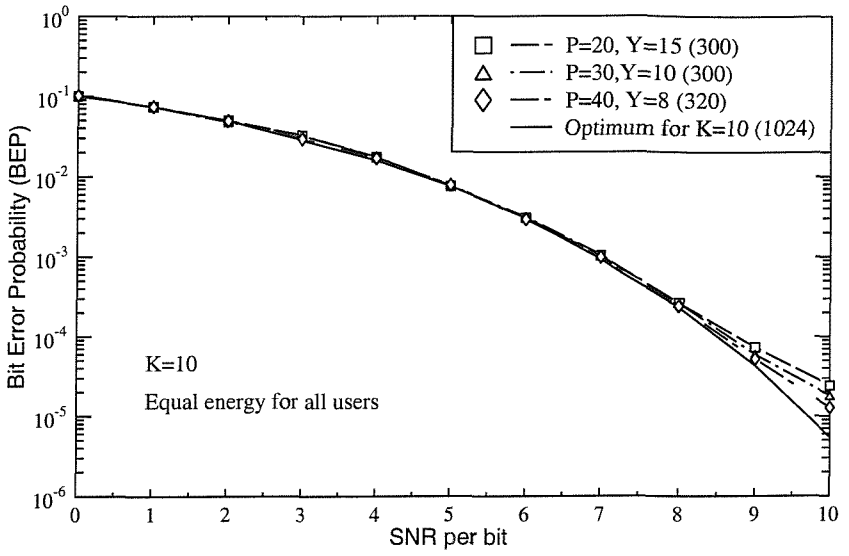

Figure 3.11: The bit error probability performance of the GA-assisted multiuser detector as a function of the SNR per bit with population sizes of $P = 20, 30, 40$ using binary random signature sequences of length $N_c = 31$ for $K = 10$ users. The GA configuration used is listed in Table 3.9. The values in round brackets in the legend denote the maximum number of times the objective function of Equation (3.25) was evaluated upon detecting the bit vector $\hat{\boldsymbol{b}}$ during a bit interval.

Figure 3.11 shows the average BEP as a function of the SNR per bit for the GA-assisted multiuser detector for various population sizes P and different number of generations Y for $K = 10$. The values of P and Y are assigned such that the maximum number of times the objective function of Equation (3.25) was evaluated upon detecting the bit vector $\hat{\boldsymbol{b}}$ during a bit interval is approximately 300. The optimum performance of the multiuser detector utilising an exhaustive search for $K = 10$ is also shown. In this case, the optimum multiuser detector has to compute the objective function of Equation (3.25) $2^{10} = 1024$ times, which corresponds to every possible combination of $\boldsymbol{b}$. Upon observing Figure 3.11, we notice that the GA-assisted multiuser detector is capable of achieving a near-optimum performance up to an SNR of 8 dB at a lower computational complexity than that of the optimum multiuser detector. Specifically, the minimum reduction in the computational complexity offered by the GA-assisted multiuser detector over its optimum counterpart is $[(1024-320)/1024] \times 100 = 68.75\%$. As mentioned previously in Section 3.5, this reduction in the computational complexity is expected to be higher if the repeated fitness value evaluation of the same individual is circumvented. From Figure 3.11, we can see that the BEP performance curves began to flatten at an

SNR of 10 dB. This is due to the inadequate population size and/or number of generations required for the GA to converge to the optimum performance. Recall that in Section 2.1 we stated that the GAs are not guaranteed to find the optimal solution, unless a sufficiently large population size and an appropriate number of generations are guaranteed. On the other hand, it is not a prerequisite that the optimum performance must be achieved for every SNR value. The integrity of detection required is usually dependent on the type of service the detection scheme is intended for. For example, a speech signal may tolerate a relatively high BEP of 10^{-3} but no latency, while a data signal may require a BEP performance below 10^{-6}, but it can tolerate a higher detection delay. Hence we can immediately see that the GA-assisted multiuser detector is capable of offering this trade-off by simply adjusting the values of P and Y.

Let us now consider the scenario when the number of users K is increased to 20. In the context of the optimum multiuser detector, an exhaustive search would required a staggering $2^{20} = 1,048,576$ number of objective function evaluations, in order to obtain the optimum solution. The BEP performance of the GA-assisted multiuser detector for various values of P and Y is shown in Figure 3.12. Again, we see that by simply expanding the population size P and by extending the number of generations Y, the near-optimal BEP performance of the GA-assisted multiuser detector found for $K = 10$ can be maintained, when the number of users is increased to $K = 20$. While this will increase the associated computational complexity of the GA-assisted multiuser detector, the maximum number of objective function evaluations given by $P \times Y$ is still significantly lower, than that required by the optimum detector.

Figure 3.13 shows the average BEP performance of the GA-assisted multiuser detector as a function of the number of users K for an SNR value of 7 dB. As we can see, for a given number of generations Y, the population size P must be increased, in order to maintain the same level of BEP performance as K is increased. However, the required increase in the population size P is not exponentially proportional to the number of users. Furthermore, there is a gradual degradation in the BEP performance for a given population size P and termination generation Y, as the number of users K increased.

3.6.2 Single-path Rayleigh Fading Channel

In this section, the BEP performance of the GA-assisted multiuser detector is evaluated for a bit-synchronous K-user CDMA system over a non-dispersive Rayleigh fading channel. The signature sequences were randomly generated $N_c = 31$-chip

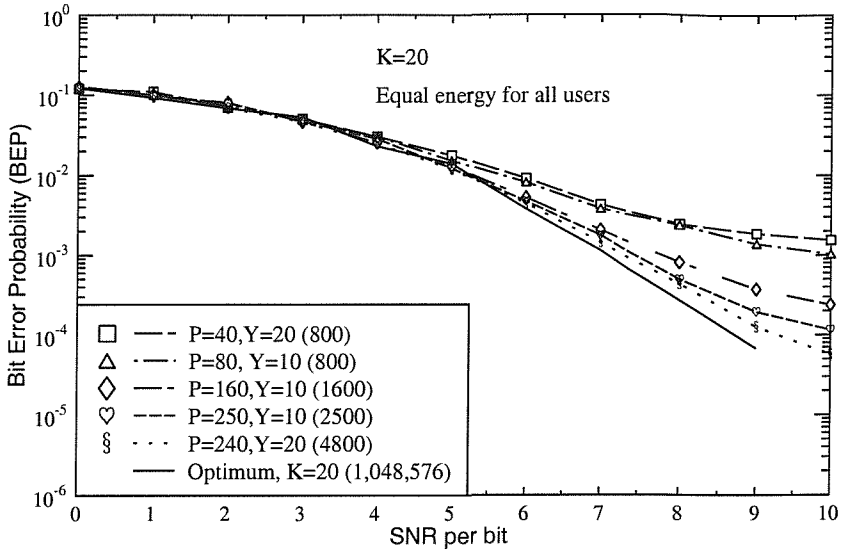

Figure 3.12: The bit error probability performance of the GA-assisted multiuser detector as a function of the SNR per bit with various population sizes P and number of generations Y for $\boldsymbol{K = 20}$ using binary random signature sequences of length $N_c = 31$. The GA configuration used is listed in Table 3.9. The values in round brackets in the legend denote the number of times the objective function of Equation (3.25) was evaluated upon detecting the bit vector $\hat{\boldsymbol{b}}$ during a bit interval.

per bit sequences and the users' CIR coefficients $\alpha_k e^{j\phi_k}$ were assumed to be known at the receiver. With the exception of Figure 3.17, the transmit bit energy ξ_k was assumed to be equal for all users.

Figure 3.14 shows the BEP performance of the GA-assisted multiuser detector for different number of generations Y and for different population sizes P. The optimum performance for $K = 10$ users was also plotted for comparison. As it can be seen from the figure, the combination of $P = 40$ and $Y = 10$ – which constitutes a maximum of $40 \times 10 = 400$ number of objective function evaluations according to Equation (3.23) – was capable of achieving a near-optimal BEP performance. For SNR values beyond 40 dB, the system exhibited an error floor due to the performance limitations of the GA in conjunction with the given P and Y values studied. At lower values of Y and P, the error floor occured at a lower SNR value. For instance, at $Y = 10$ and $P = 20$, which requires a maximum of 200 number of objective function evaluations according to Equation (3.23), the error floor occured at an SNR value of about 32 dB, while for SNR values up to 24 dB, the detector exhibited near-optimum BEP performance. Hence, again it was shown

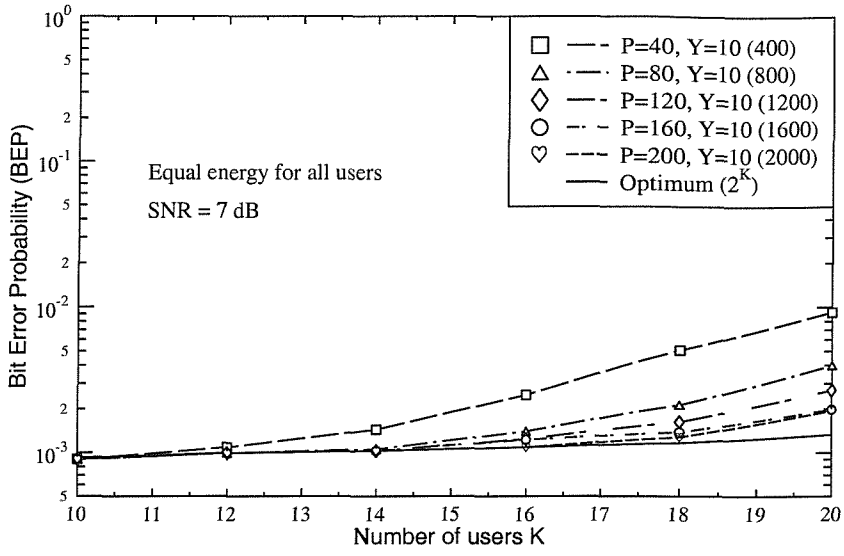

Figure 3.13: The bit error probability performance of the GA-assisted multiuser detector as a function of the number of K users with population sizes of $P = 40, 80, 120, 160, 200$ and $Y = 10$ using binary random signature sequences of length $N_c = 31$. The GA configuration used is listed in Table 3.9. The values in round brackets in the legend denotes the number of times the objective function of Equation (3.25) was evaluated upon detecting the K-bit vector $\hat{\boldsymbol{b}}$ during a bit interval.

here that the GA-assisted multiuser detector was capable of offering a trade-off between computational complexity and the optimum BEP performance.

In order to show that the computational complexity of the GA is not exponentially dependent on the number of users K, the BEP performance was evaluated in Figure 3.15 for various number of users, employing $P = 40, 80, 120, 160, 200$ in conjunction with $Y = 10$. The results are shown in Figure 3.15. At $P = 40$ and $Y = 10$, we can see that the BEP performance gradually degrades upon increasing the number of users, due to the limited population size P, which was too small for adequately exploring a significantly larger search space. As the population size P is increased, the BEP improves. For a population size of $P = 160$, we can see that the GA-assisted detector is capable of attaining a near-optimal performance, while supporting $K = 20$ users. More importantly, we noted that the number of correlation metric evaluations, seen within the brackets in the legend of Figure 3.15 increases slower than exponentially as a function of the number of users. For example, when K is increased from 10 to 16, the population size P has to be increased from 40 to 120, in order to maintain the same level of performance. This constituted a factor of $1200/400 = 3$ increased computational complexity, when K was increased from 10

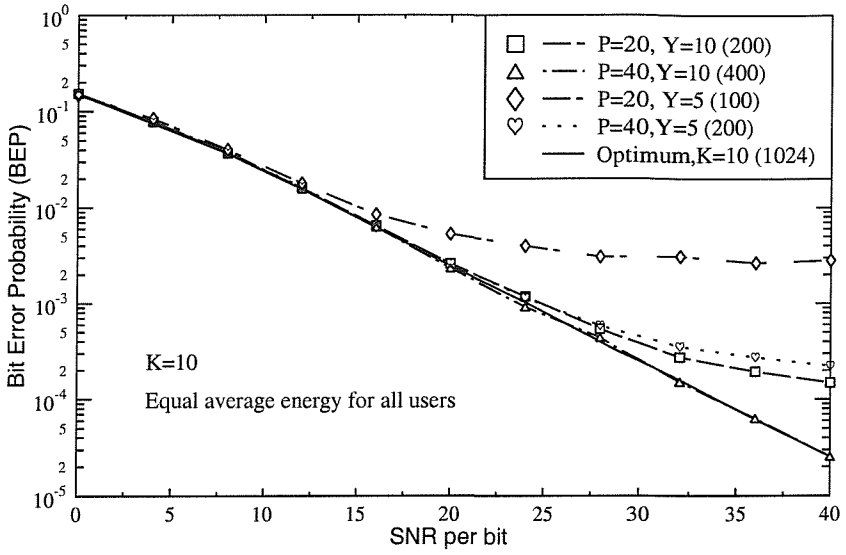

Figure 3.14: The bit error probability performance of the GA-assisted multiuser detector as a function of the SNR per bit for $K = 10$ users with various combinations of P and Y in conjunction with perfect channel estimation using binary random signature sequences of length $N_c = 31$. The GA configuration used is listed in Table 3.9. The values in round brackets in the legend denote the maximum number of times the objective function of Equation (3.25) was evaluated upon detecting the bit vector $\hat{\boldsymbol{b}}$ during a bit interval.

to 16, while maintaining a near-optimum BEP performance. By contrast, the computational complexity of the optimum multiuser detection using exhaustive search would be increased by a factor of $2^{16}/2^{10} = 64$. Similarly, when K is increased to 20, a population size of $P = 160$ is sufficient for attaining the same level of BEP performance. This constituted only a factor of $1600/400 = 4$ increased computational complexity. Furthermore, in contrast to the reduced-complexity tree-search type algorithms [26, 27] – which can also achieve a near-optimum BEP performance at a complexity lower than that of the optimum detector – the detection time required by our GA-based multiuser detector to reach a decision is independent of the number of users. Additionally, for the tree-search algorithms a noise whitening filter is required. Figure 3.16 portrays the achievable complexity reduction factor of the GA-assisted multiuser detector, which was defined as $\frac{2^K}{P \times Y}$. Specifically, the numerator quantifies the number of correlation metric evaluations required by the optimum multiuser detector, while the denominator indicates the number of correlation metric evaluations required by the GA-assisted multiuser detector, in order to attain the optimum performance at an SNR value of 24 dB. This figure

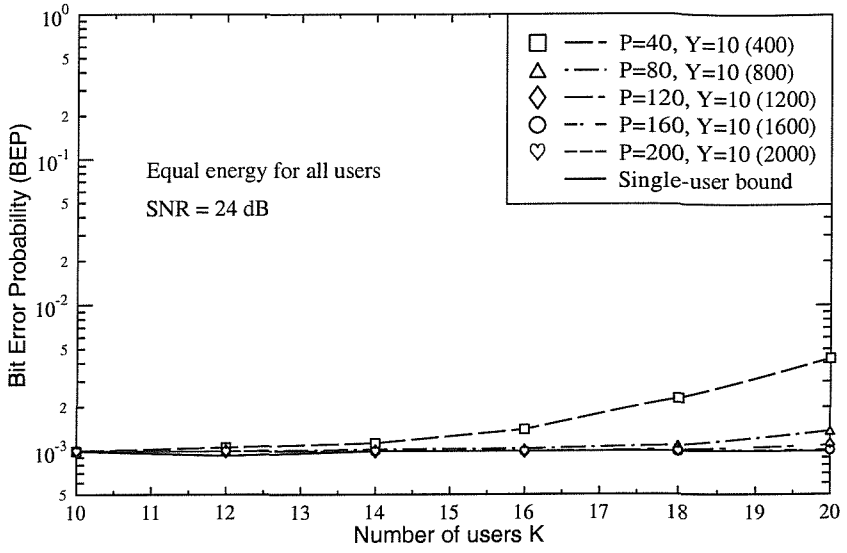

Figure 3.15: The bit error probability performance of the GA-assisted multiuser detector as a function of the number of K users with populations size of $P = 40, 80, 120, 160, 200$ and $Y = 10$ in conjunction with perfect channel estimation using binary random signature sequences of length $N_c = 31$. The GA configuration used is listed in Table 3.9. The values in round brackets in the legend denote the number of times the objective function of Equation (3.25) was evaluated upon detecting the K-bit vector $\hat{\boldsymbol{b}}$ during a bit interval.

was extracted from the results obtained in Figure 3.15. As seen from the figure, the complexity reduction offered by the GA-assisted multiuser detector over the optimum detector becomes more significant, as the number of users is increased.

Figure 3.17 shows the near-far resistence of the proposed GA-assisted multiuser detector in conjunction with perfect CIR estimation. The average received bit energy ξ_1 of the desired user remained unchanged, while the energies of all other users ξ_k for $k = 2, \ldots, K$ were either 6 dB or 10 dB higher, than that of the desired user. We can see that the GA-assisted multiuser detector was near-far resistent.

3.7 Chapter Summary and Conclusions

In this chapter, our model of a bit-synchronous CDMA system communicating over a single-tap Rayleigh fading channel was presented in Section 3.2 and its equivalent discrete representation was considered in Section 3.3. Based on this model, the optimum multiuser detector based on the maximum likelihood criterion was derived in Section 3.4. It was shown that the correlation metric of Equation (3.23) for the

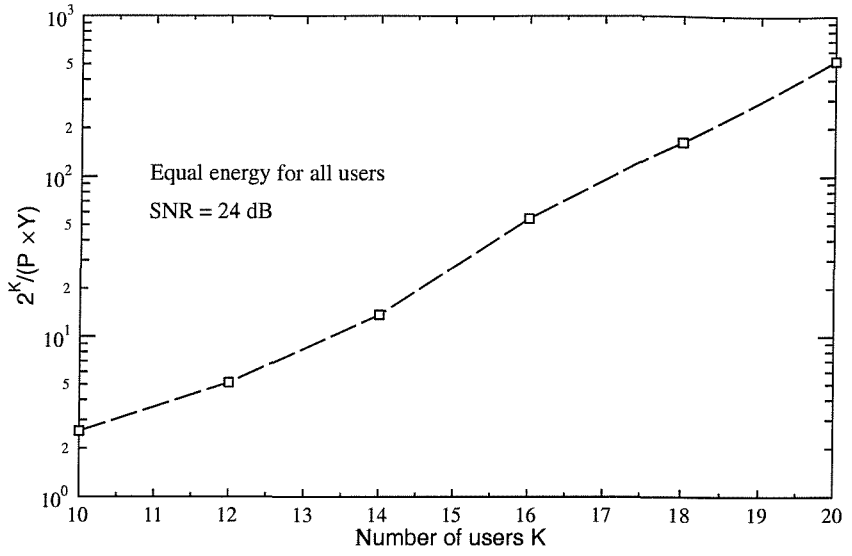

Figure 3.16: The complexity reduction factor between the optimum multiuser detector and the GA-assisted multiuser detector according to $\frac{2^K}{P \times Y}$, where the numerator denotes the number of correlation metric evaluations required by the optimum multiuser detector, while the denominator denotes that required by the GA-assisted multiuser detector, in order to attain the optimum performance at an SNR value of 24 dB, based on the results of Figure 3.15.

optimum multiuser detection scheme is cast in the form of a combinatorial optimisation function and its computational complexity is exponentially proportional to the number of users. Thus its implementation becomes impractical, when there is a high number of users. A GA-assisted multiuser detector was proposed in this chapter, in order to circumvent the above-mentioned complexity problem. According to the results obtained from other similar GA-assisted multiuser detector proposals [65–68] found in the literature, which were summarised in Section 3.5.2, traditional GAs generally have a slow convergence rate, rendering them unsuitable for real-time data detection. In order to mitigate this impediment, we conducted a series of experiments presented in Section 3.5, for finding a particular GA configuration, from the family of techniques highlighted in Chapter 2, which can offer the best trade-off between the detection delay, computational complexity and BEP performance. Based on the results obtained from our experiments, the GA configuration that we have adopted in our GA-assisted multiuser detector was given in Table 3.9. The notable differences between our favoured GA configuration and those utilised in [65–68], as shown in Table 2.3, are the probability of mutation p_m and the employment of the incest prevention strategy. As suggested by in Figure 3.3 and in Figure 3.6, these

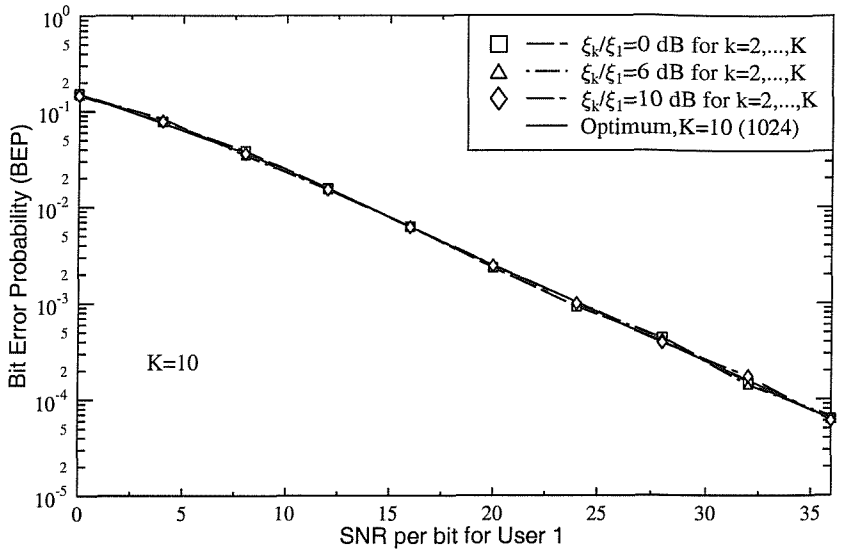

Figure 3.17: The bit error probability performance of the GA-assisted multiuser detector for $K = 10$ users with ξ_k/ξ_1 at 0 dB, 6 dB and 10 dB for $k = 2, \ldots, K$ in conjunction with perfect channel estimation using binary random signature sequences of length 31. The GA configuration used is listed in Table 3.9. The values in round brackets in the legend denote the number of times the objective function of Equation (3.25) was evaluated upon detecting the K-bit vector $\hat{\boldsymbol{b}}$ during a bit interval.

two features can have a significant impact on the convergence rate and hence on the achievable BEP performance of the GA-assisted multiuser detector. For our advocated GA configuration, the incest prevention strategy and a relatively high value of p_m were invoked, since a faster convergence and an improved BEP performance can be achieved, as illustrated in Figure 3.3 and in Figure 3.6. Last but not least, the BEP performance of the GA-assisted multiuser detector was assessed in Section 3.6 for a bit-synchronous CDMA system for transmission over an AWGN channel as well as a single-path Rayleigh fading channel. We have shown that with the aid of a sufficiently high population size P and for a reasonable number of generations Y, the BEP performance of the GA-assisted multiuser detector approaches that of the optimum multiuser detector at the cost of a significantly lower computational complexity. Our results for a single-tap Rayleigh fading channel were obtained based on the perfect knowledge of each user's CIR coefficients at the receiver. In reality, these CIR coefficients have to be estimated by some means. In our next chapter, we will show that it is possible to extend the GA-assisted multiuser detector introduced in this chapter, such that the users' CIR coefficients can be estimated concurrently with the data detection without the assistance of any pilot signals.

CHAPTER 4

Joint Genetic Algorithm-Assisted Channel Estimation and Multiuser Detection

4.1 Introduction

Our work in the previous chapter was based on the assumption that perfect channel estimation is available at the receiver, in order to perform coherent detection of the received signals. Conventionally, the fading CIR coefficients of Equation (3.5) are usually estimated using a pilot signal, as for example on the downlink of the IS-95 system [6], or employing a sequence of pilot symbols [77], in order to facilitate coherent detection. However this technique becomes inefficient on the uplink, since an independent pilot signal is required for each user in order to estimate the independent fading CIR coefficients experienced by each user's signal. Nonetheless, in order to support multiuser detection, this approach was used in the third-generation UTRA system [5]. According to our proposal, the associated inefficiency can be eliminated by invoking joint channel and data estimation, which is the topic of this chapter.

The notion of joint multiuser symbol detection and channel estimation was addressed for example in [30,78–80]. In [78], symbol detection was accomplished using

a tree-search algorithm, while the users' complex signal amplitudes were estimated using recursive least-squares techniques. In [79], Gauss-Seidel iterations were applied, in order to solve the joint symbol detection and channel estimation problem. The channel estimation was performed using the Expectation Maximization (EM) algorithm, while a multistage detection algorithm was used for detecting the data packets. In [80], joint multiuser detection and channel estimation was performed using two different types of decorrelators in conjunction with a channel estimator. A path-by-path decorrelator was used to provide noisy channel information for the channel estimator, while a channel-matched decorrelator decides on the symbols transmitted and these decisions were fed back to the channel estimator as reference signals. In [30], a decorrelator and a Kalman filter were used for symbol detection and channel estimation, respectively. A so-called per-survivor approach was also proposed in [30], which used a bank of Kalman filters for channel estimation. We note that in all the proposed methods mentioned above [30, 78–80], the symbol detection and channel estimation were performed using two separate but interlinked techniques, which potentially incurs additional complexity.

In this chapter, we present a novel approach to the problem of joint symbol detection and channel estimation in DS/CDMA for transmissions over flat-fading channels based on a GA-assisted innovation. In Chapter 3, GAs were invoked, in order to detect a particular combination of the users' transmitted bits $\boldsymbol{b}$ that maximises the objective function of Equation (3.23). Hence the search space was discrete, having a finite number of search points that is exponentially dependent on the number of users. However, in the context of joint CIR estimation and symbol detection solely by the GAs – as considered in this treatise – the search space is continuous having an infinite number of possible points, simply because the fading attenuation and phase trajectories are continuous. A GA-based channel estimation technique has been proposed previously in [81], which employed the Viterbi algorithm for data detection in a single-user receiver. We will show in Section 4.3 that the CIR estimation can be performed jointly with the symbol detection using the same GAs simultaneously, without incurring any additional computational complexity. Hence, unlike the research presented in the previous chapter, the CDMA multiuser detector proposed here takes into account the channel estimation error. Furthermore, in contrast to Kalman filter-based CIR estimation [18], which is CIR-dependent, no knowledge of the CIR is required for our proposed estimator. Since the CIR estimation can be conducted without explicit training sequences or decision feedback, our proposed detector is capable of offering a potentially higher throughput and a shorter detection delay, than that of explicitly trained CDMA multiuser

detectors.

This chapter is organised as follows. Section 4.2 describes the system model used in this chapter, which is only slightly different from the model we detailed in Section 3.2 of the previous chapter. This modification is introduced, in order to take into account the correlation of the CIR coefficients between consecutive bit intervals. Section 4.3 describes the GAs used to implement our proposed joint multiuser channel estimator and symbol detector. The GA configuration used in this chapter will be slightly different from the one listed in Table 3.9, since floating point or real-valued variables are involved here. Our simulation results are presented in Section 4.4, while Section 4.5 concludes the chapter.

4.2 System Model

We will again adopt the symbol-synchronous CDMA system model highlighted in Section 3.2, where K users transmit data packets over a single-path frequency-nonselective Rayleigh fading channel, as depicted in Figure 4.1. The channel impulse response (CIR) of each user is as given by Equation (3.5). However, in this chapter we will assume that the CIR coefficients $c_k = \alpha_k e^{j\phi_k}$ for $k = 1, \ldots, K$ are varied over the duration T_f of the M-bit transmission frame according to the maximum Doppler frequency f_d. For mobile terrestrial communications, the maximum Doppler frequency is related to the user's velocity v and the transmission wavelength λ by $f_d = v/\lambda$ [30]. Hence, the superscript (m) in Equation (3.1), which denotes the mth bit interval, has to be included in our analysis. There are numerous models that can be used to describe the fading channel characteristics, for example Jakes' model [22] or a first-order Gauss-Markov model, as given by [82]:

$$c_k^{(m+1)} = a c_k^{(m)} + \nu_k^{(m)}, \tag{4.1}$$

where $c_k^{(m)}$ is the CIR coefficient associated with the kth user during the mth symbol interval, $a = \exp(-2\pi f_d T_b)$, T_b is the bit duration and $\nu_k^{(m)}$ is a zero-mean white Gaussian variable. Kalman filter-based CIR estimation requires exact knowledge of a and that of the variance $\nu_k^{(i)}$ of the kth user, which must be acquired with the aid of training symbols and has to be updated frequently over a time-variant channel [83, 84]. Alternatively, we can express the relation between $c_k^{(m)}$ and $c_k^{(m+1)}$ as :

$$c_k^{(m+1)} = c_k^{(m)} + \Delta_k^{(m)}, \tag{4.2}$$

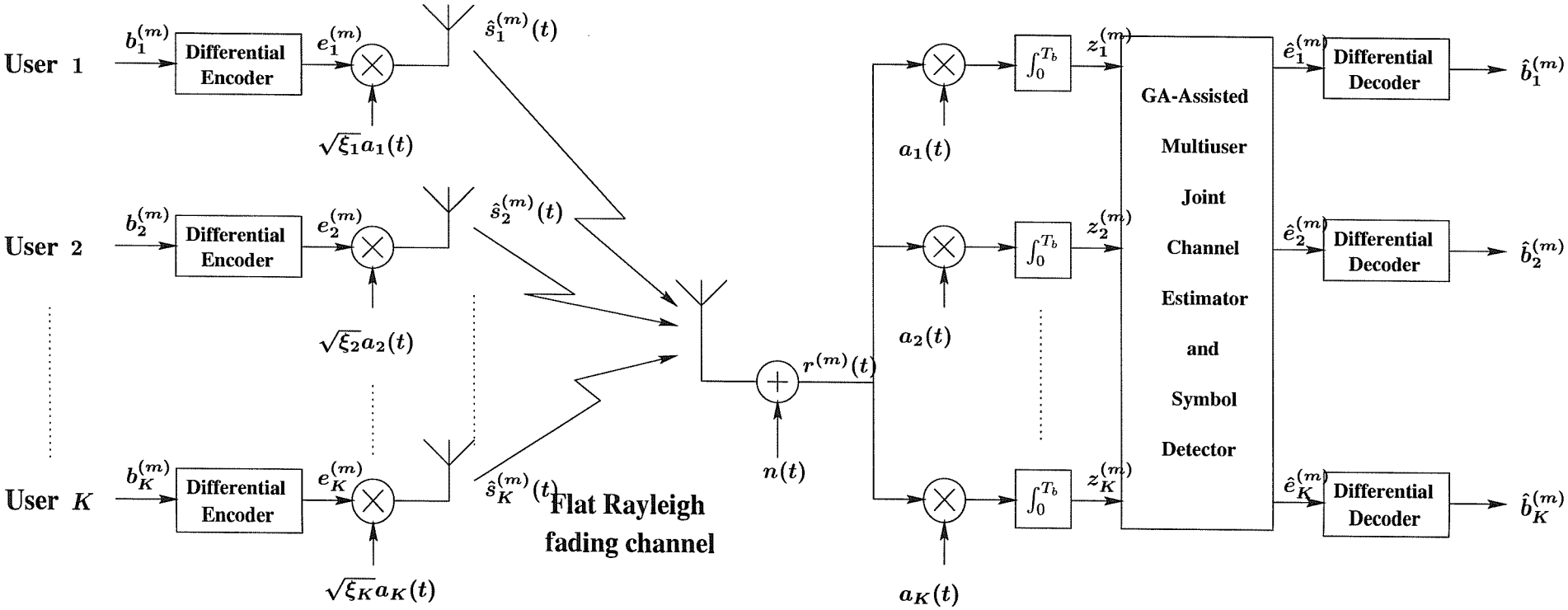

Figure 4.1: Block diagram of the K-user synchronous CDMA system communicating over a flat Rayleigh fading channel using differential encoding.

where $\Delta_k^{(m)}$ is a random variable whose value is dependent on a and $\nu_k^{(m)}$. Note that Equation (4.2) is analogous to the Least Mean Square (LMS)-based CIR estimator [85]), in which $\Delta_k^{(m)} = \mu b_k^{(m)*}\left[c_k^{(m)} b_k^{(m)} + n_k^{(m)} - \hat{c}_k^{(m)} b_k^{(m)}\right]$ (see Equation (8) of [85]), where μ is the step size.

In the context of joint channel estimation and symbol detection using Phase Shift Keying (PSK), there is always the inherent problem of a phase ambiguity of π in the estimated CIR coefficients. In order to overcome this problem, the incoming antipodal data bit stream $b_k^{(m)}$, $m = 0, \ldots, M-1$, is differentially encoded [15, 86], as shown in Figure 4.1. Then according to [22] we have :

$$e_k^{(m)} = e_k^{(m-1)} b_k^{(m)}, \tag{4.3}$$

where $e_k^{(m)}$ for $m = 0, \ldots, M-1$ constitutes the differentially encoded bit stream. From Equation (4.3), we can see that the differentially encoded bit stays at the same logical value as the previous differentially encoded bit, when $b_k^{(m)} = 1$ and vice versa. The differential encoder is initialised with $e_k^{(-1)} = 1$, which is known to the receiver. Hence we will transmit the pilot symbol $e_k^{(-1)}$ together with the encoded bits $e_k^{(m)}$, $m = 0, \ldots, M-1$. However, in Section 4.3 we will show that it is not necessary to transmit the pilot symbol, for reasons to be highlighted at a later stage. Hence in conjunction with differential encoding, the transmitted signal $\hat{s}_k(t)$ of the kth user, as illustrated in Figure 4.1, becomes :

$$\hat{s}_k(t) = \sqrt{\xi_k} \sum_{m=-1}^{M-1} e_k^{(m)} a_k(t - mT_b), \quad \forall k = 1, \ldots, K \tag{4.4}$$

where $(M+1)$ is the number of data bits in a frame transmitted by each user, ξ_k is the bit energy of the kth user and $a_k(t)$ is the signature sequence of the kth user, as given by Equation (3.2).

At the receiver, upon detecting the differentially encoded bits $\hat{e}_k^{(m)}$ of Figure 4.1, the actual data bits are obtained according to :

$$\hat{b}_k^{(m)} = \hat{e}_k^{(m-1)} \hat{e}_k^{(m)} \quad \text{for} \quad m = 0, \ldots, M-1. \tag{4.5}$$

Hence, if the CIR coefficients are estimated with a phase offset of π for at least two consecutive bits, such that $e^{-j\phi_k^{(m-1)}}$ and $e^{-j\phi_k^{(m)}}$ are detected instead of the actual values of $e^{j\phi_k^{(m-1)}}$ and $e^{j\phi_k^{(m)}}$, respectively, then the sign of the differentially encoded detected bits $\hat{e}_k^{(m-1)}$ and $\hat{e}_k^{(m)}$ will be the opposite of the actual transmitted differentially encoded bit, since again their phase is shifted by π. In this case it is assumed that the bits are detected 'correctly'. Differential decoding can cancel out

this CIR-estimation-induced phase shift according to Equation (4.5). Therefore we can see that differential encoding is important, if the channel estimation is not aided by pilot signals/symbols. On the other hand, systems utilising differential encoding suffer from a 3 dB SNR loss compared to coherently detected BPSK modulation, since a detection error in a differentially encoded bit $e_k^{(m)}$ results in two errors of the decoded bits, as it can be deduced from Equation (4.5).

In this chapter, we are interested in determining the unknown differentially encoded data bits $e_k^{(m)}$ as well as the CIR coefficients $c_k^{(m)}$ for $m = 0, \ldots, M-1$ and $k = 1, \ldots, K$ at the receiver, in order to perform coherent detection of the received signals. Following the analysis conducted in Sections 3.2–3.4, it can be shown that the correlation metric conditioned on the matrix $\boldsymbol{C}^{(m)}$ containing the CIR coefficients in its diagonal and on the vector $\boldsymbol{e}^{(m)}$ incorporating the data bits is given by [27, 79] :

$$\Omega\left(\boldsymbol{e}^{(m)}, \boldsymbol{C}^{(m)}\right) = 2\Re\left[\boldsymbol{e}^{(m)T}\boldsymbol{\xi}\boldsymbol{C}^{(m)*}\boldsymbol{Z}^{(m)}\right] - \boldsymbol{e}^{(m)T}\boldsymbol{\xi}\boldsymbol{C}^{(m)}\boldsymbol{R}\boldsymbol{C}^{(m)*}\boldsymbol{\xi}\boldsymbol{e}^{(m)}, \tag{4.6}$$

where $\boldsymbol{e}^{(m)} = \left[e_1^{(m)}, \ldots, e_K^{(m)}\right]^T$, $\boldsymbol{C}^{(m)}$ and $\boldsymbol{\xi}$ are as given by Equation (3.14), with the inclusion of the superscript (m) for denoting the mth signalling interval. Furthermore, $\boldsymbol{Z}^{(m)} = \left[z_1^{(m)}, \ldots, z_K^{(m)}\right]^T$ denotes the matched filter outputs at the mth signalling interval, as shown in Figure 4.1, whose elements are given by Equation (3.8) with b_k replaced by $e_k^{(m)}$ for $k = 1, \ldots, K$. The $K \times K$-dimensional signature sequence cross-correlation matrix $\boldsymbol{R}$ is identical to that given by Equation (3.17). The decision rule for the optimum joint multiuser channel estimation and symbol detection scheme is to choose the channel coefficient matrix $\hat{\boldsymbol{C}}^{(m)}$ and the differentially encoded symbol vector $\hat{\boldsymbol{e}}^{(m)}$, which maximises the correlation metric given in Equation (4.6), under a constraint on the channel coefficient matrix $\boldsymbol{C}^{(m)}$ as imposed by Equation (4.2). Hence,

$$\begin{aligned}\left(\hat{\boldsymbol{e}}^{(m)}, \hat{\boldsymbol{C}}^{(m)}\right) &= \arg\left\{\max_{\boldsymbol{e}^{(m)}, \boldsymbol{C}^{(m)}}\left[\Omega\left(\boldsymbol{e}^{(m)}, \boldsymbol{C}^{(m)}\right)\right]\right\} \\ \text{subject to} \quad & \boldsymbol{C}^{(m)} = \boldsymbol{C}^{(m-1)} + \boldsymbol{\Delta}^{(m-1)}.\end{aligned} \tag{4.7}$$

According to Equation (4.7), when both the CIR cofficients and the transmitted data sequence are unknown, their optimal estimates can, in fact, be jointly obtained by optimising the correlation metric. Equation (4.7) constitutes a global optimisation problem, which is non-linear, since it entails taking the maximum of $\Omega\left(\boldsymbol{e}^{(m)}, \boldsymbol{C}^{(m)}\right)$. Furthermore, Equation (4.7) cannot be solved using a conventional linear optimisation approach or employing an exhaustive tree search, because the

actual values of the channel coefficient matrix $\boldsymbol{C}^{(m)}$ in Equation (4.6) are unknown, unless a separate CIR estimator is incorporated, as in [78].

4.3 Joint GA-assisted Multiuser Channel Estimation and Symbol Detection

In this section, GAs are developed, in order to solve the joint CIR estimation and symbol detection optimisation problem, where the required objective function is defined by the correlation metric in Equation (4.6). Again, we will take the exponential of Equation (4.6), in order to ensure that all the fitness values calculated from this equation become positive. Hence the modified objective function becomes :

$$\exp\left\{\Omega\left(\boldsymbol{e}^{(m)}, \boldsymbol{C}^{(m)}\right)\right\} = \exp\left\{2\Re\left[\boldsymbol{e}^{(m)^T}\boldsymbol{\xi}\boldsymbol{C}^{(m)^*}\boldsymbol{Z}^{(m)}\right] - \boldsymbol{e}^{(m)^T}\boldsymbol{\xi}\boldsymbol{C}^{(m)}\boldsymbol{R}\boldsymbol{C}^{(m)^*}\boldsymbol{\xi}\boldsymbol{e}^{(m)}\right\}. \tag{4.8}$$

In this case, we are interested in determining the CIR matrix $\boldsymbol{C}^{(m)}$ for $m = -1, \ldots, M-1$ and the data vector $\boldsymbol{e}^{(m)}$ for $m = 0, \ldots, M-1$ that maximise the modified objective function of Equation (4.8). Hence, each individual of the GA will consist of two K-variable vectors, namely the CIR coefficient vector $\tilde{\boldsymbol{C}}_p^{(m)}(y) = \left[\tilde{c}_{p,1}^{(m)}(y), \tilde{c}_{p,2}^{(m)}(y), \ldots, \tilde{c}_{p,K}^{(m)}(y)\right]$, which is composed of continuous-valued real and imaginary parts, and the data vector $\tilde{\boldsymbol{e}}_p^{(m)}(y) = \left[\tilde{e}_{p,1}^{(m)}(y), \tilde{e}_{p,2}^{(m)}(y), \ldots, \tilde{e}_{p,K}^{(m)}(y)\right]$, which is composed of the binary-valued antipodal bits of the K users at instant m. The parameters m, y and p denote the mth signalling interval, the yth generation and the pth individual, respectively. Each individual is associated with a certain fitness value. The fitness value of the pth individual, denoted by $f_p\left[\tilde{\boldsymbol{C}}_p^{(m)}(y), \tilde{\boldsymbol{e}}_p^{(m)}(y)\right]$ is computed by substituting its corresponding CIR coefficient vector estimate $\tilde{\boldsymbol{C}}_p^{(m)}(y)$ and data vector estimate $\tilde{\boldsymbol{e}}_p^{(m)}(y)$ into the objective function of Equation (4.8). The individual that corresponds to the highest-fitness value at the end of the evolution is finally chosen as the descriptor of the estimated users' CIR coefficients $\hat{\boldsymbol{C}}^{(m)}$ and the transmitted encoded bits $\hat{\boldsymbol{e}}^{(m)}$.

4.3.1 Initialisation

In the previous chapter, we were only interested in detecting the users' transmitted bits per signalling interval. Since the transmitted bits are independent of each other in consecutive bit intervals, the initialisation of the GA, as invoked in Chapter 3 is also independent for consecutive signalling intervals. On the other hand, in this chapter, the CIR coefficients to be estimated are correlated for consecutive

bit intervals according to Equation (4.2). Hence we can use the CIR coefficients estimated during the previous bit interval for initialising the CIR coefficient vector associated with each individual of the population in the current bit interval. More explicitly, assuming that the current signalling interval is the mth interval, we have :

$$\begin{aligned} \tilde{\boldsymbol{C}}_1^{(m)}(0) &= \hat{\boldsymbol{C}}^{(m-1)} \\ \tilde{\boldsymbol{C}}_p^{(m)}(0) &= MUTATION\left[\hat{\boldsymbol{C}}^{(m-1)}\right] \quad \text{for} \quad p = 2, \ldots P, \end{aligned} \tag{4.9}$$

where $\hat{\boldsymbol{C}}^{(m-1)}$ consists of the K users' estimated CIR coefficients accruing from the previous signalling interval. The mutation operation applied to the pth individual for $p = 2, \ldots, P$ is necessary, in order to diversify the initial population as well as to provide dissimilar individuals for preventing incest mating, as highlighted in Section 2.4.2. The mutation process of the CIR coefficients will be detailed further in Section 4.3.3.

Recall from our discourse in the previous section that at $m = -1$ the users' data has to be a known bit, since the transmitted bit sequences are differentially encoded. We also mentioned that we will transmit this known symbol, even though it is demonstrated in Section 4.2 that it is not absolutely necessary. The reason for transmitting it is that we can use this pilot symbol, in order to assist in estimating the CIR coefficients $\hat{\boldsymbol{C}}^{(-1)}$. Hence based on this known data bit, the CIR coefficient vectors $\tilde{\boldsymbol{C}}_p^{(0)}(0)$ associated with the P individuals of the initial population can be assigned by estimating the CIR coefficients with the aid of the output of the matched filters according to :

$$\begin{aligned} \tilde{\boldsymbol{C}}_1^{(-1)}(0) &= \boldsymbol{Z}^{(-1)^T} \text{diag}\left[\frac{1}{\sqrt{\xi_1}}, \frac{1}{\sqrt{\xi_2}}, \ldots, \frac{1}{\sqrt{\xi_K}}\right] \\ \tilde{\boldsymbol{C}}_p^{(-1)}(0) &= MUTATION\left[\tilde{\boldsymbol{C}}_1^{(-1)}(0)\right] \quad \text{for} \quad p = 2, \ldots, P \end{aligned} \tag{4.10}$$

where $\boldsymbol{Z}^{(-1)}$ is given by Equation (3.16) with $b_k^{(-1)}$ replaced by $e_k^{(-1)} = 1$ for $k = 1, \ldots, K$. The estimated CIR coefficients will be contaminated by the MAI, as it is evidently seen from Equation (3.8), and hence will be inaccurate. Nevertheless, these CIR coefficient estimates will provide a good foundation for the GA to evolve from. Again, for the individuals $\tilde{\boldsymbol{C}}_p^{(-1)}(0)$, where $p = 2, \ldots, P$, the associated CIR coefficient vectors are randomly mutated versions of $\tilde{\boldsymbol{C}}_1^{(-1)}(0)$ for the reasons highlighted above.

Similarly to the previous chapter, the K-bit data vector associated with each individual is generated at the beginning by randomly mutating the hard decisions

generated from the matched filter outputs, as it was highlighted in Section 3.5.7 for the method M2. However, in this case, the CIR coefficients for the current signalling interval are unknown. Since the CIR coefficients are highly correlated between consecutive signalling intervals, as indicated by Equation (4.2), we can use the estimated CIR coefficients $\hat{\boldsymbol{C}}^{(m-1)}$ generated during the previous signalling interval for coherently detecting the hard decisions derived from the matched filter outputs during the current signalling interval, in order to obtain an adequately biased initial population. Hence we have :

$$\tilde{\boldsymbol{e}}_p^{(m)}(0) = MUTATION\left\{\text{sgn}\left[\Re\left(\boldsymbol{Z}^{(m)^T}\hat{\boldsymbol{C}}^{(m-1)^*}\right)\right]\right\} \quad \text{for } p = 1, \ldots, P \tag{4.11}$$

After the initialisation of the individuals in the population, the GA is then invoked, in order to find the individual that yields the highest fitness value according to Equation (4.8). A flowchart depicting the structure of the proposed GA used to jointly estimate the users' CIR coefficients $\hat{\boldsymbol{C}}^{(m)}$ and to detect the transmitted differentially encoded bits $\hat{\boldsymbol{e}}^{(m)}$ at the mth signalling interval is shown in Figure 4.2. As we can see, the GA that is adopted here is similar to that employed in the previous chapter, as shown in Figure 3.10. However, due to the continuous-valued nature of the CIR coefficients, there will be an infinite number of possible solutions for the CIR coefficient vector that the GAs will handle. Hence, the GA configuration specified in Table 3.9 that is used to search for the optimum CIR coefficient vector in this chapter is slightly different from that used for finding the optimum data vector. Specifically, the mutation operation designed for real-valued decision variables, as highlighted in Section 2.4.4, will be adopted for determining the CIR coefficient vector associated with each individual, which requires the determination of the maximum mutation size λ_{max}. Furthermore, the mating pool size T will have a significant impact on the CIR estimation performance, since we are unlikely to come across identical individuals in a given population due to the infinite number of possible solutions of the continuous-valued CIR coefficient vectors. Because of this, all the individuals in the population are likely to be considered as potential parents. However, due to the high number of potential parents in the mating pool, insufficient selection emphasis might be placed on any individual, since each continuous-valued CIR tap estimate is likely to be encountered only once, despite having a range of similar continuous-valued CIR taps.

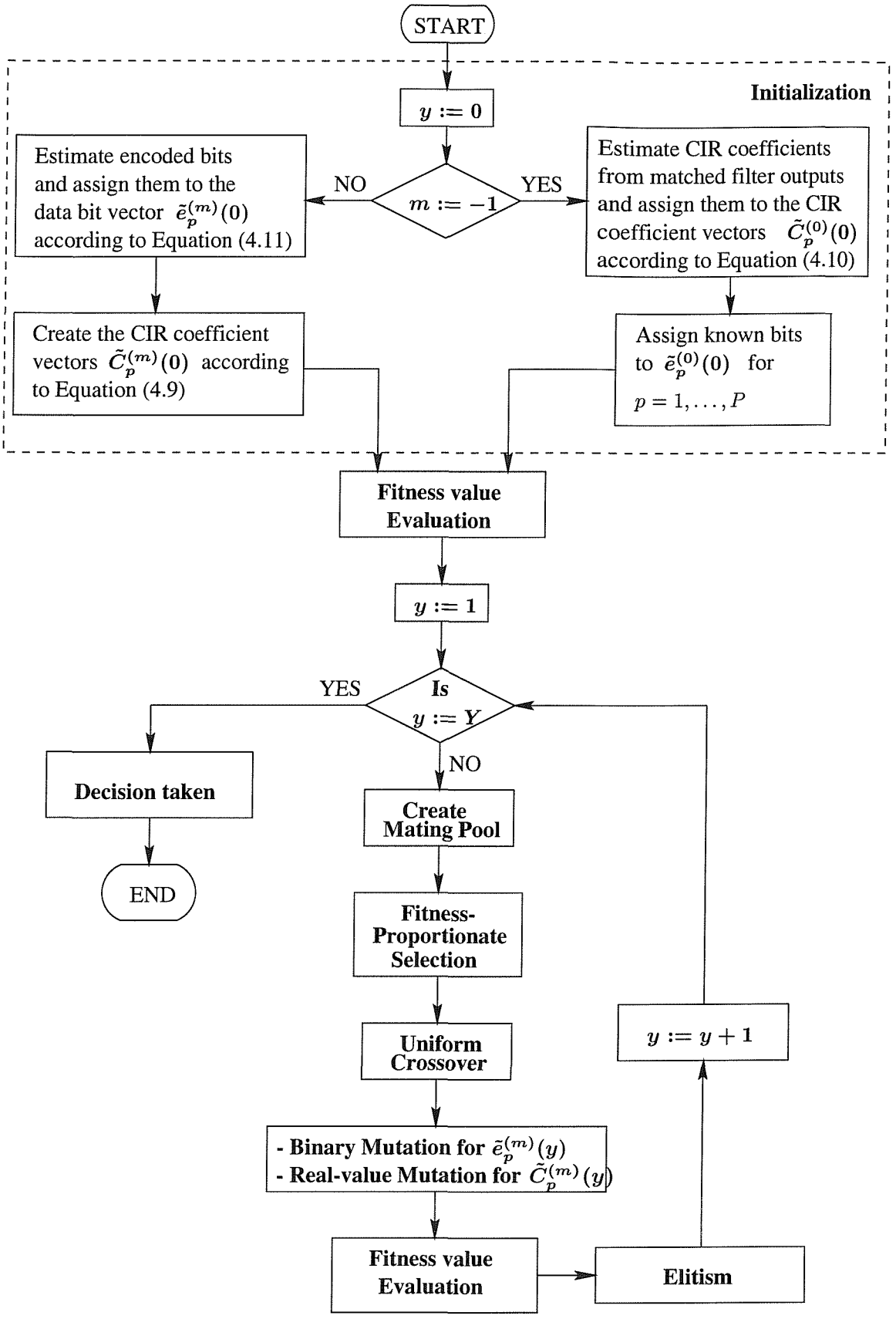

Figure 4.2: A flowchart depicting the structure of the proposed genetic algorithm used to jointly estimate the users' CIR coefficients and to detect the transmitted differentially encoded bits at the mth signalling interval.

Parameter	Value
Spreading factor N_c	31
Modulation mode	Differential Encoded BPSK
Number of CDMA users K	10
SNR per bit ξ_k/N_0	Infinity for $k = 1, \ldots, K$
Doppler frequency f_d	200 Hz
Data rate R_b	64 kbps
Packet size M	100

Table 4.1: Simulation parameters for the experiments of Figures 4.3-4.4.

Setup/Parameter	Method/Value
Individual initialisation method	According to Equation (4.9) for $m = 0, \ldots, M-1$ and Equation (4.10) for $m = -1$
Selection method	Fitness-proportionate
Crossover operation	Uniform crossover
Mutation operation	Standard floating point mutation
Elitism	Yes
Incest Prevention	Yes
Population size P	Given in the associated plots
Number of generations Y	Given in the associated plots
Mating pool size T	Given in the associated plots
Probability of mutation p_m	0.1
Mutation size λ_{max}	0.1

Table 4.2: Configuration of the GA used to obtain the results of Figure 4.3 and Figure 4.4. Explicit description of the fitness-proportionate selection scheme, the uniform crossover operation and the floating point mutation operation can be found in Section 2.4.2, Section 2.4.3 and Section 2.4.4, respectively. The definition of the mutation size will be given in Section 4.3.3.

4.3.2 Effects of the Mating Pool Size

In this section, we will investigate the effects of the mating pool size T on the performance of the CIR estimator section of our proposed GA-assisted multiuser detector. Hence we shall assume that the received data bits are known. In other words, the data vectors $\tilde{\boldsymbol{e}}_p^{(m)}(y)$ associated with all the individuals $p = 1, \ldots, P$ and $y = 0, \ldots, Y-1$ in the population are equal to the transmitted data vector $\boldsymbol{e}^{(m)}$. In order to quantify the channel estimator's performance, the Mean Squared Error (MSE) between the true value and the estimated value of the channel's attenuation was obtained. A summary of the various parameters and the GA configuration that are used in our simulations in this section are shown in Table 4.1 and Table 4.2, respectively.

Figure 4.3 shows the achievable CIR estimation MSE over 20 generations at the end of the $M = 100$-bit data packet for various mating pool sizes T with a

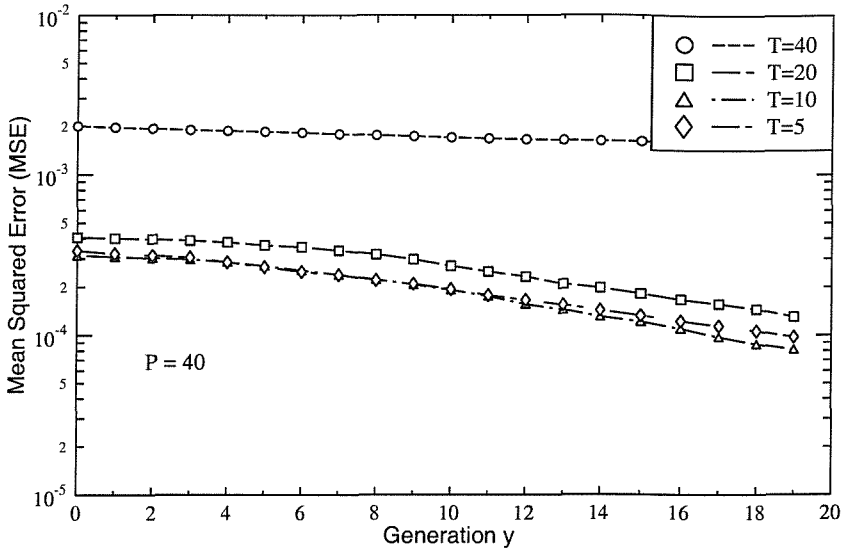

Figure 4.3: The mean squared error performance of the GA-assisted CIR estimator as a function of the number of generations y for a population size of $P = 40$ in conjunction with various mating pool sizes T using binary random signature sequences of length $N_c = 31$. The GA configuration and the simulation parameters used are listed in Table 4.2 and Table 4.1, respectively.

population size of 40 individuals. As it can be seen, when $T = P = 40$, the lowest achievable MSE of the GA-assisted CIR estimator is relatively high, in the region of 0.02. Furthermore, the convergence rate is relatively low. As the mating pool size is reduced, an MSE improvement can be observed, reaching values as low as 0.0001 for $T = 10$ and 5.

Figure 4.4 shows the achievable MSE for various population sizes P in conjunction with different mating pool sizes T. As it can be seen, the value of T has a significant impact on the achievable MSE. Specifically, the MSE becomes higher as T increases. The MSE is less sensitive to small values of T. This is justified with the aid of the following simple example. Let us assume that $T = 4$, in which case the lowest possible probability of selection associated with the individual having the highest fitness value is 0.25. On the other hand, in case of $T = 10$, the lowest possible probability of selection of the same individual becomes 0.1. Hence we can see that the emphasis placed on the best individual is lower for the latter case, which resulted in a slower convergence. This phenomenon will be investigated in more depth in the context of Figure 6.6 in conjunction with asynchronous GA-assisted multiuser detector. Hence in our case, we will adopt a mating pool size of $T = 5$ for our simulations in this chapter.

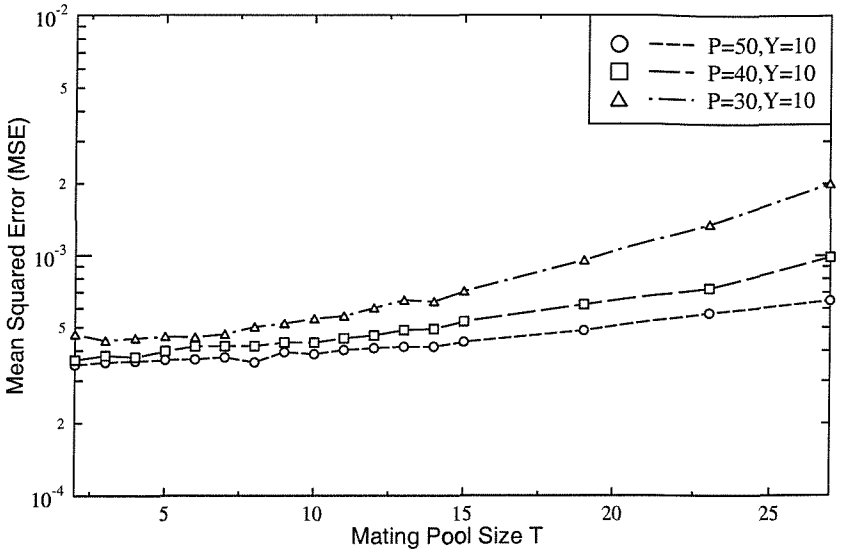

Figure 4.4: The mean squared error performance of the GA-assisted CIR estimator as a function of the mating pool size T in conjunction with various population sizes P using binary random signature sequences of length $N_c = 31$. The GA configuration and the simulation parameters used are listed in Table 4.2 and Table 4.1, respectively.

4.3.3 Effects of the Mutation Size

The mutation operation that is adopted to alter the value of the estimated CIR coefficients is conducted as follows. When a complex-valued variable associated with the CIR coefficient vector is picked for mutation, the direction of mutation is chosen randomly with equal probability for both the real and imaginary-part of the CIR coefficient. Then a real-valued random mutation size $\hat{\Delta}_k^{(m)}(y)$ is generated in the range of $[0, \lambda_{max}]$, having a uniform PDF. The value of both the real and imaginary part of the CIR coefficient is then increased or decreased accordingly by a magnitude prescribed by the mutation size :

$$\begin{aligned} \Re\left[\tilde{c}_{p,k}^{(m)}(y)\right] &= \Re\left[\tilde{c}_{p,k}^{(m)}(y-1)\right] \pm \hat{\Delta}_k^{(m)}(y-1) \\ \Im\left[\tilde{c}_{p,k}^{(m)}(y)\right] &= \Im\left[\tilde{c}_{p,k}^{(m)}(y-1)\right] \pm \hat{\Delta}_k^{(m)}(y-1). \end{aligned} \tag{4.12}$$

Notice that a limit is imposed on the value of $\hat{\Delta}_k^{(m)}(y)$ by the parameter λ_{max}, in order to ensure that the associated phase ambiguity becomes significantly less than π. This is to ensure that the phase ambiguity will not change from the $(m-1)$th symbol to the mth symbol, unless the phase is near zero, as we shall see in the context of one of our simulation results in Section 4.4. On the other hand, the

Parameter	Value
Spreading factor N_c	31
Modulation mode	Differential Encoded BPSK
Number of CDMA users K	10
SNR per bit ξ_k/N_0	Given in the associated plots
Doppler frequency f_d	200 Hz
Data rate R_b	64 kbps
Packet size M	200

Table 4.3: Simulation parameters for the experiments of Figures 4.5-4.6.

Setup/Parameter	Method/Value
Individual initialisation method	According to Equation (4.9) for $m = 0, \ldots, M-1$ and Equation (4.10) for $m = -1$
Selection method	Fitness-proportionate
Crossover operation	Uniform crossover
Mutation operation	Standard floating point mutation
Elitism	Yes
Incest Prevention	Yes
Population size P	40
Number of generations Y	10
Mating pool size T	5
Probability of mutation p_m	0.1
Mutation size λ_{max}	Given in the associated plots

Table 4.4: Configuration of the GA used for obtaining the results of Figure 4.5 and Figure 4.6. Explicit description of the fitness-proportionate selection scheme, the uniform crossover operation and the floating point mutation operation can be found in Section 2.4.2, Section 2.4.3 and Section 2.4.4, respectively.

value of λ_{max} should be sufficiently high – especially for high Doppler shifts – in order to track the evolving CIR coefficients from one symbol to the next. In other words, the ideal value of λ_{max} is directly related to the Doppler frequency f_d. Hence in this section, we will attempt to determine the appropriate value of λ_{max} that is acceptable for our application. Again, we will consider the MSE performance of the CIR estimator section of our proposed detector in conjunction with known transmitted bits. The simulation parameters and the GA configuration used for our study in this section are given in Table 4.3 and Table 4.4, respectively.

In Figure 4.5 we examined the effects of different λ_{max} values on the lowest achievable CIR estimation MSE for various Doppler frequencies f_d and SNR values. In order to characterise the worst case scenarios in terms of the vehicular speeds in Figure 4.5, we opted for using extremely high Doppler frequencies. Explicitly, we found that the GA-assisted multiuser detector MSE reached its best possible value even for a Doppler frequency of $f_d = 600$ Hz at the SNR value investigated.

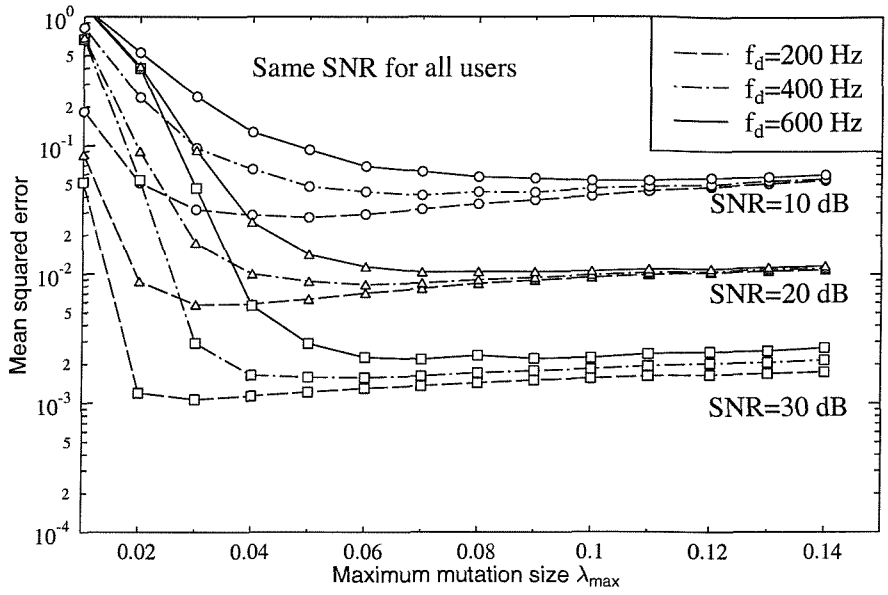

Figure 4.5: Average mean squared channel estimation error after convergence in a $K = 10$-user synchronous CDMA system transmitting known bits and having equal averaged received bit energy for all users over a narrowband Rayleigh-fading channel at various Doppler frequencies f_d. The GA configuration and the simulation parameters used are listed in Table 4.4 and Table 4.3, respectively.

From the figure we can see that the value of λ_{max} can have a significant impact on the lowest achievable CIR estimation MSE for different f_d values. In an effort to quantify the worst-case performance of the algorithm, we tested it in high-speed scenarios, such as for example a vehicular speed of 114 km/h - 342 km/h at 1.9 GHz carrier frequency. This resulted in a Doppler frequency of 200-600 Hz. For example, when $f_d = 200$ Hz, $\lambda_{max} \approx 0.04$ gives the optimal MSE for all SNR values. However, for the same value of $\lambda_{max} = 0.04$, the MSE for $f_d = 600$ Hz becomes excessive due to the fact that a low λ_{max} value is incapable of tracking the rapidly changing CIR coefficients between symbols. Moreover, we can see that the achievable MSE is more sensitive to lower values of λ_{max} for the various Doppler frequencies assumed. On the other hand, only a slight degradation in the achievable MSE is observed, as λ_{max} increases to a higher value.

Figure 4.6 compares the average MSE performance versus symbol index of the GA-assisted CIR estimator in conjunction with known bits for different SNR values and for $\lambda_{max} = 0.05$ as well as for $\lambda_{max} = 0.1$ measured over a frame of 200 known bits. Averaging over 200 transmitted frames was carried out with equal average

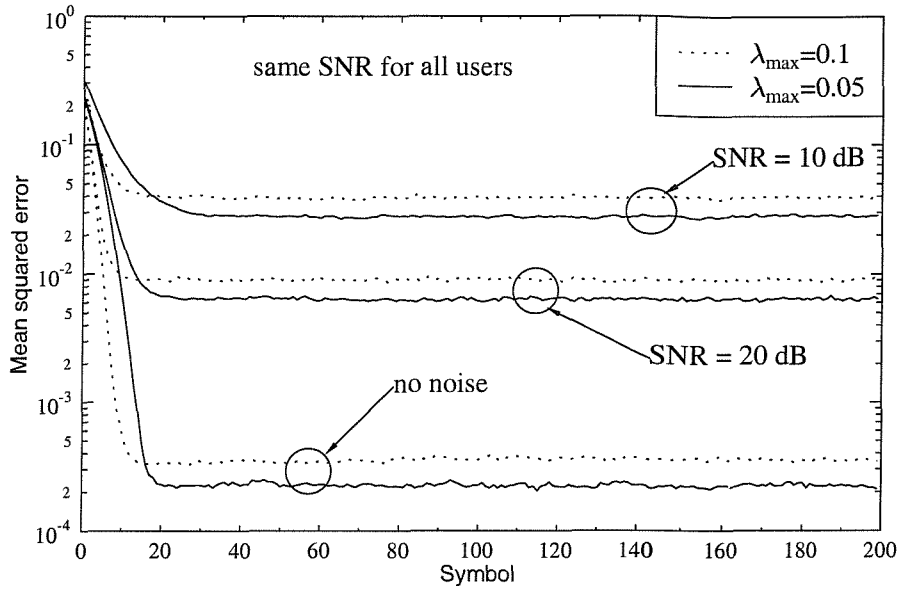

Figure 4.6: Average mean squared CIR estimation error versus transmitted symbol index in a $K = 10$-user synchronous CDMA system for a frame of 200 known bits. Averaging over 200 transmitted frames was carried out with equal averaged received bit energy for all users over a narrowband Rayleigh-fading channel at $f_d = 200$ Hz. The GA configuration and the simulation parameters used are listed in Table 4.4 and Table 4.3, respectively.

received bit energy for all users. It is seen in the figure that GAs using $\lambda_{max} = 0.05$ can achieve a lower MSE, than in conjunction with $\lambda_{max} = 0.1$. However, the former suffered from a longer convergence period.

Based on the results obtained in Figure 4.5 and in Figure 4.6, we decided to adopt $\lambda_{max} = 0.1$ for our simulations hereafter, since this value resulted in a fairly consistent MSE over an f_d range of 200 Hz to 600 Hz as well as ensuring a fast convergence rate. Finally, due to its moderate value it avoided the phase-ambiguity problem.

4.4 Simulation Results

In this section our simulation results are presented in order to characterise the performance of the proposed joint multiuser CIR estimator and symbol detector. A summary of the various parameters and the GA configuration that are used in our simulations are shown in Table 4.5 and Table 4.6, respectively.

Parameter	Value
Spreading factor N_c	31
Modulation mode	Differential Encoded BPSK
Number of CDMA users K	10
Doppler frequency f_d	200 Hz
Data rate R_b	64 kbps
Packet size M	640

Table 4.5: Simulation parameters for the experiments of Figures 4.7-4.12.

Setup/Parameter	Method/Value
Individual initialisation method	According to the flowchart of Figure 4.2
Selection method	Fitness-proportionate
Crossover operation	Uniform crossover
Mutation operation	- Floating point mutation for $\tilde{\boldsymbol{C}}_p^{(m)}(y)$ - Binary mutation for $\tilde{\boldsymbol{e}}_p^{(m)}(y)$
Elitism	Yes
Incest Prevention	Yes
Population size P	40, unless specified otherwise
Number of generations Y	10
Mating pool size T	5
Probability of mutation p_m	0.1
Mutation size λ_{max}	0.1

Table 4.6: Configuration of the GA used to obtain the results of Figures 4.7-4.12. Explicit description of the fitness-proportionate selection scheme, the uniform crossover operation and the floating point mutation operation can be found in Section 2.4.2, Section 2.4.3 and Section 2.4.4, respectively.

Before we examine the BEP performance of the proposed detector, let us first consider the tracking capability of the GA-assisted CIR estimator both in conjunction with known and unknown bits, as characterised in Figure 4.7 and Figure 4.8, respectively. Specifically, a snap-shot of the estimated real and imaginary components of the CIR coefficient of a user is compared with its corresponding true value. Notice the mirror image of the estimated components after about 400 symbols with respect to the zero level of the y-axis in Figure 4.8, when the transmitted bits and the CIR are jointly estimated by the proposed GA-assisted multiuser detector. This will result in the phase ambiguity we have mentioned previously due to the 180^o change in the CIR's phase potentially changing the sign of the estimated bit in the case of BPSK. More explicitly, this change in the phase is caused by the mutation process in an attempt to estimate the desired CIR coefficients. The bits in this ambiguity region will be detected in error, unless differential encoding and decoding are invoked. However, on the whole the GA-assisted CIR estimator was capable of

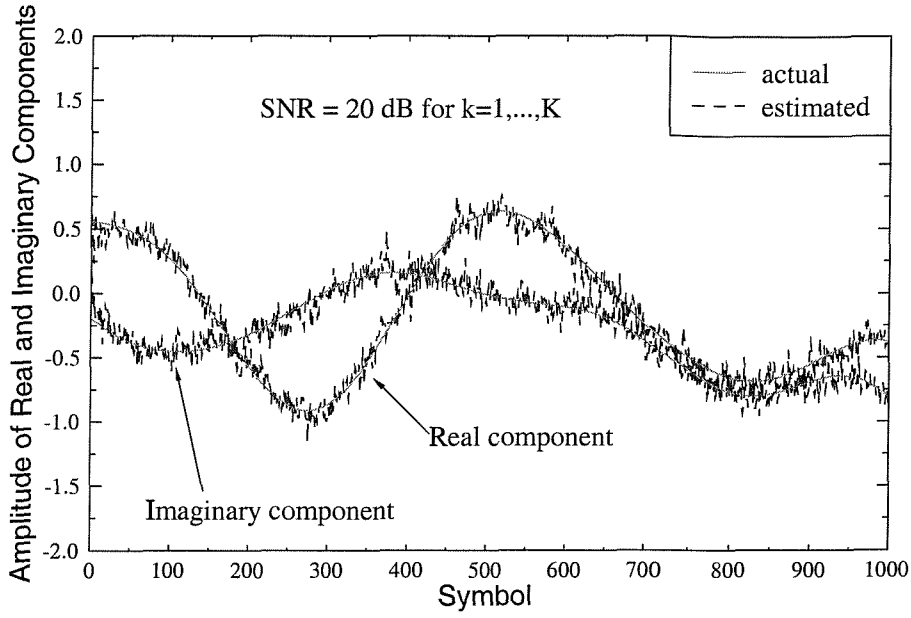

Figure 4.7: A snap-shot of the estimated real and imaginary components of the CIR coefficients in conjunction with known transmitted bits corresponding to one user compared to its true value for a narrowband Rayleigh-fading channel at $f_d = 200$ Hz, where the GA configuration and the simulation parameters used are listed in Table 4.6 and Table 4.5, respectively.

tracking the channel variations closely, regardless of whether the bits were known or unknown.

Figure 4.9 compares the MSE of the proposed CIR estimator to that of the conventional correlation-type estimator [18]. The single-user bound using the Linear Minimum Mean Squared Error (LMMSE) CIR estimator given in [87] was also plotted for comparison. It can be seen that our proposed GA-assisted CIR estimator exhibited a significantly lower MSE value, than that of the conventional CIR estimator.

Figure 4.10 shows the BEP performance of the proposed GA-assisted joint CIR estimator and symbol detector for spreading factors of $N_c = 31$ and $N_c = 127$. The BEP performance of the GA-assisted symbol detector using imperfect CIR estimation having a MSE of 0.01 and 0.001 is also shown. Furthermore, we plotted in the figure the differentially-coded single user bound in conjunction with perfect CIR estimation, which is given by [75] :

$$P_2 = \frac{1}{2}\left(1 - \frac{\bar{\gamma}_c}{1+\bar{\gamma}_c}\right), \tag{4.13}$$

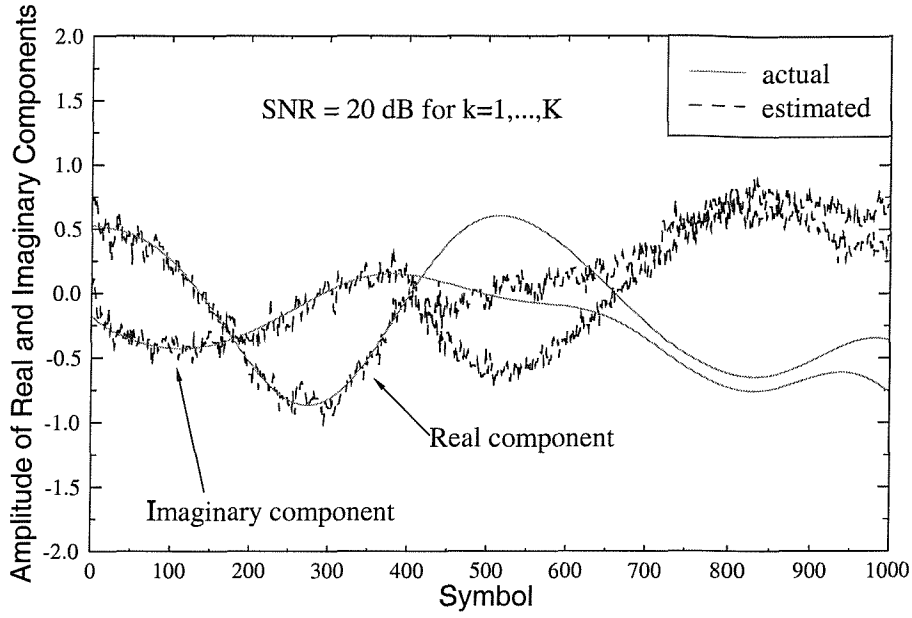

Figure 4.8: A snap-shot of the estimated real and imaginary components of the CIR coefficients in conjunction with unknown transmitted bits corresponding to one user compared to its true value for a narrowband Rayleigh-fading channel at $f_d = 200$ Hz, where the GA configuration and the simulation parameters used are listed in Table 4.6 and Table 4.5, respectively.

as well as the differentially decoded BEP performance of the proposed GA-assisted symbol detector using perfect CIR estimation. As it can be observed, the joint CIR and data detector exhibited an error floor due to the imperfect CIR estimation and the MSE of the CIR estimation was somewhere between 0.01 and 0.001, which conforms to our results obtained previously in Figure 4.6. The error floor phenomenon can also be observed in the context of other multiuser detectors suffering from CIR estimation errors [82]. For the sake of comparison, the joint symbol detection and CIR estimation using a decorrelator and an ideal Kalman filter shown in [82] achieved a BEP of 10^{-3} for $K = 10$ users and for a processing gain of 127. As shown in Figure 4.10, our proposed joint data and CIR detector is attaining a BEP performance close to 10^{-3}. Furthermore, it should be noted that our BEP is calculated over the entire length of the transmitted bit sequence, i.e. from the 0th symbol to the $(M-1)$th symbol, rather than after the initial convergence. Hence the bit errors observed during the acquisition of the CIR estimates were also taken into account. The CIR estimation error induced BEP floor can also be observed for a single-user transmission scenario, i.e. for $K = 1$ using the matched filter based

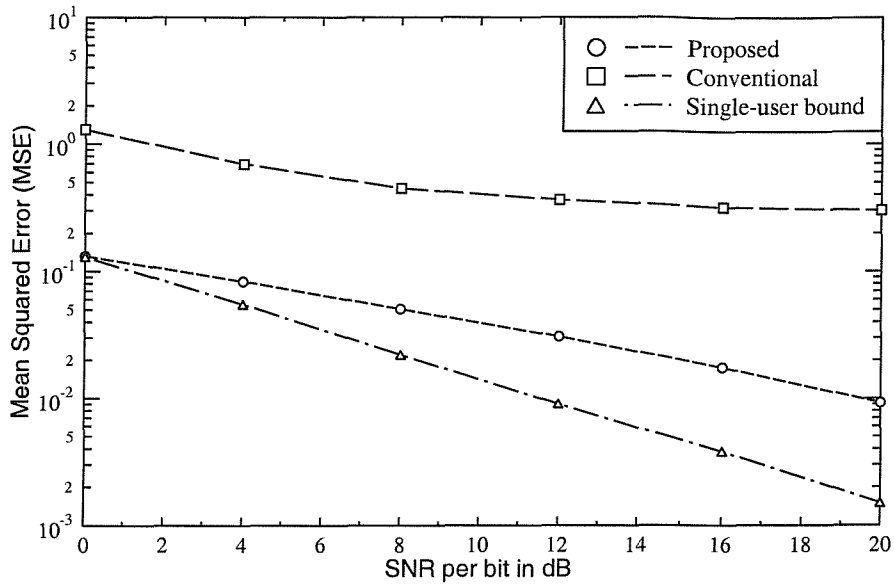

Figure 4.9: Average mean squared CIR estimation error in a $K = 10$-user synchronous CDMA system with known transmitted bits compared to that of a conventional correlator-type CIR estimator in a $K = 10$ user system and to that of a single user LMMSE estimator over a narrowband Rayleigh-fading channels at $f_d = 200$ Hz. The GA configuration and the simulation parameters used are listed in Table 4.6 and Table 4.5, respectively.

coherent receiver, as shown in Figure 4.11. It can be seen that the BEP performance of both the matched filter detector supporting $K = 1$ user and that of the GA-assisted multiuser detector for $K = 10$ is almost identical for CIR estimation MSE values of 0.01 and 0.001. This shows that the GA-assisted multiuser detector is operating near its optimum performance.

Figure 4.12 characterises the BEP performance of the proposed GA-assisted joint multiuser CIR estimator and symbol detector for different population sizes P. As it can be seen from the figure, no significant BEP performance improvement can be achieved by increasing the population size. This is an expected observation, since in Figure 4.4 the achievable MSE was observed to be almost the same for the different population sizes studied.

4.5 Chapter Summary and Conclusion

In this chapter, GAs were developed in order to jointly estimate the CIR coefficients as well as the transmitted bits simultaneously for all users in a symbol-synchronous CDMA system based on the ML decision rule. The system model used in this

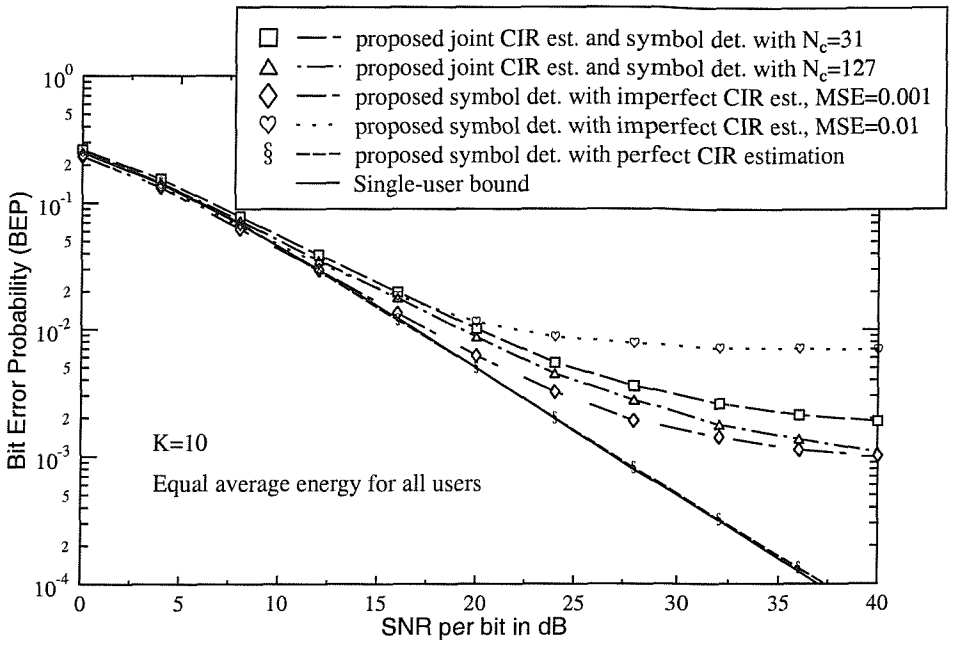

Figure 4.10: BEP performance of the proposed GA-assisted joint CIR estimator and symbol detector for $K = 10$ users over narrowband Rayleigh-fading channels at $f_d = 200$ Hz after the differential decoder. Results were shown for spreading factors of $N_c = 31$ and $N_c = 127$. Also shown are the BEP performances of the GA-assisted data detector with imperfect CIR estimation for MSE values of 0.01 and 0.001. The GA configuration and the simulation parameters used are listed in Table 4.6 and Table 4.5, respectively.

chapter was highlighted in Section 4.2. Differential encoding was invoked, in order to circumvent the phase ambiguity problem, when the CIR coefficients were estimated without the aid of pilot symbols. The GA-assisted joint multiuser CIR estimator and symbol detector was introduced in Section 4.3. Because of the continuous nature of the CIR coefficients as well as due to their correlation between consecutive bit intervals, the configuration of the GA used in this chapter is slightly different from that employed in Chapter 3. In particular, investigations were carried out in Section 4.3.2 and Section 4.3.3, in order to determine the ideal mating pool size T and the best possible mutation size λ_{max} for our application, respectively. The BEP performance of the GA-assisted joint multiuser CIR estimation and symbol detection scheme was then examined using computer simulations in Section 4.4.

Our results showed that as a channel estimator, the GA was capable of tracking the variations of the fading channel, while achieving a channel gain estimation MSE as low as 10^{-3} in a noiseless channel with a Doppler frequency $f_d = 200$ Hz. Upon exploiting its capabilities as a channel estimator as well as a symbol detector, as seen from the previous chapter, the proposed joint channel estimator

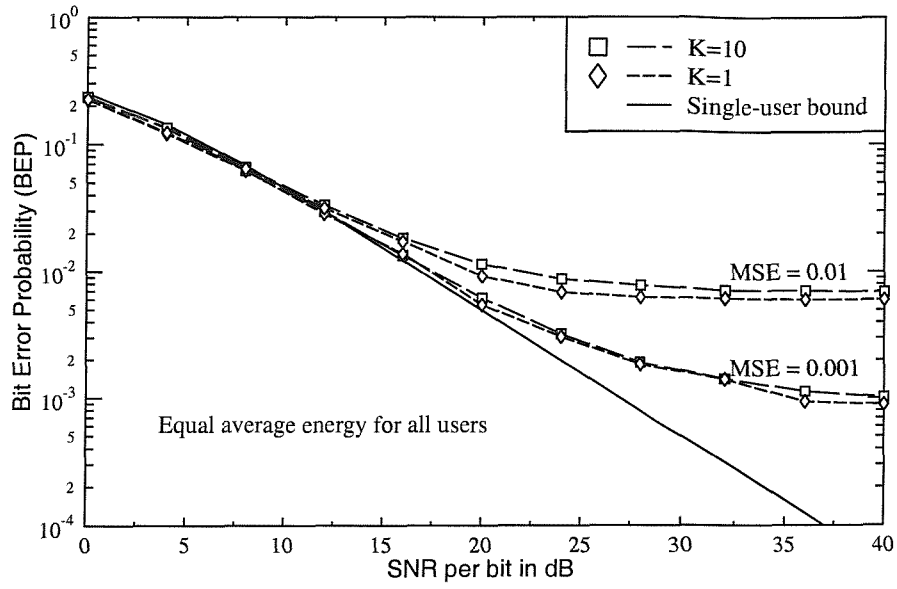

Figure 4.11: BEP performance comparison between the proposed GA-assisted CIR and symbol detector for $K = 10$ users and the matched filter for $K = 1$ over narrowband Rayleigh-fading channels at $f_d = 200$ Hz after the differential decoder using imperfect CIR estimation with MSE values of 0.01 and 0.001. Results were shown for a spreading factor of $N_c = 31$.

and symbol detector can achieve a BEP as low as 2×10^{-3} at a SNR value of 30 dB in a 10-user CDMA environment without channel coding or diversity. An error floor was observed beyond SNR = 30 dB due to the imperfect channel estimation. Furthermore, since the channel estimation and symbol detection are performed simultaneously, no pilot symbols or decision feedback are necessary, which results in a higher throughput and shorter detection time, than that of explicitly trained CDMA multiuser detectors.

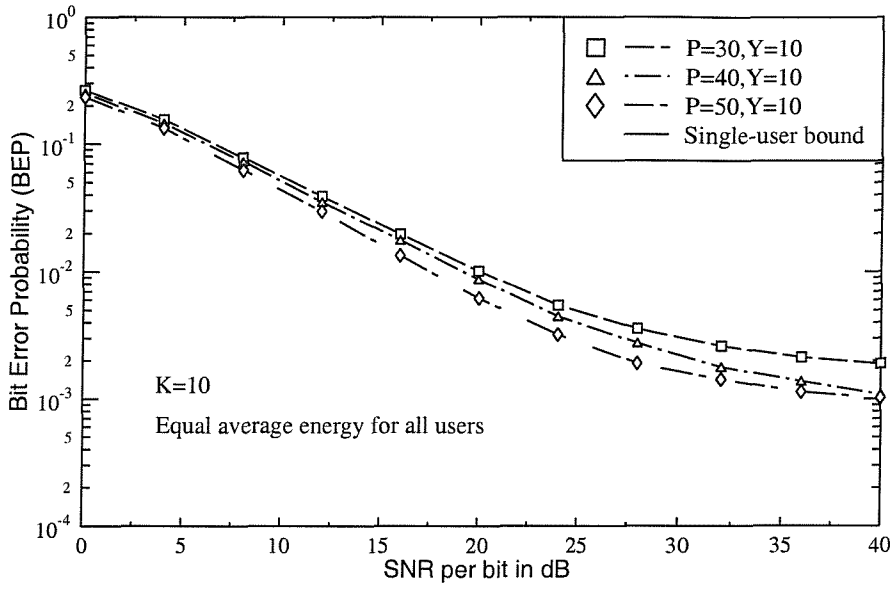

Figure 4.12: BEP performance of the proposed GA-assisted joint CIR estimator and symbol detector for $K = 10$ users with various population sizes P over narrowband Rayleigh-fading channels at $f_d = 200$ Hz after the differential decoder. The GA configuration and the simulation parameters used are listed in Table 4.6 and Table 4.5, respectively.

CHAPTER 5

Genetic Algorithm-Assisted, Antenna Diversity Aided Multiuser Detection

5.1 Introduction

It is well known that the hostile effects of fading constitute a major limitation of the system performance, which can be mitigated by diversity techniques [88, 89]. A commonly used diversity technique is receiver *antenna diversity* [75]. The distance between the receiving antennas is expected to be higher than half the wavelength, such that the signals received by the antennas become uncorrelated, experiencing sufficiently different path loss, fading and shadowing conditions [88]. Antenna diversity in conjunction with CDMA has been investigated for example in [21, 90, 91].

In this chapter, we present a novel approach to the problem of multiuser detection in DS/CDMA over flat Rayleigh-fading channels assisted by antenna diversity based on the GA-assisted multiuser detector developed in Chapter 3. The antennas are assumed to be sufficiently far apart, such that the received signals at the antennas are faded independently, resulting in an independent correlation metric obeying Equation (3.23) for each antenna. This poses a problem to the optimisation process

due to the fact that while a specific bit sequence $\boldsymbol{b}$ may optimise the correlation metric of one antenna, the same bit sequence may not necessarily optimise the correlation metric of the other antennas. In order to resolve this dilemma two different strategies of creating the mating pool are considered. In our first approach, all the non-identical individuals in a given population of the GA are picked for the mating pool. This approach is identical to that adopted so far in Chapter 3 and Chapter 4. According to our second strategy, the individuals in a given population associated with the GA are picked for the mating pool based on the concept of the so-called *Pareto optimality* [31], which uses the information from the antennas independently.

This chapter is organised as follows. Section 5.2 describes our system model, which again is assumed to be a K-user symbol-synchronous CDMA system communicating over uncorrelated non-frequency-selective Rayleigh fading channels and receiving using L_d number of antennas. We note, however that the proposed GA-assisted multiuser detector can also be applied to asynchronous systems transmitting over frequency-selective Rayleigh fading channels using multiple receiving antennas. This can be achieved by simply modifying the correlation metric of Equation (3.23), as it will be presented in Chapter 6. The GA-assisted joint multiuser CIR estimator and symbol detector proposed in the previous chapter can also be applied in the context of multiple receiver antennas. Section 5.3 describes the GAs used for implementing our proposed detector in conjunction with diversity reception invoking two different strategies of creating the mating pool, as mentioned previously. Our simulation results are presented in Section 5.4, where the BEP performance of the GA-assisted multiuser detector using two diversity antennas will be investigated under the assumption of perfect CIR estimation. The BEP performance of the GA-assisted joint multiuser CIR estimator and symbol detector proposed in Chapter 4 using two diversity antennas will also be evaluated. Finally, Section 5.5 concludes this chapter.

5.2 System Model

The system model used in this chapter is depicted in Figure 5.1, where the transmitted signals of the K users are received at the base station over L_d receiver antennas. The transmitted signal $\hat{s}_k(t)$, $k = 1, \ldots, K$, of each user is given by Equation (3.1) of Chapter 3. We assumed that the L_d antennas are sufficiently separated spatially, such that the received signals of the K users at each antenna are statistically

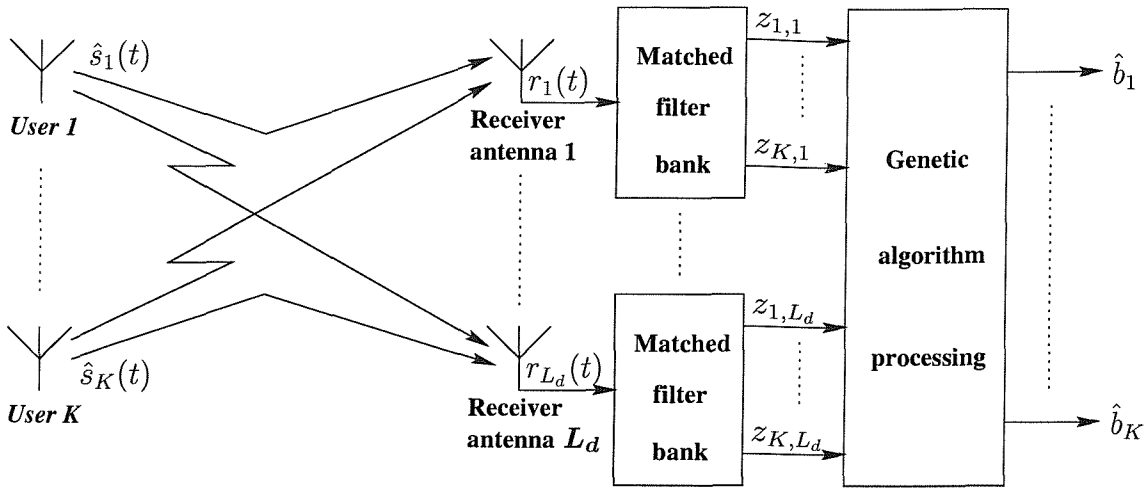

Figure 5.1: Block diagram of the K-user system model incorporating L_d-antenna diversity.

independent. Hence we can express the received signal at the ith antenna as :

$$r_i(t) = \sum_{k=1}^{K} s_{k,i}(t) + n_i(t), \tag{5.1}$$

with

$$s_{k,i}(t) = \sqrt{\xi_k}\alpha_{k,i}b_k a_k(t)e^{j\phi_{k,i}}, \quad \forall k = 1, \ldots, K \tag{5.2}$$

where ξ_k, b_k and $a_k(t)$ correspond to the bit energy, the transmitted bit and the signature sequence associated with the kth user, respectively. Furthermore, $\alpha_{k,i}$ and $\phi_{k,i}$ describe the channel attenuation and phase for the link between the kth user and the ith antenna, which was given by Equation (3.5) for a single antenna. The path amplitudes are normalised, such that $\sum_{i=1}^{L_d} E\left[\alpha_{k,i}^2\right] = 1$ for $k = 1, \ldots, K$. Following the analysis carried out in Section 3.2, the output $\boldsymbol{Z}_i$ of the matched filter bank at the ith diversity antenna, as portrayed in Figure 5.1, is given by the vector :

$$\boldsymbol{Z}_i = [z_{1,i}, z_{2,i}, \ldots, z_{K,i}]^T = \boldsymbol{R}\boldsymbol{\xi}\boldsymbol{C}_i\boldsymbol{b} + \boldsymbol{n}_i, \tag{5.3}$$

where

$$\begin{aligned} \boldsymbol{C}_i &= \text{diag}\left[\alpha_{1,i}e^{j\phi_{1,i}}, \ldots, \alpha_{K,i}e^{j\phi_{K,i}}\right] \\ \boldsymbol{\xi} &= \text{diag}\left[\sqrt{\xi_1}, \ldots, \sqrt{\xi_K}\right] \\ \boldsymbol{b} &= [b_1, \ldots, b_K]^T \\ \boldsymbol{n}_i &= [n_{1,i}, \ldots, n_{K,i}]^T \end{aligned} \tag{5.4}$$

and $\boldsymbol{R}$ is a $K \times K$-dimensional user signature sequence cross-correlation matrix, as given by Equation (3.17). Hence based on the observation vector $\boldsymbol{Z}_i$ given in Equation (5.3), we can express the correlation metric corresponding to the ith antenna as [75] :

$$\Omega_i(\boldsymbol{b}) = 2\Re\left[\boldsymbol{b}^T\boldsymbol{\xi}\boldsymbol{C}_i^*\boldsymbol{Z}_i\right] - \boldsymbol{b}^T\boldsymbol{\xi}\boldsymbol{C}_i\boldsymbol{R}\boldsymbol{C}_i^*\boldsymbol{\xi}\boldsymbol{b} \quad \forall i = 1, \ldots, L_d \tag{5.5}$$

The decision rule for the optimum multiuser detector associated with the ith antenna is to choose the specific bit vector $\hat{\boldsymbol{b}}$, which maximises the correlation metric given in Equation (5.5). Hence, the estimated transmitted bit vector of the K users is given by :

$$\hat{\boldsymbol{b}} = \arg\left\{\max_{\boldsymbol{b}} \Omega_i(\boldsymbol{b})\right\}. \tag{5.6}$$

Since the channel characteristics for each antenna are statistically independent, we have typically $\Omega_i(\boldsymbol{b}) \neq \Omega_{j\neq i}(\boldsymbol{b})$ for the correlation metrics of the L_d diversity antennas. In certain scenarios such as during deep fades, the above inequality implies that :

$$\arg\left\{\max_{\boldsymbol{b}} [\Omega_i(\boldsymbol{b})]\right\} = \hat{\boldsymbol{b}} \neq \arg\left\{\max_{\boldsymbol{b}} [\Omega_{j\neq i}(\boldsymbol{b})]\right\} \quad \forall i = 1, \ldots, L_d \tag{5.7}$$

In other words, there may not exist a single solution $\hat{\boldsymbol{b}}$, which is the best with respect to all the L_d correlation metrics. This creates a so-called *optimisation conflict* [92], since the optimisation of the L_d correlation metrics may sometimes lead to two or more possible solutions and any one of them is an acceptable solution. Nevertheless, for optimum detection, the correlation metrics corresponding to the L_d number of diversity antennas are combined according to [79] :

$$\begin{aligned}\Omega(\boldsymbol{b}) &= \sum_{i=1}^{L_d} \Omega_i(\boldsymbol{b}) \\ &= 2\Re\left\{\boldsymbol{b}^T\vec{\boldsymbol{C}}^H\vec{\boldsymbol{\xi}}\vec{\boldsymbol{Z}}\right\} - \boldsymbol{b}^T\vec{\boldsymbol{C}}^H\vec{\boldsymbol{\xi}}\vec{\boldsymbol{R}}\vec{\boldsymbol{\xi}}\vec{\boldsymbol{C}}\boldsymbol{b},\end{aligned} \tag{5.8}$$

where $\vec{\boldsymbol{Z}} = [z_{1,1}, \ldots, z_{1,L_d}, \ldots, z_{K,1}, \ldots, z_{K,L_d}]^T$, $\vec{\boldsymbol{\xi}} = \text{diag}\left[\sqrt{\xi_1}\boldsymbol{I}, \ldots, \sqrt{\xi_K}\boldsymbol{I}\right]$ with $\boldsymbol{I}$ being a unity vector of length L_d. Furthermore, $(\cdot)^H$ denotes a Hermitian matrix and $\vec{\boldsymbol{C}} = \text{diag}\left[(\alpha_{1,1}e^{j\theta_{1,1}}, \ldots, \alpha_{1,L_d}e^{j\theta_{1,L_d}})^T, \ldots, (\alpha_{K,1}e^{j\theta_{K,1}}, \ldots, \alpha_{K,L_d}e^{j\theta_{K,L_d}})^T\right]$. The decision rule is then to find the estimated transmitted bit vector $\hat{\boldsymbol{b}}$ that maximizes $\Omega(\boldsymbol{b})$ in Equation (5.8).

In the next section we will highlight the philosophy of our GA-assisted diversity-aided multiuser detector with emphasis on the strategies invoked in creating the

mating pool, in order to detect the users' transmitted bits.

5.3 GA-Assisted Diversity-Aided Multiuser Detection

The flowchart of the GA invoked in this chapter is depicted in Figure 5.2. Apart from the specific approach used in creating the mating pool, the structure of the GA invoked here is identical to the one highlighted in Chapter 3. Similarly to Chapter 3, there are P number of individuals in a population, where the pth individual is represented by a K-bit vector as $\tilde{\boldsymbol{b}}_p(y) = \left[\tilde{b}_{p,1}(y), \ldots, \tilde{b}_{p,K}(y)\right]$ and y denotes the generation index. The individuals during the initialisation phase of Figure 5.2 are generated based on the maximal ratio combining [75] of the matched filter outputs corresponding to all the antennas. Hence we have [75] :

$$\begin{aligned} \tilde{\boldsymbol{b}}_1(0) &= \text{sgn}\left[\Re\left(\sum_{i=1}^{L_d} \boldsymbol{Z}_i \boldsymbol{C}_i^*\right)\right] \\ \tilde{\boldsymbol{b}}_p(0) &= MUTATION\left[\tilde{\boldsymbol{b}}_1(0)\right] \text{ for } p = 2, \ldots, P \end{aligned} \tag{5.9}$$

In a system consisting of L_d receiving antennas, each individual is associated with L_d number of antenna-specific figures of merit denoted as $\Omega_i\left(\tilde{\boldsymbol{b}}_p(y)\right)$ for $i = 1, \ldots, L_d$, which are derived by evaluating Equation (5.7) for the corresponding antenna, where $\boldsymbol{b}$ is defined by the individual. We shall refer to these figures of merit as antenna-specific fitness values. We also introduced an additional fitness value referred to as the diversity-specific fitness value $\Omega\left(\tilde{\boldsymbol{b}}_p(y)\right)$, which is derived according to Equation (5.8). The diversity-based fitness value associated with each individual will determine its probability of selection. Hence in summary, each individual will be associated with L_d number of antenna-specific fitness values and a diversity-based fitness value. We will now consider, how we can make use of these information in order to create the mating pool and to aid our search for the optimum K-bit vector $\boldsymbol{b}$.

5.3.1 Direct Approach

The direct approach of creating the mating pool is similar to that implemented in Chapter 3. Basically, only the diversity-based fitness value associated with each individual will be considered here. **All dissimilar individuals will be placed in the mating pool** and their probability of selection is computed following the

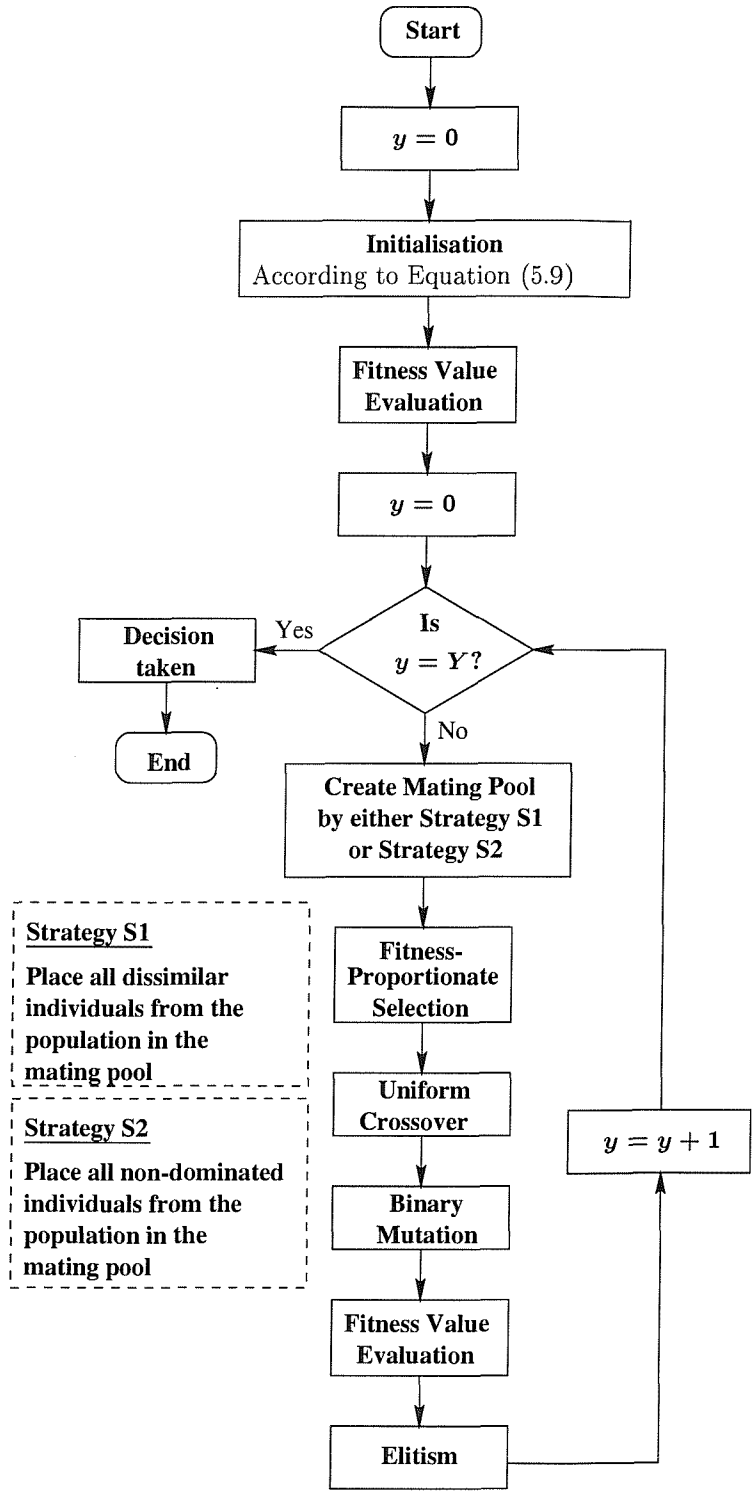

Figure 5.2: A flowchart depicting the structure of a generic genetic algorithm used for function optimisation.

philosophy of Equation (2.9) according to :

$$p_i = \frac{\exp\left[\Omega\left(\tilde{\boldsymbol{b}}_i(y)\right)\right]}{\sum_{j=1}^{T}\exp\left[\Omega\left(\tilde{\boldsymbol{b}}_j(y)\right)\right]}, \tag{5.10}$$

where $T \leq P$ is the number of dissimilar individuals in a given population. Again, we have considered the exponent of the diversity-based fitness value associated with each individual, in order to ensure that the probability of selection becomes positive. We shall refer to this direct approach strategy as S1.

5.3.2 Pareto Optimality Approach

Our second individual-selection strategy of the GA-assisted multiuser detector is based on the concept of the so-called *Pareto optimality* [31]. This strategy favours the so-called *non-dominated* individuals by retaining them for the mating pool and discards the so-called *dominated* individuals. Then the pth K-bit individual is considered to be dominated by the qth individual iff [93] :

$$\forall i \in \{1,2\} : \Omega_i\left(\tilde{\boldsymbol{b}}_q^{(y)}\right) \geq \Omega_i\left(\tilde{\boldsymbol{b}}_p^{(y)}\right) \wedge \exists j \in \{1,2\} : \Omega_j\left(\tilde{\boldsymbol{b}}_q^{(y)}\right) > \Omega_j\left(\tilde{\boldsymbol{b}}_p^{(y)}\right). \tag{5.11}$$

where $\wedge$ and $\exists$ denote 'or' and 'exists', respectively. In more explicit verbal terms Equation (5.11) implies that the pth individual is considered to be dominated by the qth individual if all the ith antenna-specific fitness values associated with the qth individual, where $i = 1, 2$ for dual antenna diversity, are higher than that of the pth individual, or there exists at least one jth antenna-specific fitness value associated with the qth individual that is higher than the fitness of the pth individual, provided that all their ith antenna-specific fitness values, where $i = 1, 2, i \neq j$, are equal. If an individual is not dominated in the sense of Equation. (5.11) by any other K-bit individuals in the population, then by definition it is considered to be non-dominated. The non-dominated individuals are also known as Pareto-optimal individuals [92]. Since GAs work with a population of candidate solutions, a number of Pareto-optimal individuals may be captured using GAs. *According to our second individual-selection strategy, all the non-dominated K-bit individuals are selected and placed in the mating pool.* The probability of selection of these individuals in the mating pool is then computed according to Equation (5.10) using their corresponding diversity-based figure of merit, where T in this case denotes the number of Pareto-optimal individuals in a given population. If there is only one non-dominated individual in a given population, then the next set of non-dominated

individuals in the population will be found and placed in the mating pool, together with the ultimate non-dominated individual.

Observe that this strategy uses the information provided by the L_d antennas independently, in order to decide which individuals are placed in the mating pool. By contrast, the direct approach of Section 5.3.1 based its decisions on only the diversity-based fitness values. We shall refer to the pareto-optimality approach as S2. Note that the Pareto optimality concept can only be applied to GAs or population-based algorithms, since non-dominated individuals can only be identified if more than one candidate solutions are evaluated at a time.

¿From a detection point of view, the concept of Pareto optimality does not give the most likely transmitted bit sequence. Upon termination of the GA, if there is only one Pareto-optimal individual in the final population, then this solution will be deemed as the detected bit sequence $\hat{\boldsymbol{b}}$. On the other hand, there may exist a number of Pareto-optimal individuals in the final population. In this case, we will adopt the optimum criteria according to Equation. (5.8) and then the individual that corresponds to the highest diversity-specific fitness value will be the detected bit sequence $\hat{\boldsymbol{b}}$.

5.4 Simulation Results

In this section our computer simulation results are presented, in order to characterise the BEP performance of the GA-assisted multiuser detector in conjunction with L_d number of received antennas employing both strategies of creating the mating pool, which were highlighted in Section 5.3. All the results in this chapter were based on evaluating the BEP performance of a bit-synchronous K-user CDMA system using L_dth-order antenna diversity reception over Rayleigh fading channels, where the signals of the diversity channels were uncorrelated with each other. The spreading factor was $N_c = 31$ and the signature sequences were randomly generated. The results shown in Figures 5.3–5.4 were based on the asumption that perfect CIR estimation is invoked at each antenna, while in Figures 5.5-5.6, imperfect CIR estimation was assumed. A summary of the simulation parameters and the GA configuration invoked is listed in Table 5.1 and Table 5.2, respectively.

Specifically, Figure 5.3 shows the BEP performance over a narrow-band Rayleigh channel against the average SNR per bit for the GA-assisted $K = 10$-user detector employing both strategy S1 and S2 assuming equal average received energy at the $L_d = 2$ antennas, i.e. for $E\left[\alpha_{k,1}^2\right] = E\left[\alpha_{k,2}^2\right] = 0.5$. Perfect power control and CIR estimation was assumed. The number in parentheses denotes the maximum number

Parameter	Value
Spreading factor N_c	31
Modulation mode	BPSK
Number of CDMA users K	10
Number of diversity antennas L_d	2

Table 5.1: Simulation parameters for the experiments of Figures 5.3-5.6.

Setup/Parameter	Method/Value
Individual initialisation method	According to Equation (5.10)
Selection method	Proportionate-Fitness
Crossover operation	Uniform crossover
Mutation operation	Standard binary mutation
Elitism	Yes
Incest Prevention	Yes
Population size P	Given in the associated plots
Number of generations Y	10
Mating pool size T	– Strategy S1 : All dissimilar individuals in the population – Strategy S2 : All non-dominated individuals in the population
Probability of mutation p_m	0.1

Table 5.2: Configuration of the GA used to obtain the results of Figure 5.3 and Figure 5.6. Explicit description of the fitness-proportionate selection scheme, the uniform crossover operation and the floating point mutation operation can be found in Section 2.4.2, Section 2.4.3 and Section 2.4.4, respectively.

of times the correlation metric of Equation (5.8) is evaluated by the GA-assisted multiuser detector. Again, this complexity figure is compared to the complexity of the optimum multiuser detector, which requires 2^K correlation metric evaluations. The single-user bound, which assumed an equal average received energy at both antennas, was computed using [75] :

$$P_2 = \left[\frac{1}{2}(1-\mu)\right]^{L_d} \sum_{k=0}^{L_d-1} \binom{L_d-1+k}{k} \left[\frac{1}{2}(1+\mu)\right]^k, \tag{5.12}$$

where $\mu = \sqrt{\frac{\bar{\gamma}_k}{1+\bar{\gamma}_k}}$ and $\bar{\gamma}_k$ is the average SNR per bit of the kth user. An error floor is observed in Figure 5.3. Again, this is due to the limitations of the GAs for a given population size P and for a number of generations Y. However, the BEP performance improved, when the population size P was increased from $P = 10$ to $P = 16$. However, this also increased the computational complexity. Hence the value of P can be selected, in order to find a trade-off between computational complexity and performance. More importantly, we can see from Figure 5.3 that

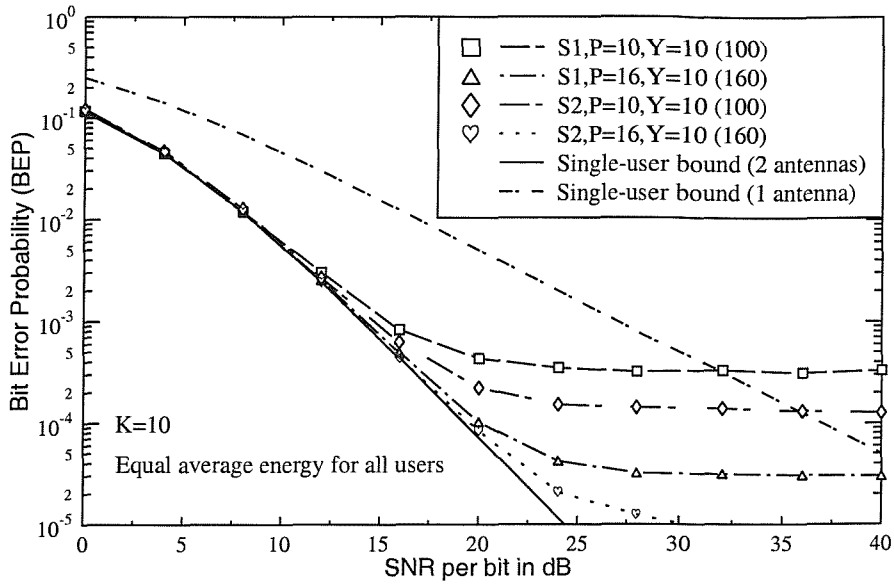

Figure 5.3: BEP performance of the proposed GA-assisted multiuser detector over narrow-band Rayleigh channels employing strategies S1 and S2 in creating the mating pool with population sizes of $P = 10, 16$ using binary random signature sequences of length $N_c = 31$ and supporting $K = 10$ users. The average received energy at the antennas was assumed to be equal, i.e. for $E\left[\alpha_{k,1}^2\right] = E\left[\alpha_{k,2}^2\right] = 0.5$. The GA configuration and the simulation parameters used are listed in Table 5.2 and Table 5.1, respectively.

the GA employing strategy S2 performs better, exhibiting a lower error floor, as compared to employing strategy S1. Nevertheless, both strategies were capable of matching the single-user bound performance up to SNRs of $\bar{\gamma}_k = 16$ dB and $\bar{\gamma}_k = 20$ dB for $P = 10$ and $P = 16$, respectively.

We then investigated the BEP performance of the GA-based multiuser detector employing both selection strategy S1 and S2 in conjunction with unequal average received energy at the two antennas, setting $E\left[\alpha_{k,1}^2\right] = 0.8$ and $E\left[\alpha_{k,1}^2\right] = 0.2$. Perfect power control and CIR estimation were assumed again. The associated results are shown in Figure 5.4 in comparison to the single-user bound given by Equation (5.12). Again, we can see that GAs invoking strategy S2 exhibit a lower BEP compared to strategy S1.

Figure 5.5 and Figure 5.6 portray the BEP performance of the GA-assisted multiuser detector in the context of imperfect CIR estimation having a CIR estimation MSE of 0.01 and 0.001, respectively. Perfect power control is assumed with equal average received energy at both antennas. In Figure 5.5 we can see that there is no significant difference in the achievable BEP performance between S1 and S2 at

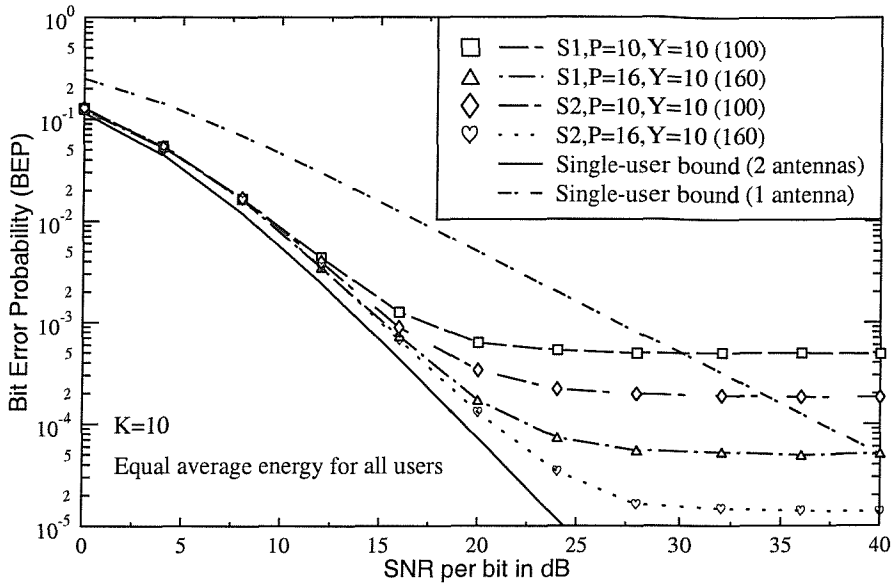

Figure 5.4: BEP performance of the proposed GA-assisted multiuser detector over narrow-band Rayleigh channels employing strategies S1 and S2 in creating the mating pool with population sizes of $P = 10, 16$ using binary random signature sequences of length $N_c = 31$ and supporting $K = 10$ users. The average received energy at the antennas was assumed to be unequal with $E\left[\alpha_{k,1}^2\right] = 0.8$ and $E\left[\alpha_{k,2}^2\right] = 0.2$. The GA configuration and the simulation parameters used are listed in Table 5.2 and Table 5.1, respectively.

$P = 16$. This is due to the high MSE of the CIR estimation, which limits the performance, as also highlighted in [94] in the context of conventional CDMA detectors. The BEP for a single-user transmission scenario using a matched filter and maximal ratio combining in conjunction with a CIR estimation MSE of 0.01 constitutes the lower bound, as shown in Figure 5.5. At the lower CIR estimation MSE of 0.001, we can see from Figure 5.6 that the BEP was lower and the detector was capable of matching the single-user bound up to an SNR of about 20 dB. We can also see from Figure 5.3, which assumed perfect CIR estimation, and from Figure 5.6, which assumed a CIR estimation MSE of 0.001 for both $P = 10$ and $P = 16$ that the error floors in both figures occur at the same BEP. Hence the BEP floor was deemed to be due to the limitations of the GAs and not the CIR estimation error, since the single-user bound is much lower.

Finally, the BEP performance of the joint GA-assisted multiuser CIR estimation and symbol detection scheme introduced in Chapter 4 was evaluated in conjunction with two diversity antennas. Apart from the creation of the mating pool, which follows the strategies highlighted in Section 5.3, the entire detection process is the

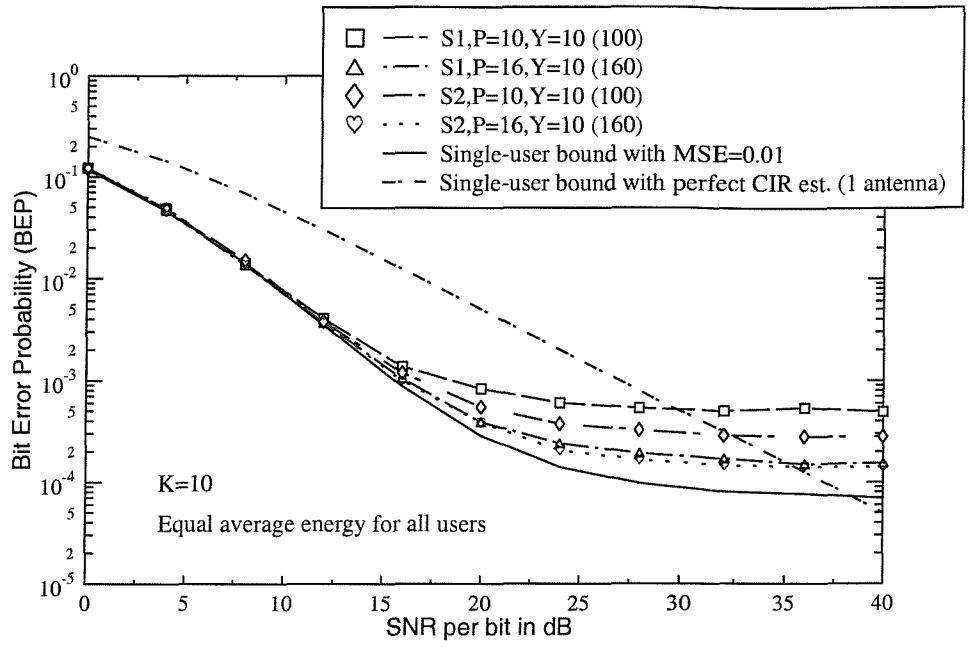

Figure 5.5: BEP performance of the proposed GA-assisted multiuser detector over narrow-band Rayleigh channels employing strategies S1 and S2 in creating the mating pool with population sizes of $P = 10, 16$ using binary random signature sequences of length $N_c = 31$ and supporting $K = 10$ users. Both antennas were assumed to exhibit a CIR estimation error of 0.01. The GA configuration and the simulation parameters used are listed in Table 5.2 and Table 5.1, respectively.

same as that implemented in Chapter 4. In this case, the antenna-specific fitness values corresponding to each individual are evaluated according to Equation (4.6) associated with each antenna and the diversity-based fitness value of each individual is obtained by combining its corresponding antenna-specific fitness values. The GA configuration used for this simulation is characterised in Table 5.3. Note that for strategy S1, only $T = 5$ non-identical individuals associated with the highest fitness values in the population were placed in the mating pool. The reason for this course of action was highlighted in Section 4.3.2. The BEP achievable performance is shown in Figure 5.7.

Firstly, we compared the performance gain achieved by utilising two antennas instead of one without increasing the computational complexity. This is represented in Figure 5.7 by the curves corresponding to $P = 40, Y = 10, L_d = 1$ for a single antenna and to $P = 20, Y = 10, L_d = 2$ for two antennas. We can see that there is a significant BEP performance improvement for the twin-antenna assisted system. However, there is no performance difference between S1 and S2, since the BEP is limited by the CIR estimation error. We can reduce the CIR estimation error by

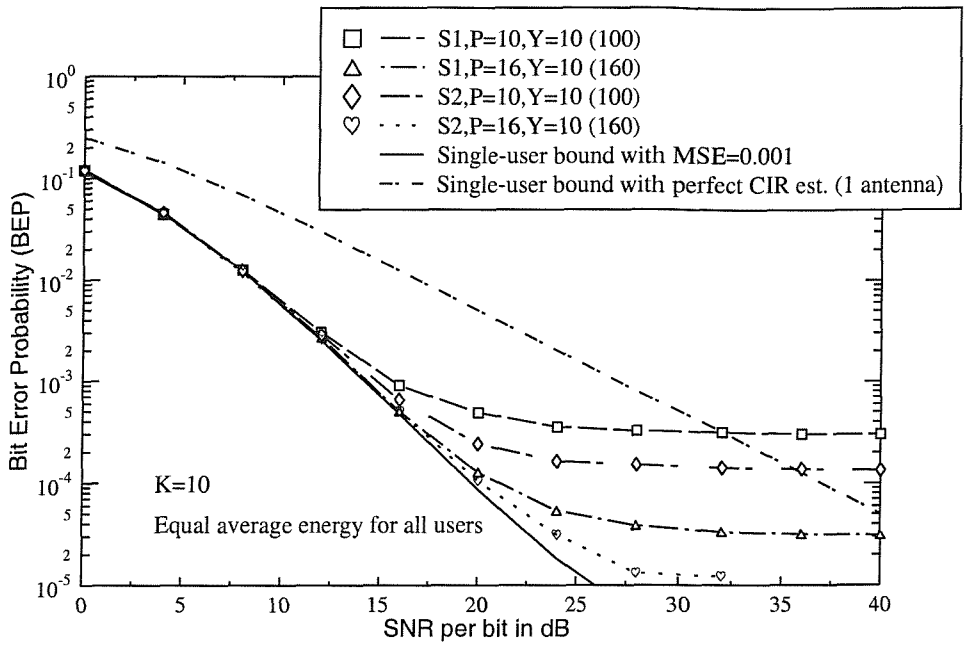

Figure 5.6: BEP performance of the proposed GA-assisted multiuser detector over narrow-band Rayleigh channels employing strategies S1 and S2 in creating the mating pool with population sizes of $P = 10, 16$ using binary random signature sequences of length $N_c = 31$ and supporting $K = 10$ users. Both antennas were assumed to exhibit a CIR estimation error of 0.001. The GA configuration and the simulation parameters used are listed in Table 5.2 and Table 5.1, respectively.

increasing the population size P, as seen previously in Figure 4.4, which in turn will reduce the BEP. This is explicitly shown in Figure 5.7, where there is a BEP improvement, when the population size is increased from $P = 20$ to $P = 40$.

5.5 Chapter Summary and Conclusions

In this chapter, we developed a GA-assisted multiuser detector for a symbol synchronous CDMA system incorporating L_d number of diversity antennas. These antennas are expected to be separated by a distance higher than half the wavelength, so that the received signal at each antenna transmitted from any of the users becomes uncorrelated. However, the GA's figure of merit that is obtained from the correlation metrics associated with each antenna is typically different. As a result, there may not exist a particular bit sequence, which is the best with respect to all the antennas' correlation metric.

We have resolved this optimisation conflict to our advantage by selecting only the so-called non-dominated individuals of a given population for the mating pool.

Setup/Parameter	Method/Value
Individual initialisation method	According to the flowchart of Figure 4.2 and Equation (5.9)
Selection method	Proportionate-Fitness
Crossover operation	Uniform crossover
Mutation operation	- Floating point mutation for $\tilde{C}_p^{(m)}(y)$ - Binary mutation for $\tilde{e}_p^{(m)}(y)$
Elitism	Yes
Incest Prevention	Yes
Population size P	Given in Figure 5.7
Number of generations Y	10
Mating pool size T	– Strategy S1 : $T = 5$ dissimilar individuals associated with the highest diversity-specific fitness values in the population – Strategy S2 : All non-dominated individuals in the population
Probability of mutation p_m	0.1
Mutation size λ_{max}	0.1

Table 5.3: Configuration of the GA used to obtain the results of Figure 5.7. Explicit description of the fitness-proportionate selection scheme, the uniform crossover operation and the floating point mutation operation can be found in Section 2.4.2, Section 2.4.3 and Section 2.4.4, respectively.

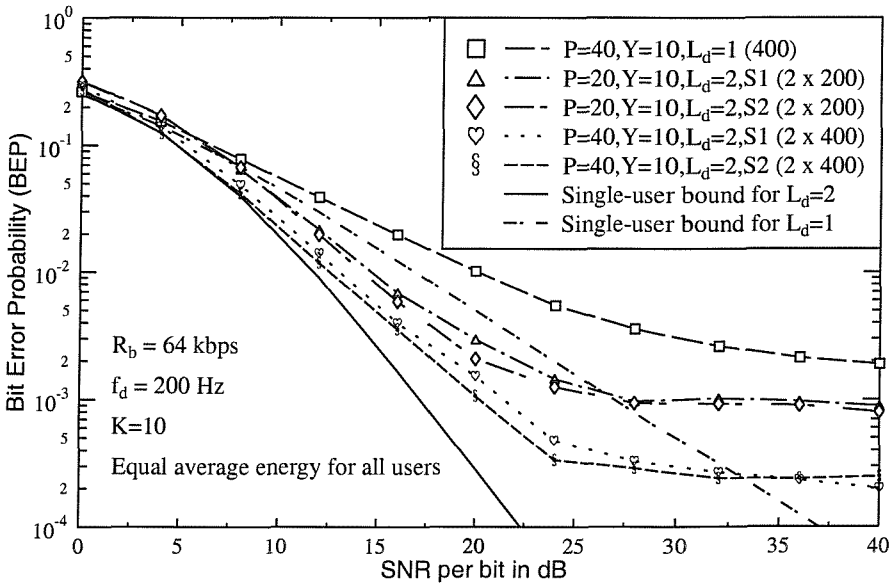

Figure 5.7: BEP performance of the proposed GA-assisted joint channel estimator and symbol detector for $K = 10$ users over narrowband Rayleigh-fading channels at $f_d = 200$ Hz after the differential decoder. Results were shown for spreading factors of $N_c = 31$. The GA configuration and the simulation parameters used are listed in Table 5.3 and Table 4.5, respectively.

This process was based on exploiting the Pareto optimality. The creation of the mating pool based on Pareto optimality was referred to here as Strategy S2. This strategy was then compared with the direct approach, which was used previously in Chapter 3 and Chapter 4, whereby all non-identical individuals in a given population were selected for the mating pool. This direct approach was referred to here as Strategy S1.

We have shown that GAs employing Strategy S2 in creating the mating pool always exhibit a lower BEP compared to those employing Strategy S1. We have also shown that the BEP performance can be improved by increasing the population size. Finally, we showed, in Figure 5.7 that a significant BEP performance gain can be achieved by the joint GA-assisted CIR estimator and symbol detector, when utilising two receiving antennas instead of a single antenna without increasing the computational complexity.

CHAPTER 6

Genetic Algorithm-Assisted Multiuser Detection for Asynchronous CDMA Systems

6.1 Introduction

So far, we have assumed that all the users transmit their signals synchronously. In order to accomplish this symbol-synchronism, a form of closed-loop timing control would be required between the base station's receiver and all the mobile users' transmitters [22]. In practice symbol-synchronous CDMA reception is not easy to implement. However, one of the advantages of CDMA over the more traditional Frequency Division Multiple Access (FDMA) and Time Division Multiple Access (TDMA) is its capability of supporting uncoordinated uplink signal transmission. Hence it is possible to allow the users to transmit their signals in an asynchronous manner.

In an asynchronous DS-CDMA system, every bit of each user is interfered by two bits of every other user in the system, which are overlapping with the bit of interest, assuming an identical channel bit rate for all users. Hence the multiuser detector must have knowledge of these two overlapping bits, in order to efficiently

detect the desired bit. Conventional multiuser detectors, such as the decorrelator [14], operate on the entire length M of the users' bit sequence at once. This results in a long detection delay as well as in a significant receiver complexity, when M is high. Several methods [95–99] have been proposed in order to reduce the detection delay and the receiver complexity in asynchronous DS-CDMA systems. The simplest way is to periodically cease transmission for a fixed time interval for all users [27, 95]. This will effectively break the continuous transmissions into frames and hence reduce the complexity of the multiuser detector. However, this method still requires synchronisation amongst the users, although not as strictly, as in symbol-synchronous transmissions. Furthermore, this method will degrade the bandwidth efficiency of the system. In the proposal by Xie *et al.* [96], the detection observation window is truncated, such that only a portion of the bit sequence length M is considered by the detector at a time. In [96] the bits that coincide with the window's edge, referred to as the *edge bits* in this chapter, are tentatively estimated employing the conventional single-user correlator. The desired bits within the truncated observation window are then detected using conventional multiuser detection techniques. The overall performance of this technique is largely dependent on the estimation reliability of the edge bits by the single-user correlator, which degrades as K increases. In order to reduce the effects of the edge bits the adjacent subsequences input to the detector can be arranged to overlap. Wijayasuriya *et al.* [97] proposed a technique, where the edge bits are predicted using previously detected bits with the aid of convolutional decoding, although other channel codecs can also be used. Juntti *et al.* [98] proposed a finite-memory-length detector, referred to as a Finite Impulse Response (FIR) detector, in order to reduce the high memory length associated with traditional multiuser detectors employed in asynchronous CDMA systems. In the contribution by Shen *et al.* [99], the edge bits are estimated using a modified decorrelator. These proposals [96, 97, 99] demonstrated that maintaining a low edge bit error probability is essential, in order to attain a high overall bit error rate performance.

Using a similar approach to that in [96, 97, 99] we proposed a multiuser detector for an asynchronous DS-CDMA system transmitting over L-path Rayleigh fading channels based on a GA. In order to reduce the complexity of the detector, as well as to decrease the detection time, the observed window is truncated such that it encompasses at most one complete symbol interval of all users in any detection window. Let us assume that we are interested in detecting the ith bit of all users. Then the edge bits will be the $(i-1)$st bits and the $(i+1)$st bits of all interfering users, referred to in this chapter as the start edge bits (SEB) and the end edge

bits (EEB), respectively. The SEBs have been detected in the previous observed window and hence they are known to the receiver. Two different strategies are adopted, in order to estimate the EEBs of all users. In our first strategy, the EEBs are estimated employing the conventional single-user correlator, a technique similar to that in [96]. GAs are then developed, in order to estimate the desired ith bits of all users. In our second strategy, we extend the same GAs in order to simultaneously improve the EEB error probability (EBEP). In contrast to the previously proposed techniques [97,99], the EEB and the desired bits in the latter strategy are estimated simultaneously using the same process. This results in minimal detection delay and no additional computation is required for predicting the EEB.

The performance of the proposed multiuser detector is examined by computer simulations, whereby the measure of interest is the desired bit error probability (DBEP). We will investigate the effects of the ambiguity of the edge bits on the DBEP. The improvement in the EBEP using our second strategy, i.e. the GA-based estimation, over that of our first strategy employing the single-user correlator based edge-bit predictor is also shown. Furthermore, we will evaluate the effects of varying the GA parameters on the DBEP performance, in order to strike a balance between detection complexity and performance. Our simulation results showed that the DBEP performance corresponding to the first detection strategy is limited by the high EBEP. On the other hand, upon using GAs for improving the accuracy of the edge bits, our proposed multiuser detector can achieve a near-optimum DBEP performance, while imposing a lower complexity compared to that of the optimum multiuser detector [1].

The remainder of this chapter is organised as follows. Section 6.2 describes our asynchronous CDMA system communicating over multipath Rayleigh fading channels. The correlation metric required for the optimisation process in conjunction with an asynchronous CDMA system is also developed. Section 6.3 describes the GAs used for implementing our proposed multiuser detector. The structure of the GAs will be slightly different from that invoked in Chapter 3, since the SEBs and the EEBs have to be taken into acount. Our simulation results are presented in Section 6.4, while Section 6.5 concludes the chapter.

6.2 Asynchronous CDMA System Model

We consider Binary Phase Shift Keying (BPSK) transmissions over a common AWGN channel shared by K asynchronous users employing DS-CDMA, as illustrated in Figure 6.1. The signal of each user is assumed to be propagating over L

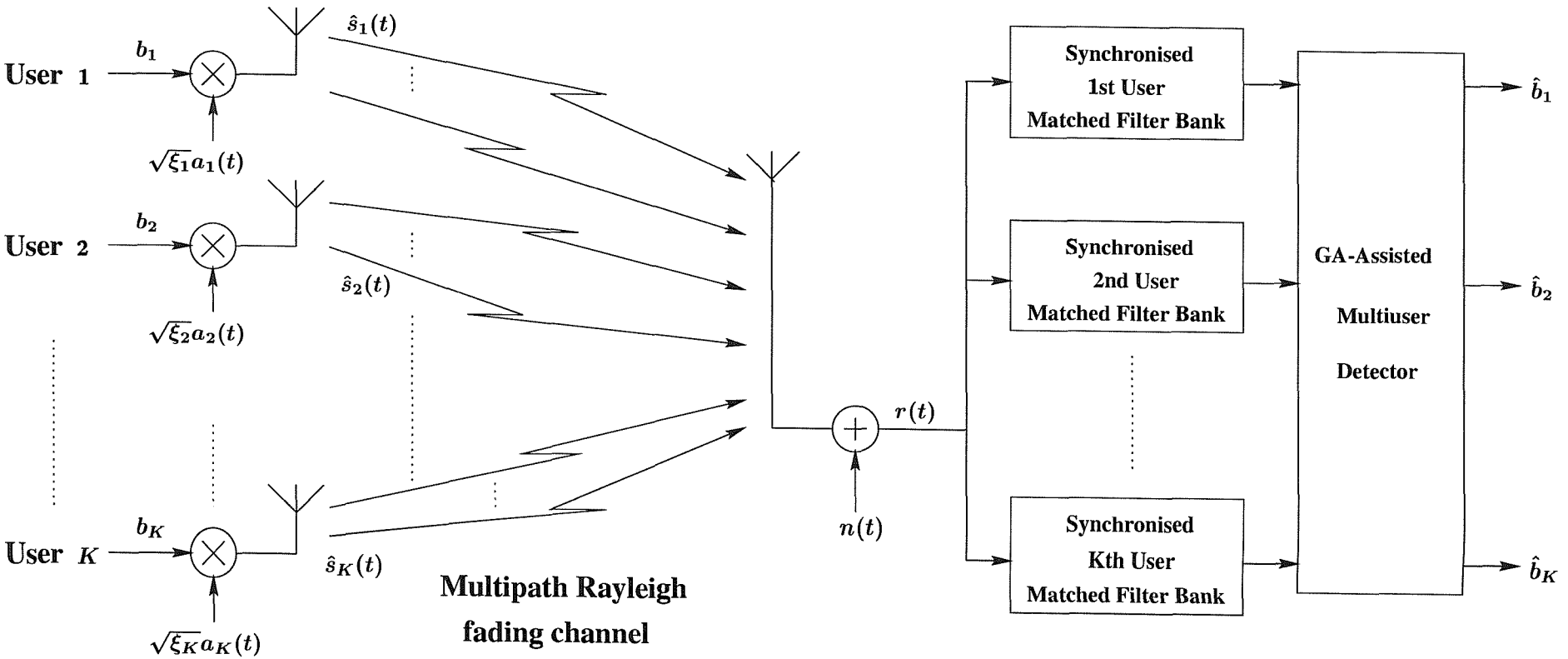

Figure 6.1: Block diagram of the K-user asynchronous CDMA system model in a multipath Rayleigh fading channel.

independent slowly Rayleigh fading paths to the base station's receiver. The complex lowpass impulse response of the channel for the kth user over the mth symbol interval of the M-bit transmission burst can be expressed as :

$$h_k^{(m)}(t) = \sum_{l=1}^{L} \alpha_{k,l}^{(m)} \exp(j\theta_{k,l}^{(m)})\delta(t - \tau'_{k,l}), \tag{6.1}$$

where $\alpha_{k,l}^{(m)}$, $\tau'_{k,l}$ and $\theta_{k,l}^{(m)}$ are the lth path gain, propagation delay and phase, respectively.

Assuming ideal lowpass receiver filtering for removing the high-frequency noise components, the baseband received signal as shown in Figure 6.1 can be written as :

$$r(t) = \sum_{m=0}^{M-1} \sum_{k=1}^{K} \sum_{l=1}^{L} \sqrt{\xi_k} b_k^{(m)} c_{k,l}^{(m)} a_k(t - mT_b - \tau_{k,l}) + n(t), \tag{6.2}$$

where M is the number of transmitted data symbols in a frame, ξ_k is the energy per bit of the kth user and $b_k^{(m)}$ is the mth data symbol of the kth user. Furthermore, $c_{k,l}^{(m)} = \alpha_{k,l}^{(m)} \exp(j\theta_{k,l}^{(m)})$ is the complex channel gain associated with the lth path of the kth user at the mth symbol interval, $a_k(t)$ is the normalised signature sequence of the kth user, as given by Equation (3.2) and $\tau_{k,l}$ is the random delay[1] corresponding to user k. Over Rayleigh fading channels the channel gain is a zero mean complex Gaussian random variable, where the amplitude $\alpha_{k,l}^{(m)}$ is Rayleigh distributed and the phase $\theta_{k,l}^{(m)}$ is uniformly distributed between $[0, 2\pi)$. For simplicity and without loss of generality, we assumed an ordering of the random delays $\tau_{k,l}$ such that $0 = \tau_{1,1} < \tau_{1,2} < \ldots < \tau_{1,L} < \tau_{2,1} < \ldots < \tau_{K,L} < T_b$. We also assumed that the energies, channel gains and random delays of all users are known to the receiver and that the channel gain is normalised so that the average signal energy levels at the output and input of the channel are the same, which is formulated as :

$$E\left[\sum_{l=1}^{L} \left|c_{k,l}^{(m)}\right|^2\right] = 1, \quad \text{for } k = 1, 2, \ldots, K. \tag{6.3}$$

The channel noise $n(t)$ is modelled by a zero mean, complex white Gaussian process exhibiting independent real and imaginary components, each having a double-sided power spectral density of $N_0/2$.

[1]The random delay $\tau_{k,l}$ takes into account the asynchronous nature of the transmission as well as the propagation delay $\tau'_{k,l}$ given in Equation (6.1).

Again, we can represent the received signal due to the M-bit transmission burst by using the vector notation as :

$$r(t) = \sum_{m=0}^{M-1} \boldsymbol{a}^T(t - mT_b)\boldsymbol{\xi}\boldsymbol{c}^{(m)}\boldsymbol{b}^{(m)} + n(t), \tag{6.4}$$

where $\boldsymbol{a}(t) = [a_1(t-\tau_{1,1}), \ldots, a_1(t-\tau_{1,L}), \ldots, a_K(t-\tau_{K,L})]^T$ is the K users' signature sequence vector, $\boldsymbol{\xi} = \text{diag}\left[\sqrt{\xi_1}\boldsymbol{I}, \sqrt{\xi_2}\boldsymbol{I}, \ldots, \sqrt{\xi_K}\boldsymbol{I}\right]$ is a $KL \times KL$-dimensional diagonal matrix containing the energy of the K users, while $\boldsymbol{I}$ is an $L \times L$-dimensional identity matrix, $\boldsymbol{c}^{(m)} = \text{diag}\left[c_{1,1}^{(m)}, \ldots, c_{1,L}^{(m)}, \ldots, c_{K,L}^{(m)}\right]$ is the $KL \times KL$ diagonal CIR matrix of the K users for the L-path Rayleigh channels, $\boldsymbol{b}^{(m)} = \left[\boldsymbol{b}_1^{(m)}, \boldsymbol{b}_2^{(m)}, \ldots, \boldsymbol{b}_K^{(m)}\right]^T$ is the $KL \times 1$ data vector of the K users transmitting over their respective L-path channels, where $\boldsymbol{b}_k^{(m)}$ is the kth $1 \times L$ user bit vector.

We can define the $KL \times KL$-dimensional cross-correlation matrix $\boldsymbol{R}(m)$ of the signature sequences, such that the (p,q)th element is given by :

$$\rho_{p,q}(m) = \int_{-\infty}^{+\infty} a_{k_p}(t - \tau_{k_p,l_p}) a_{k_q}(t + mT_b - \tau_{k_q,l_q}) dt, \tag{6.5}$$

where $k_p = \lceil \frac{p}{L} \rceil$, $k_q = \lceil \frac{q}{L} \rceil$, $l_p = p - \lfloor \frac{p-1}{L} \rfloor \cdot L$ and $l_q = q - \lfloor \frac{q-1}{L} \rfloor \cdot L$. Since the modulating signals are time-limited, $\boldsymbol{R}(m) = \boldsymbol{0}\ \forall |m| > 1$ and $\boldsymbol{R}(-1) = \boldsymbol{R}^T(1)$. Note that $\boldsymbol{R}(1)$ is an upper triangular matrix having a zero diagonal.

The front end of the receiver illustrated in Figure 6.1 consists of a bank of KL filters, matched to the signature sequences of the K users transmitting over their L-path channels. Assuming perfect synchronisation for each individual user, which transmit asynchronously with respect to each other, the output of the kth user's matched filter corresponding to the lth path sampled at the end of the ith symbol interval is given as [24] :

$$\begin{aligned} z_{k,l}^{(i)} &= \int_{-\infty}^{+\infty} r(t) a_k(t - iT_b - \tau_{k,l}) dt \\ &= \sum_{j=(k-1)L+l+1}^{KL} \rho_{(k-1)L+l,j}(1) \sqrt{\xi_{k_j}} c_{k_j,l_j}^{(i-1)} b_{k_j}^{(i-1)} \\ &\quad + \sum_{j=1}^{(k-1)L+l-1} \rho_{(k-1)L+l,j}(-1) \sqrt{\xi_{k_j}} c_{k_j,l_j}^{(i+1)} b_{k_j}^{(i+1)} \\ &\quad + \sum_{j=1}^{KL} \rho_{(k-1)L+l,j}(0) \sqrt{\xi_{k_j}} c_{k_j,l_j}^{(i)} b_{k_j}^{(i)} + n_{k,l}^{(i)}. \end{aligned} \tag{6.6}$$

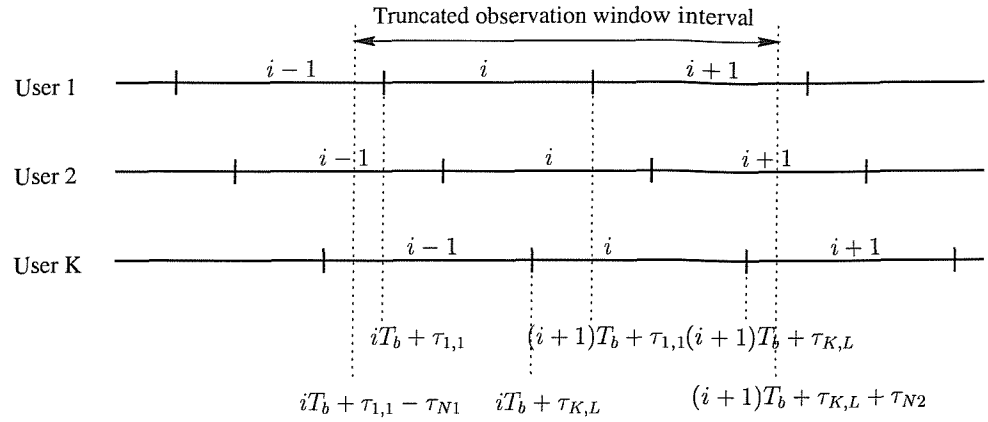

Figure 6.2: Received sequences of an asynchronous DS-CDMA system assuming a non-dispersive channel associated with $L = 1$.

Using vector notation, the output $\boldsymbol{z}^{(i)}$ of the matched filter bank at the ith symbol interval can be written as :

$$\begin{aligned} \boldsymbol{z}^{(i)} &= \left[z_{1,1}^{(i)}, \ldots, z_{1,L}^{(i)}, \ldots, z_{K,L}^{(i)}\right]^T \\ &= \boldsymbol{R}(1)\boldsymbol{\xi}\boldsymbol{c}^{(i-1)}\boldsymbol{b}^{(i-1)} + \boldsymbol{R}(0)\boldsymbol{\xi}\boldsymbol{c}^{(i)}\boldsymbol{b}^{(i)} + \boldsymbol{R}^T(1)\boldsymbol{\xi}\boldsymbol{c}^{(i+1)}\boldsymbol{b}^{(i+1)} + \boldsymbol{n}^{(i)}. \quad (6.7) \end{aligned}$$

¿From Equation (6.7) given by the first and third terms we can see the presence of the interference contributed by the edge bits. Hence any joint decision made on the ith bits of the K users has to take into account the decisions on either the $(i-1)$st bit or the $(i+1)$st bit of each user, as shown in Figure 6.2.

Let us first assume that the receiver has explicit knowledge of the SEB and EEB of all the users. Let us also introduce :

$$\boldsymbol{R}'(0) = \begin{bmatrix} \rho'_{1,1} & \cdots & \rho'_{1,L} & \cdots & \rho'_{1,KL} \\ \rho'_{2,1} & \cdots & \rho'_{2,L} & \cdots & \rho'_{2,KL} \\ \vdots & \vdots & & \vdots & \\ \rho'_{KL,1} & \cdots & \rho'_{KL,L} & \cdots & \rho'_{KL,KL} \end{bmatrix} \quad (6.8)$$

and

$$\boldsymbol{R}''(0) = \begin{bmatrix} \rho''_{1,1} & \cdots & \rho''_{1,L} & \cdots & \rho''_{1,KL} \\ \rho''_{2,1} & \cdots & \rho''_{2,L} & \cdots & \rho''_{2,KL} \\ \vdots & \vdots & & \vdots & \\ \rho''_{KL,1} & \cdots & \rho''_{KL,L} & \cdots & \rho''_{KL,KL} \end{bmatrix}, \quad (6.9)$$

where the (p,q)th element is given by :

$$\rho'_{p,q} = \int_{\tau_{1,1}+T_b-\tau_{N1}}^{\tau_{k_p,l_p}+T_b} a_{k_p}(t-\tau_{k_p,l_p})a_{k_q}(t-\tau_{k_q,l_q})dt$$

$$\rho''_{p,q} = \int_{\tau_{k_p,l_p}+T_b}^{\tau_{K,L}+T_b+\tau_{N2}} a_{k_p}(t-\tau_{k_p,l_p})a_{k_q}(t-\tau_{k_q,l_q})dt,$$

which will be used at a later stage in Equation (6.11) and Equation (6.12). The truncated observation window duration is governed by τ_{N1} and τ_{N2}, where $0 \leq \tau_{N1}, \tau_{N2} < \tau_{1,1} - \tau_{K,L} + T_b$. As illustrated by Figure 6.2, the truncated observation window interval can span from the most recently received $(i-1)$st bit of the Kth user to the end of the first received $(i+1)$st bit of the 1st user, i.e. $[(i-1)T_b + \tau_{K,L}, (i+2)T_b + \tau_{1,1}]$. In this way, the decisions made on the desired ith bits of the K users will only depend on either the $(i-1)$st or $(i+1)$st bits of all users.

Let us from now on consider the simplified scenario of non-dispersive channels associated with $L = 1$. Based on the observation vector $\boldsymbol{z}^{(i)}$ given in Equation (6.7) and then following the analysis carried out in Section 3.4 in the context of a synchronous CDMA system, it can be shown that the correlation metric required for detecting the ith bit of all users within the truncated observation window, given that the K-dimensional vectors $\boldsymbol{b}^{(i-1)}$ and $\boldsymbol{b}^{(i+1)}$ are known to the receiver, can be written as :

$$\Omega\left(\boldsymbol{b}^{(i)}\right) = 2\Re\left\{\boldsymbol{B}^T\boldsymbol{C}^*\boldsymbol{W}\boldsymbol{Z}\right\} - \boldsymbol{B}^T\boldsymbol{C}\boldsymbol{W}\boldsymbol{R}\boldsymbol{W}\boldsymbol{C}^*\boldsymbol{B}, \tag{6.10}$$

where

$$\begin{aligned}
\boldsymbol{B} &= \left[\boldsymbol{b}^{(i-1)^T}, \boldsymbol{b}^{(i)^T}, \boldsymbol{b}^{(i+1)^T}\right]^T \\
\boldsymbol{C} &= \text{diag}\left[\boldsymbol{c}^{(i-1)}, \boldsymbol{c}^{(i)}, \boldsymbol{c}^{(i+1)}\right] \\
\boldsymbol{W} &= \text{diag}\left[\boldsymbol{\xi}, \boldsymbol{\xi}, \boldsymbol{\xi}\right] \\
\boldsymbol{Z} &= \left[\boldsymbol{z}^{(i-1)'}, \boldsymbol{z}^{(i)}, \boldsymbol{z}^{(i+1)''}\right]^T \\
\boldsymbol{R} &= \begin{bmatrix} \boldsymbol{R}'(0) & \boldsymbol{R}^T(1) & \boldsymbol{0} \\ \boldsymbol{R}(1) & \boldsymbol{R}(0) & \boldsymbol{R}^T(1) \\ \boldsymbol{0} & \boldsymbol{R}(1) & \boldsymbol{R}''(0) \end{bmatrix}.
\end{aligned}$$

The vectors $\boldsymbol{z}^{(i-1)'}$ and $\boldsymbol{z}^{(i+1)''}$ represent the correlations of the partial matched filter outputs at instances $[iT_b+\tau_{1,1}-\tau_{N1}, iT_b+\tau_{k,l}]$ and $[(i+1)T_b+\tau_{k,l}, (i+1)T_b+\tau_{K,L}+\tau_{N2}]$, respectively, for $k = 1, 2, \ldots, K$, which are given by :

$$\boldsymbol{z}^{(i-1)'} = \boldsymbol{R}'(0)\boldsymbol{w}\boldsymbol{c}^{(i-1)}\boldsymbol{b}^{(i-1)} + \boldsymbol{R}^T(1)\boldsymbol{w}\boldsymbol{c}^{(i)}\boldsymbol{b}^{(i)} + \boldsymbol{n}^{(i-1)'} \tag{6.11}$$

$$\boldsymbol{z}^{(i+1)''} = \boldsymbol{R}(1)\boldsymbol{w}\boldsymbol{c}^{(i)}\boldsymbol{b}^{(i)} + \boldsymbol{R}''(0)\boldsymbol{w}\boldsymbol{c}^{(i+1)}\boldsymbol{b}^{(i+1)} + \boldsymbol{n}^{(i+1)''}. \tag{6.12}$$

The optimum decision concerning the K-dimensional user bit-related vector $\boldsymbol{b}^{(i)}$, provided that $\boldsymbol{b}^{(i-1)}$ and $\boldsymbol{b}^{(i+1)}$ are known to the receiver, is formulated as

$\hat{\boldsymbol{b}}^{(i)} = \left[\hat{\boldsymbol{b}}_1^{(i)}, \hat{\boldsymbol{b}}_2^{(i)}, \ldots, \hat{\boldsymbol{b}}_K^{(i)}\right]^T$, which maximises the correlation metric given in Equation (6.10). However, in practice the receiver is oblivious of the EEB-related K-dimensional vectors $\boldsymbol{b}^{(i+1)}$ during the detection of $\boldsymbol{b}^{(i)}$, unless they are pilot bits. On the other hand, the SEBs $\boldsymbol{b}^{(i-1)}$ can be derived from the previous detection process and if the DBEP of the receiver is sufficiently low, the SEB-detection errors will not significantly degrade the system's performance. We note at this stage, however that the effects of SEB-detection errors has been taken into account in all of our simulations. Hence, in order to optimise the decision concerning $\boldsymbol{b}^{(i)}$, it is imperative that the EEBs are estimated as reliably as possible. One way of estimating the EEBs is by taking a hard decision based on their maximum ratio combined correlator outputs [96]. This can be written as :

$$\tilde{\boldsymbol{b}}_{MF}^{(i+1)} = \text{sgn}\left\{\text{diag}\left[\boldsymbol{I}_L, \ldots, \boldsymbol{I}_L\right]\left[\boldsymbol{c}^{(i+1)^*}\boldsymbol{\xi}\boldsymbol{z}^{(i+1)''}\right]\right\}, \tag{6.13}$$

where $\boldsymbol{I}_L$ is a $1 \times L$ unity vector and the K-dimensional vector $\tilde{\boldsymbol{b}}_{MF}^{(i+1)}$ denotes the tentative decisions concerning the EEBs based on the hard decision of the correlator. In this treatise, this approach of detecting the EEBs is denoted as Strategy 1 or S1. GAs are then invoked in order to estimate the current bits by optimising the correlation metric of Equation (6.10) with respect to the K-dimensional vector $\boldsymbol{b}^{(i)}$, yielding :

$$\hat{\boldsymbol{b}}^{(i)} = \arg\left\{\max_{\boldsymbol{b}^{(i)}}\left[\Omega\left(\boldsymbol{b}^{(i)}\right)\right]\right\}. \tag{6.14}$$

However, due to the presence of MAI, as shown in Equation (6.12) and Equation (6.13), the EBEP is high, especially in a worst-case single-path scenario, where no diversity gain is achieved. This high EBEP will have a significant detrimental impact on the overall performance of the detector, as we shall see in Section 6.4. Hence, in order to reduce the EBEP, we invoke the proposed GA for improving the tentative decision accuracy of the EEBs $\boldsymbol{b}^{(i+1)}$, and at the same time we optimise the correlation metric in order to detect $\boldsymbol{b}^{(i)}$. In this case, the correlation metric is expressed as :

$$\Omega\left(\boldsymbol{b}^{(i)}, \boldsymbol{b}^{(i+1)}\right) = 2\Re\left\{\boldsymbol{B}^T\boldsymbol{C}^*\boldsymbol{W}\boldsymbol{Z}\right\} - \boldsymbol{B}^T\boldsymbol{C}\boldsymbol{W}\boldsymbol{R}\boldsymbol{W}\boldsymbol{C}^*\boldsymbol{B}, \tag{6.15}$$

since the desired K-dimensional bit vector $\boldsymbol{b}^{(i)}$ and the K-dimensional EEB vector $\boldsymbol{b}^{(i+1)}$ now jointly constitute the decision variables. Again, this approach of detecting the EEBs based on GAs is denoted here as Strategy 2 or S2. Hence, the estimated transmitted bit vector $\hat{\boldsymbol{b}}^{(i)}$ of the K users can be found by optimising Equation (6.10)

with respect to the desired bits $\boldsymbol{b}^{(i)}$ and the EEBs $\boldsymbol{b}^{(i+1)}$, yielding :

$$\hat{\boldsymbol{b}}^{(i)}, \tilde{\boldsymbol{b}}_{GA}^{(i+1)} = \arg \left\{ \max_{\boldsymbol{b}^{(i)}, \boldsymbol{b}^{(i+1)}} \left[\Omega \left(\boldsymbol{b}^{(i)}, \boldsymbol{b}^{(i+1)} \right) \right] \right\}, \tag{6.16}$$

where $\tilde{\boldsymbol{b}}_{GA}^{(i+1)}$ denotes the tentative decisions concerning the EEBs based on GA-assisted optimisation. In the next section we will further augment the philosophy of our GA-assisted multiuser detector used for simultaneously estimating both the desired users' bits and the EEBs.

6.3 GA-Assisted Multiuser Detection in Asynchronous CDMA Systems

The flowchart of the GAs invoked for detecting the users transmitted bits in an asynchronous CDMA system is depicted in Figure 6.3.

Apart from the initialisation phase, the main structure of the GA is identical to that employed in Figure 3.10 for detecting the users' transmitted bits in the symbol-synchronous CDMA system of Chapter 3. Hence we will be using the fitness-proportionate selection scheme in conjunction with a uniform crossover operation and a standard binary mutation operation as well as invoking the incest prevention strategy and elitism strategy, as shown in Figure 6.3. However, the structure of the individual adopted here is slightly different, since we have to take into account the SEBs and the EEBs. Each individual will consist of $3 \times K$ antipodal bits. Assuming that the current desired signalling interval is the ith interval, we shall express the pth individual here as $\tilde{\boldsymbol{b}}_p(y) = \left[\hat{\boldsymbol{b}}_{p,SEB}^{(i-1)}, \tilde{\boldsymbol{b}}_p^{(i)}(y), \tilde{\boldsymbol{b}}_{p,EEB}^{(i+1)}(y) \right]$, where $\hat{\boldsymbol{b}}_{p,SEB}^{(i-1)}$, $\tilde{\boldsymbol{b}}_p^{(i)}(y)$ and $\tilde{\boldsymbol{b}}_{p,EEB}^{(i+1)}(y)$ are K-bit vectors which denote the SEBs, the desired bits and the EEBs at the yth generation, respectively. The fitness value associated with each individual, denoted as $f\left[\tilde{\boldsymbol{b}}_p(y)\right]$ for $p = 1, \ldots, P$ is then computed by substituting the corresponding vectors $\hat{\boldsymbol{b}}_{p,SEB}^{(i-1)}$, $\tilde{\boldsymbol{b}}_p^{(i)}(y)$ and $\tilde{\boldsymbol{b}}_{p,EEB}^{(i+1)}(y)$ into the correlation metric of Equation (6.10) and then using it as exponent, in order to obtain positive fitness values. Based on the evaluated fitness value, a new population of P individuals is created for the $(y+1)$st generation with the aid of the various processes, as illustrated in Figure 6.3. The explicit description of each of the process can be found in Chapter 2 and Chapter 3. Upon the GA's termination at the Yth generation, as shown in Figure 6.3, the desired bit vector $\tilde{\boldsymbol{b}}_p^{(i)}(Y)$ of the individual corresponding to the highest fitness value in the population constitutes the detected K users' ith

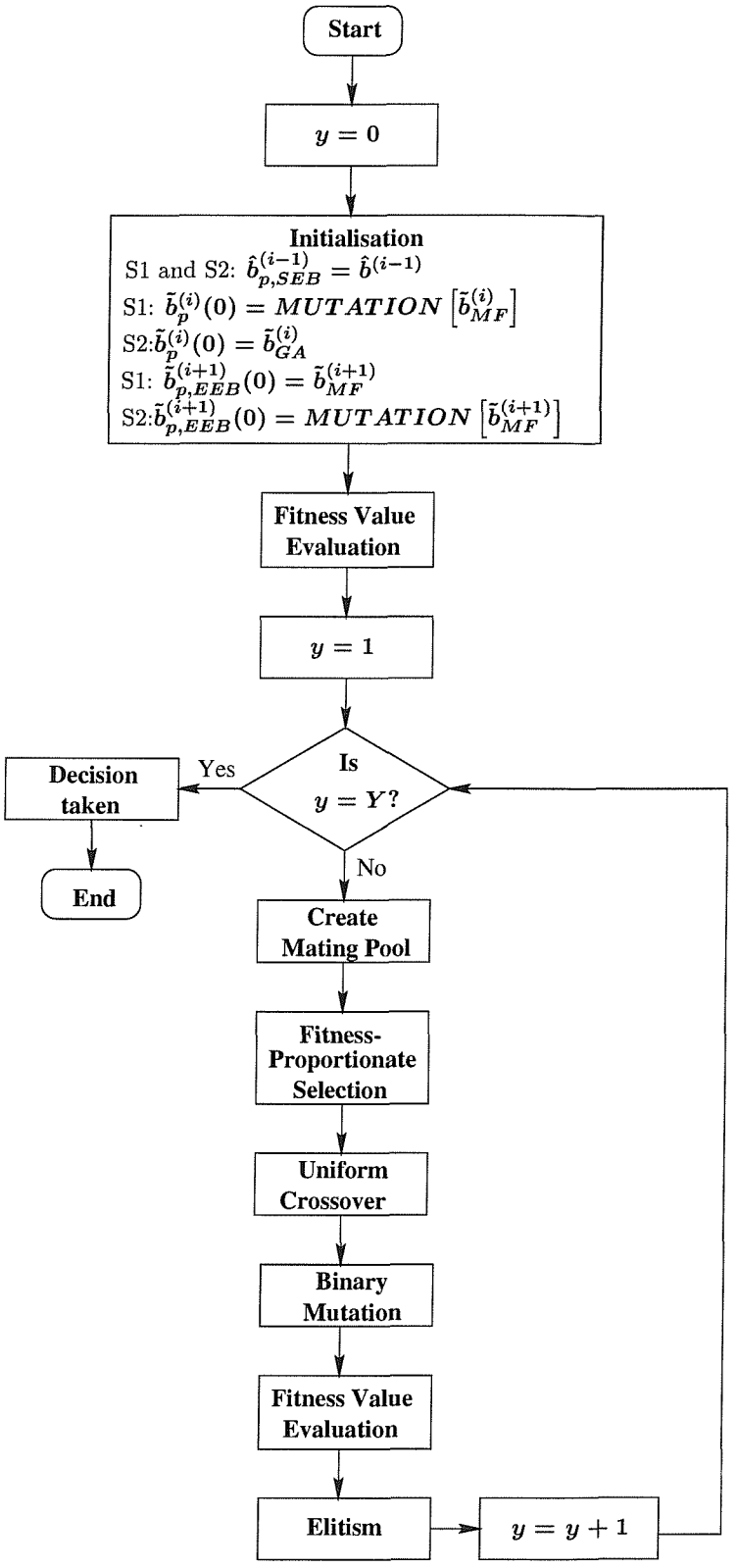

Figure 6.3: A flowchart depicting the structure of the proposed genetic algorithm used for detecting the transmitted users' bit $\boldsymbol{b}^{(i)}$ as well as providing the tentative solutions of $\boldsymbol{b}^{(i+1)}$ during the ith truncated observation window.

bit associated with the truncated observation window interval considered. In other words, we have $\hat{\boldsymbol{b}}^{(i)} = \tilde{\boldsymbol{b}}_j^{(i)}(Y)$, where $\tilde{\boldsymbol{b}}_j(Y) = \max\left\{f\left[\tilde{\boldsymbol{b}}_1(Y)\right], \ldots, f\left[\tilde{\boldsymbol{b}}_P(Y)\right]\right\}$.

As seen in Figure 6.3, the GA must be initialised for every new truncated observation window before commencing the optimisation process. Similarly to the GA initialisation invoked in the symbol-synchronous CDMA system of Chapter 3, we can exploit the information already available at the beginning of each detection step, in order to aid and accelerate the optimisation. Again, let us assume that the current bit of interest is the ith bit of all users. Hence, the SEB vector will be constituted by the $(i-1)$st bits, while the EEBs by the $(i+1)$st bits. At this point, the SEBs will have been detected in the previous truncated observation window, when the $(i-1)$st bits were the desired bits, i.e. $\hat{\boldsymbol{b}}^{(i-1)}$ will be known. Therefore, we can assign $\hat{\boldsymbol{b}}_{p,SEB}^{(i-1)} = \hat{\boldsymbol{b}}^{(i-1)}$ for all p. It is well-known that the computational complexity – in the context of the population size P and the number of generations Y – of the GA required to attain a specified level of performance increases with the number of variables to be optimised [31]. Hence, in order to reduce the computational complexity of the GA, the SEBs will not be involved in the optimisation process, since these SEBs have been detected previously and modification of the SEBs will not affect the performance of the detector significantly. Thus the generation index y is omitted for the SEB vector.

6.3.1 Matched Filter-Assisted EEB Estimation

It is now clear that the unknown variables involved in the optimisation process consist of the current desired bits as well as the EEBs. As mentioned before, here two methods are investigated in order to provide tentative solutions for the EEBs. **In our first method denoted here as S1**, we invoke the hard decisions obtained from the users' correlator outputs as the tentative EEBs, according to Equation (6.13). Hence :

$$\tilde{\boldsymbol{b}}_{p,EEB}^{(i+1)}(y) = \tilde{\boldsymbol{b}}_{MF}^{(i+1)} \quad \text{for } p = 1, \ldots, P \text{ and } y = 0, \ldots, Y. \tag{6.17}$$

The error probability of these EEBs estimated on the basis of the correlator outputs is generally excessive and therefore it will degrade the performance of the optimisation process, as we will see later in Section 6.4. Given these EEBs in this case, only the current desired bits are involved in the GA-assisted optimisation process. During the initialisation phase of Figure 6.3, the desired bit vector of each individual is a 'mutated' version of the tentative hard decisions. In other words, we will change the state of each bit of $\tilde{\boldsymbol{b}}_{MF}^{(i)}$ with a probability of p_{m1}. Typically, the value of p_{m1} is

governed by the BEP that can be achieved by the correlator and a practical choice is to set $p_{m1} = BEP$. In this treatise, we shall set a nominal value of $p_{m1} = 0.1$. Hence :

$$\tilde{\boldsymbol{b}}_p^{(i)}(0) = MUTATION\left[\tilde{\boldsymbol{b}}_{MF}^{(i)}\right]_{p_{m1}=0.1} \quad \text{for } p = 1, \ldots, P. \tag{6.18}$$

The mutation process [41] of Equation (6.18) is used for ensuring that the GA has a highly diversified search range at the beginning of its operation as well as for providing dissimilar individuals. Without this mutation process all the individuals at the initialisation stage would be identical, which is not allowed by the incest prevention strategy. After initialisation, the GA will commence searching for the optimum solution. The main advantage of the strategy S1 is that since only K variables are considered, the population size P required to attain a specified optimisation quality associated with a given DBEP can be lower.

6.3.2 GA-Assisted EEB Estimation

In our second method denoted here as S2, the GA is invoked in order to lower the EBEP. At the 0th generation, the unknown EEB $\tilde{\boldsymbol{b}}_p^{(i+1)}(0)$, $p = 1, \ldots, P$, can be initially estimated based on the hard decisions of the correlator outputs of Figure 6.1. This is equivalent to using S1 at the 0th generation. Again, these bits are mutated with a probability of $p_{m1} = 0.1$ in order to ensure a diversified search. Hence the mutation process is identical to that of Equation (6.18) used in S1, but it is applied to the edge bits at index $(i + 1)$ yielding :

$$\tilde{\boldsymbol{b}}_p^{(i+1)}(0) = MUTATION\left[\tilde{\boldsymbol{b}}_{MF}^{(i+1)}\right]_{p_{m1}=0.1} \quad \text{for } p = 1, \ldots, P. \tag{6.19}$$

Let us now assume that upon termination of the GA-assisted search at the end of every truncated observation window, the error probability of the EEBs will be sufficiently low and hence these bits can be considered as the tentative solutions for the GA during initialisation, when these EEBs become the desired bits in the next truncated observation window. Hence according to Equation (6.16) we have :

$$\tilde{\boldsymbol{b}}_p^{(i)}(0) = \tilde{\boldsymbol{b}}_{GA}^{(i)} \quad \text{for } p = 1, \ldots, P. \tag{6.20}$$

where $\tilde{\boldsymbol{b}}_{GA}^{(i)}$ is specified by Equation (6.16). After initialisation, the GAs are then invoked in order to search for the K users' desired bit vector as well as for the EEB vector that optimises the correlation metric according to Equation (6.16). The advantage of the S2 strategy is that the optimisation performance is not limited by the high EBEP exhibited by the correlator outputs. On the other hand, since

there are now $2K$ variables to be optimised, a higher population size P is required in order to attain a specified level of performance.

6.3.3 Complexity Issues

Since our proposed GA-assisted multiuser detector optimises the correlation metric of Equation (6.10), we will only consider its complexity in terms of the number of correlation metric computations required for the optimisation. The optimum multiuser detector using exhaustive search requires 2^K evaluations of the correlation. By contrast, our proposed detector requires a maximum of $Y \times P$ correlation metric evaluations. In fact, the number of such correlation metric evaluations can be reduced by avoiding repeated evaluations of identical individuals, either within the same generation or across the entire iteration process, if the receiver has the necessary memory. We note that since the EEBs of strategy S1 are fixed throughout the iteration process, the number of additions and multiplications per correlation metric evaluation will be a factor KL lower, than that of strategy S2, since they do not have to be re-computed.

Before we present our simulation results, we should note here that the employment of our proposed GA-based multiuser detector is not restricted to joint bit-by-bit detection. The truncated observation window can actually span over several users' bits. In such cases, the individuals of the GA must contain an increased number of bits. However, since there are more unknown bits to be detected, a higher P and more generations must be invoked.

6.4 Simulation Results

In this section, our computer simulation results are presented, in order to characterise the DBEP performance of the GA-assisted multiuser detector employing the two EEB estimation strategies highlighted in the previous section. All the results in this section were based on evaluating the DBEP performance of a chip-asynchronous 10-user CDMA system over both single-path and two-path Rayleigh fading channels. For ease of simulation, the relative delays between the different received signals were arranged in the single-path scenario such that $\tau_{j+1,1} - \tau_{j,1} = \left[\frac{T_c}{8}, T_c\right)$. Hence for a system supporting $K = 10$ users, the maximum delay between the 1st user and the highest-delay Kth user is 10 chips. Since the chip duration is about $\frac{1}{64000} \times \frac{1}{31} \approx 0.5\mu sec$, assuming a bit rate of 64 kbps and a spreading factor of 31, the 10-chip maximum propagation delay difference corresponds to about $5\mu sec$. This scenario would be encountered by two mobiles, where the 1st user is directly at the

Parameter	Value
Spreading factor N_c	31
Modulation mode	BPSK
Number of CDMA users K	10, unless stated otherwise
Number of multipaths L	1 and 2

Table 6.1: Simulation parameters for the experiments of Figures 6.4-6.11.

base station and the Kth user is for example directly at the edge of a 1500m-radius propagation cell, where the radio waves' propagation delay becomes $5\mu sec$. Given this maximum propagation delay, the truncated observation window of Figure 6.2 can encompasses between 0 to 20 chips of the EEBs and SEBs. Hence in our simulations, we considered an average scenario associated with $t_{N1} = t_{N2} = 10$ chips in Figures 6.4-6.10. The BEP performance difference between the two extreme cases of 0 and 20 chips, respectively, will be shown in Figure 6.11. For the two-path scenario, the relative delays were arranged according to $\tau_{j,2} - \tau_{j,1} = \left[\frac{T_c}{8}, T_c\right)$ and $\tau_{j+1,1} - \tau_{j,2} = \left[\frac{T_c}{8}, T_c\right)$. The two paths were assumed to have equal average received energy, i.e. $E\left[\alpha_{k,1}\right] = E\left[\alpha_{k,2}\right] = 0.5$. The processing gain was $N_c = 31$ and the signature sequences were randomly generated. Perfect power control and CIR estimation was assumed for all the simulations. We also assumed that the first bit $\boldsymbol{b}^{(0)}$ of all the users was known to the receiver. A summary of the simulation parameters and the GA configuration is given in Table 6.1 and Table 6.2, respectively. Upon observing the GA configuration of Table 6.2, we can see that there are a couple of parameters, which are different from those presented in the previous chapters, namely the mating pool size T and the probability of mutation p_m for S2. The probability of mutation adopted here can be readily justified. As mentioned in Section 6.3.2, there are $2 \times K$ decision variables, comprising the desired bits and the EEBs, to be optimised for S2. In Section 3.5.3, it was shown that the BEP performance of the GA-assisted multiuser detector critically depends on the value of p_m for a specific number of decision variables. From Figure 3.4, we can see that for $K = 20$ users, it is desirable to have $p_m < 0.1$, in order to obtain a lower BEP. Since employing S2 for $K = 10$ users is analogous to a 20-user synchronous CDMA system scenario, we decided to adopt $p_m = 0.05$ for the mutation process. For S1, the value of p_m remains at 0.1, since it involves the same number of decision variables as in the previous chapters. This hypothesis can be extended to the case of $K = 15$ users. The choice of the mating pool size T for S2 will be explained next.

Setup/Parameter	Method/Value
Individual initialisation method	According to Figure 6.3
Selection method	Proportionate-Fitness
Crossover operation	Uniform crossover
Mutation operation	Standard binary mutation
Elitism	Yes
Incest Prevention	Yes
Population size P	Given in the associated plots
Number of generations Y	10
Mating pool size T	- S1 : All dissimilar individuals in the population - S2 : Given in the associated plots
Probability of mutation p_{m1} and p_m for $K = 10$	- S1 : 0.1 and 0.1, respectively - S2 : 0.1 and 0.05, respectively
Probability of mutation p_{m1} and p_m for $K = 15$ of Figure 6.10	- S1 : 0.1 and 0.07, respectively - S2 : 0.1 and 0.03, respectively

Table 6.2: Configuration of the GA used to obtain the results of Figures 6.4-6.11. Explicit description of the fitness-proportionate selection scheme, the uniform crossover operation and the floating point mutation operation can be found in Section 2.4.2, Section 2.4.3 and Section 2.4.4, respectively.

6.4.1 Effects of the Mating Pool Size

Let us first consider the achievable BEP over the course of 10 generations for both S1 and S2 in conjunction with a mating pool size equivalent to the number of non-identical individuals, i.e. $T \leq P$ as well as using $T = 4$. The results are shown in Figure 6.4 for an SNR value of 36 dB over single-path fading Rayleigh fading channels. It can be seen that for GAs employing S1, there is no significant difference in the BEP attained over the course of the evolution for mating pool sizes of $T \leq P$ and $T = 4$. This also proves that our results obtained in the previous chapters are relatively consistent, since the approach we adopted in those chapters is identical to GAs employing S1. On the other hand, for GAs employing S2, a substantial difference in the achievable BEP can be observed between the mating pool sizes of $T \leq P$ and $T = 4$.

This phenomenon can be explained by considering the distribution of the probability of selection p_i corresponding to the individuals having the highest fitness value after the initialisation phase of Figure 6.3. The corresponding selection distribution curves for the GAs employing S1 and S2 are shown in Figure 6.5 and Figure 6.6, respectively. ¿From Figure 6.5, the probability of selection corresponding to the individual having the highest fitness value for the GA employing S1 has a similar distribution for both $T \leq P$ and $T = 4$. From this observation, we can

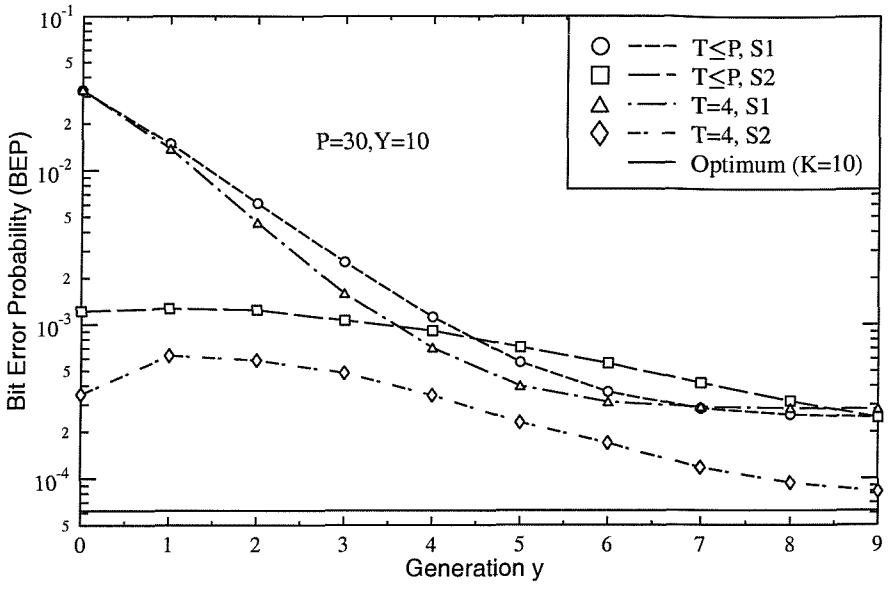

Figure 6.4: The desired bits' error probability with respect to the number of generations for the GA-assisted multiuser detector over narrow-band Rayleigh fading channels employing the EEB detection strategies S1 and S2 with a population size of $P = 30$ using random signature sequences of length $N_c = 31$ and supporting $K = 10$ users at an SNR value of 36 dB. The GA configuration and the simulation parameters used are listed in Table 6.2 and Table 6.1, respectively.

conclude that for GAs employing S1, there is only a handful of individuals having relatively high fitness values that dominate the population. Furthermore, since the initial individuals are generated based on the matched filter output according to Equation (6.18), their fitness values are far from optimum and hence the random process of mutation may substantially increase some of these fitness values.

On the other hand, the distribution of the probability of individual selection for GAs employing S2 is different for $T \leq P$ and $T = 4$, as seen from Figure 6.6. In particular, for $T \ll P$ we see that the selection pdf peak is around the region of 0.2. This implies that most of the time the selection probability of the fittest individual is only about 0.2. This implies a weakly selective process, as highlighted in Section 2.4.2, which reduces the convergence rate. The reason for this weakly selective process is because the EEBs now have a significantly lower BEP due to their GA-assisted estimation, which are used for the initialisation of the desired bits in the subsequent truncated observation window. Hence the fitness values of all the individuals are relatively high, exhibiting near-optimum values. As a result, a high number of individuals will have similar fitness values, which ultimately reduces

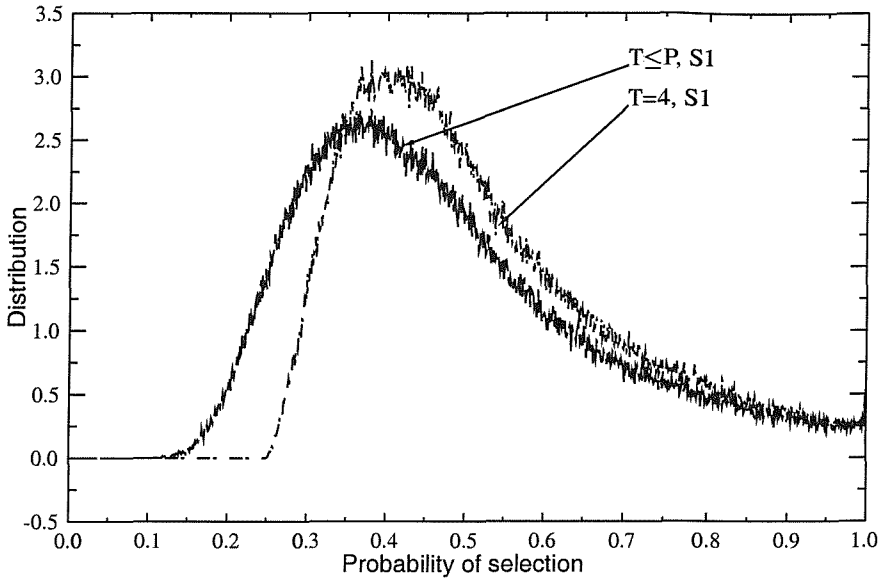

Figure 6.5: Distribution of the probability of selection corresponding to the individual having the highest fitness value at the 0th generation for the GA-assisted multiuser detector over narrow-band Rayleigh fading channels employing the EEB detection strategy S1 with a population size of $P = 30$ using random signature sequences of length $N_c = 31$ and supporting $K = 10$ users at an SNR value of 36 dB. The GA configuration and the simulation parameters used are listed in Table 6.2 and Table 6.1, respectively.

the probability of selection for each individual. By contrast, a majority of the probability of selections for $T = 4$ centres around the region of 0.3. This provides further evidence of the argument that the majority of the individuals have almost equal fitness values, since the lowest probability of selection for $T = 4$ is 0.25, when these 4 individuals have the same probability of selection. Hence, by using a small mating pool, we can place more emphasis on the individuals exhibiting high fitness values.

Figure 6.7 and Figure 6.8 shows the DBEP performance and the EBEP performance, respectively, against the average SNR per bit for the GA-assisted multiuser detector supporting $K = 10$ users, when employing the two EEB estimation strategies. The single-user bound was computed using Equation (5.12), with L_d replaced by L. As Figure 6.7 shows, the DBEP of the GA-assisted multiuser detector employing S1 was inferior compared to that of S2. The error floor observed for S1 in the single-path scenario was caused by the high EBEP, as seen in Figure 6.8. In this case, the GA-assisted multiuser detector was termed as EEB interference-limited. The same can be said for the two-path scenario. On the other hand, we

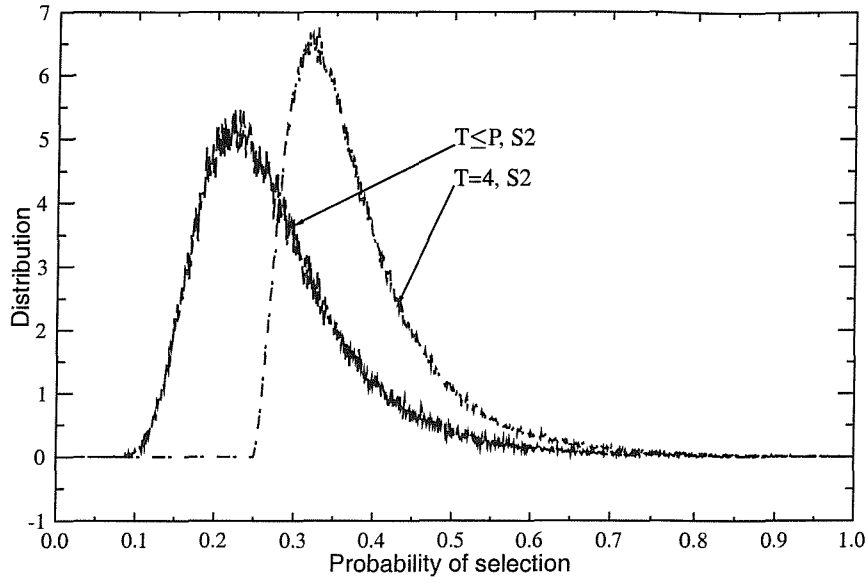

Figure 6.6: Distribution of the probability of selection corresponding to the individual having the highest fitness value at the 0th generation for the GA-assisted multiuser detector over narrow-band Rayleigh fading channels employing the EEB detection strategy S2 with a population size of $P = 30$ using random signature sequences of length $N_c = 31$ and supporting $K = 10$ users at an SNR value of 36 dB. The GA configuration and the simulation parameters used are listed in Table 6.2 and Table 6.1, respectively.

can see from Figure 6.8 that the EBEP upon employing S2 is fairly low. As a result, the performance of the GA-assisted multiuser detector utilising this strategy was not limited by the EEB errors and hence it was capable of achieving a near-optimum single-user-like DBEP performance. Furthermore, in comparison to the 'brute-force' ML detector requiring $2^{10} = 1024$ correlation metric evaluations, our proposed multiuser detector is substantially less complex, requiring only a maximum of $10 \times 30 = 300$ correlation metric evaluations, yet performing close to the optimum performance.

The notion of an EEB interference-limited DBEP performance employing strategy S1 is further substantiated in Figure 6.9, which characterises the DBEP performance of the proposed detector for a population size of $P = 20$. Naturally, we would expect the performance to degrade as compared to Figure 6.7, when the population size P decreases. As seen in the figure for both the one-path and two-path scenarios, the DBEP performance of the proposed detector employing strategy S1 did not show significant degradation in comparison to that associated with $P = 30$, as illustrated in Figure 6.7. This is due to the fact that the EBEP is the same for

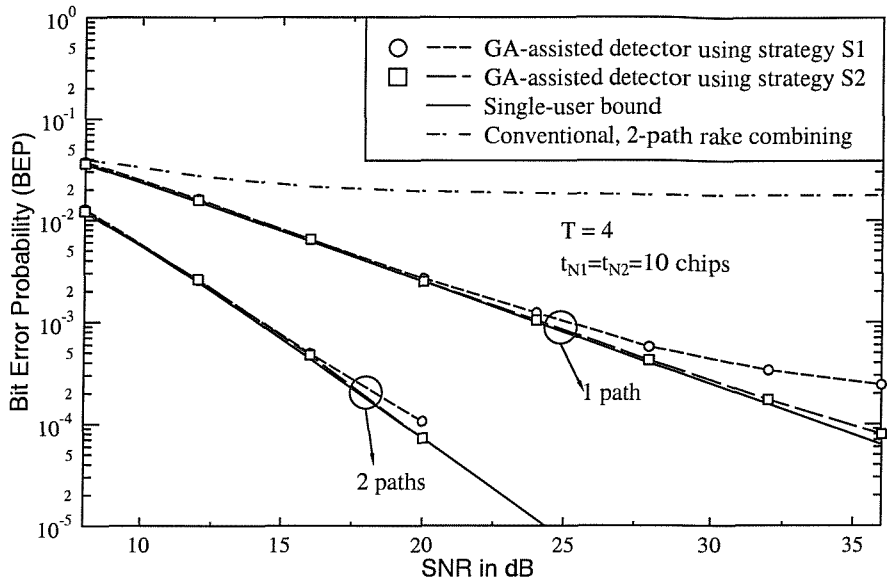

Figure 6.7: The **desired bits'** error probability for the GA-assisted multiuser detector over Rayleigh fading channels employing the EEB detection strategies S1 and S2 with a population size of $P = 30$ using random signature sequences of length 31 and supporting $K = 10$ users. The GA configuration and the simulation parameters used are listed in Table 6.2 and Table 6.1, respectively.

both $P = 30$ and $P = 20$ and hence the corresponding DBEP performances are limited by the poor reliability of the EEBs. This becomes explicit in comparison to the curve characterising the scenario using perfect knowledge of the SEBs and EEBs, which exhibited a near-single-user DBEP performance even for $P = 20$. On the other hand, for detectors employing strategy S2, a degradation can be observed for $P = 20$ compared to that for $P = 30$, as shown in Figure 6.7. This is because in this case there are $2K$ variables to be optimised and therefore a higher population size is required in order to achieve optimum performance. Hence, when $P = 20$, the performance of the detector is degraded. In this case, we referred to the DBEP performance as 'GA-limited'.

Figure 6.10 shows the DBEP performance of our proposed multiuser detector for $K = 15$ users. Because of the higher number of variables to be optimised, we increased the population size P to 40 and 50. We note from the figure that for $P = 40$, the GA employing strategy S1 now exhibits a more significant degradation in terms of its DBEP performance with respect to the single-user bound, than that employing strategy S2. This is due to the fact that as the number of users increases, the EBEP becomes higher. Increasing the population size to 50 does not show any

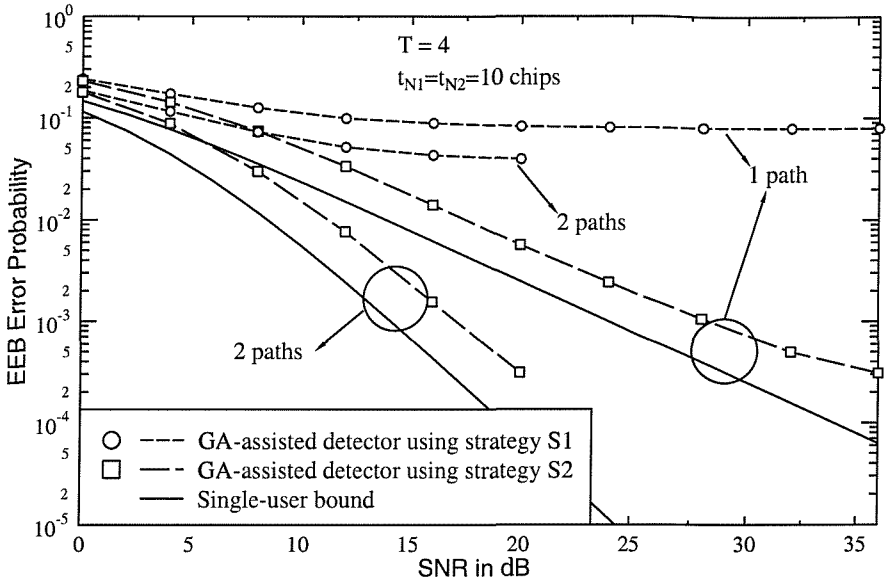

Figure 6.8: The **EEBs'** error probability performance for the GA-assisted multiuser detector over Rayleigh fading channels employing the EEB detection strategies S1 and S2 with a population size of $P = 30$ using random signature sequences of length 31 and supporting $K = 10$ users. The GA configuration and the simulation parameters used are listed in Table 6.2 and Table 6.1, respectively.

significant improvement using the same strategy, since the performance is limited by the EEB interference. We also note that for $P = 40$ the DBEP performance of GAs employing strategy S2 did not match the single-user bound, even though it outperformed strategy S1. This is due to the limited population size, which was too small for optimising 2×15 variables. However, by increasing P to 50, the DBEP performance becomes near-optimum. Hence, while achieving a superior performance, the associated additional computational complexity has to be tolerated. An important observation is that when K is increased from 10 to 15 users, a near-optimum DBEP performance can be maintained by increasing the population size P from 30 to 50, while keeping $Y = 10$ and employing strategy S2. This constitutes a factor of 5/3 increase in the number of correlation metric computations. On the other hand, the computational complexity of the conventional optimum detector using brute-force optimisation is increased by a factor of $2^5 = 32$.

All the simulation results we have seen so far were based on a truncated window size of $t_{N1} = t_{N2} = 10$ chips[2]. This corresponds to a minimum spreading factor

[2]We have set $t_{N1} = t_{N2}$ in order to arrive at a symmetric truncated window for ease of simulation

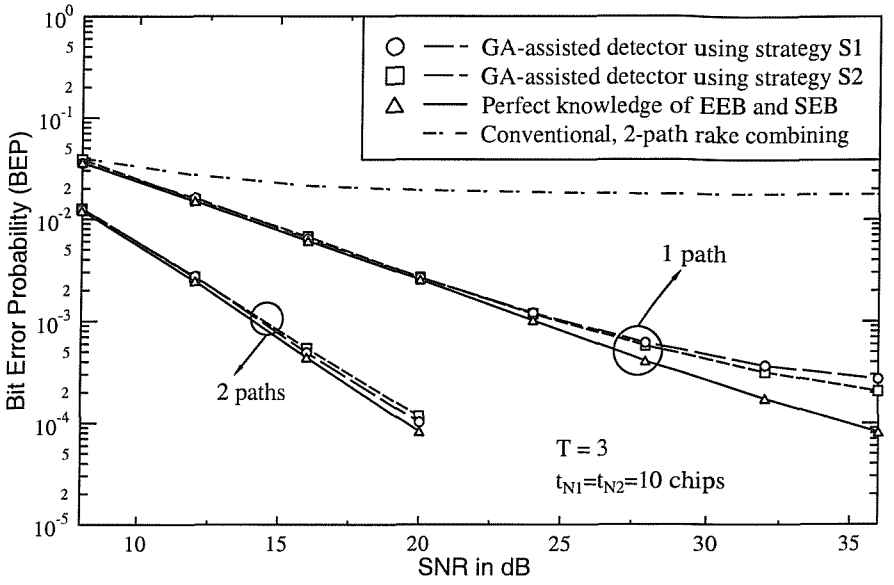

Figure 6.9: The **desired bits'** error probability performance for the GA-assisted multiuser detector over Rayleigh fading channels employing the EEB detection strategies S1 and S2 with a population size of $P = 20$ using random signature sequences of length 31 and supporting $K = 10$ users. The GA configuration and the simulation parameters used are listed in Table 6.2 and Table 6.1, respectively.

of 10 for both the SEBs and EEBs. The effects of the window size on the SEB error probability can be ignored, since these bits have been detected previously. On the other hand, the EEBs have to be tentatively detected based on only the reduced spreading factor. In practice, it is not always possible to set $t_{N1} = t_{N2} = 10$ chips. The worst case would be $t_{N1} = t_{N2} = 0$ chips, while the ideal case would be $t_{N1} = t_{N2} = \tau_{1,1} - \tau_{K,L} + T_b$ chips. We studied the effects of varying the window size on the DBEP performance based on these two settings and the associated results are shown in Figure 6.11.

We can see that for a narrow window size of $t_{N1} = t_{N2} = 0$ chips, the performance of the detectors employing strategy S1 deteriorates more significantly compared to the scenario using a wider window size of $t_{N1} = t_{N2} = 20$ chips, when employing strategy S2. This implies that the DBEP performance of detectors using the EEBs based on the hard decisions of the correlator outputs in Figure 6.1 are more sensitive to the varying window size, than those invoking GA-assisted EEB detection.

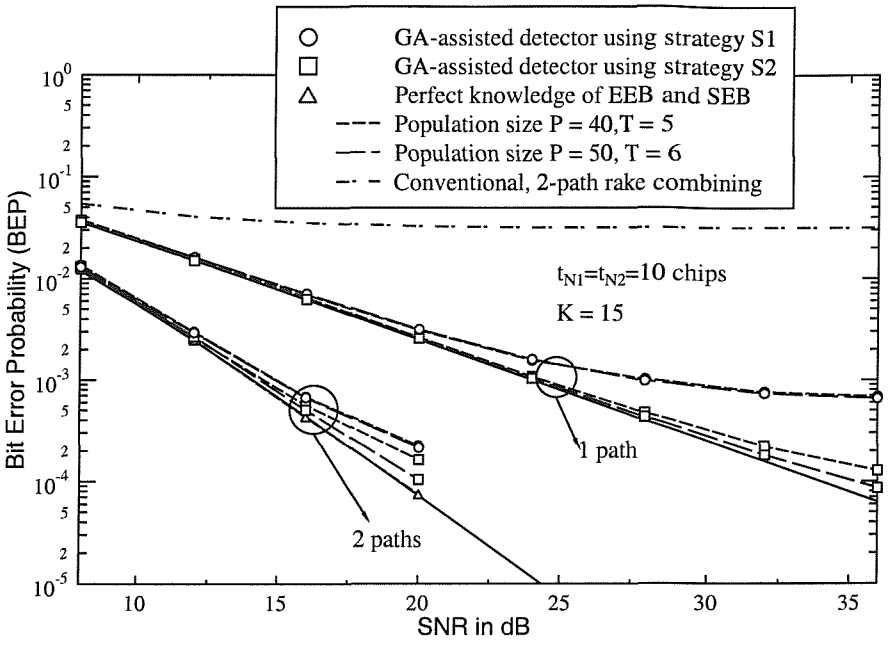

Figure 6.10: The **desired bits'** error probability performance for the GA-assisted multiuser detector over Rayleigh fading channels employing the EEB detection strategies S1 and S2 with population sizes of $P = 40$ and $P = 50$ using random signature sequences of length 31 and supporting $K = 15$ users. The GA configuration and the simulation parameters used are listed in Table 6.2 and Table 6.1, respectively.

6.5 Chapter Summary and Conclusions

In this chapter, we considered an asynchronous CDMA system communicating over a dispersive Rayleigh fading channel, as presented in Section 6.2. The correlation metric based on a truncated window size was also formulated. We then developed a GA-assisted multiuser detector for this model in Section 6.3, in order to search for the particular bit sequence that optimises the correlation metric. Two strategies were evaluated for providing tentative decisions concerning the EEBs. In the first approach, as highlighted in Section 6.3.1, the EEBs were tentatively detected based on the hard decisions at the correlator outputs. The desired bits within the truncated observation window were detected using GAs. In our second approach presented in Section 6.3.2, GAs were invoked in order to improve the EBEP and at the same time to detect the desired bits within the window. Our simulation results presented in Section 6.4 showed that the DBEP performance of the detectors using the first approach were limited by the high error rate of the EEBs. On the other hand, using the same number of correlation metric evaluations, detectors employing the second approach can achieve a near-optimal DBEP performance at the cost of a

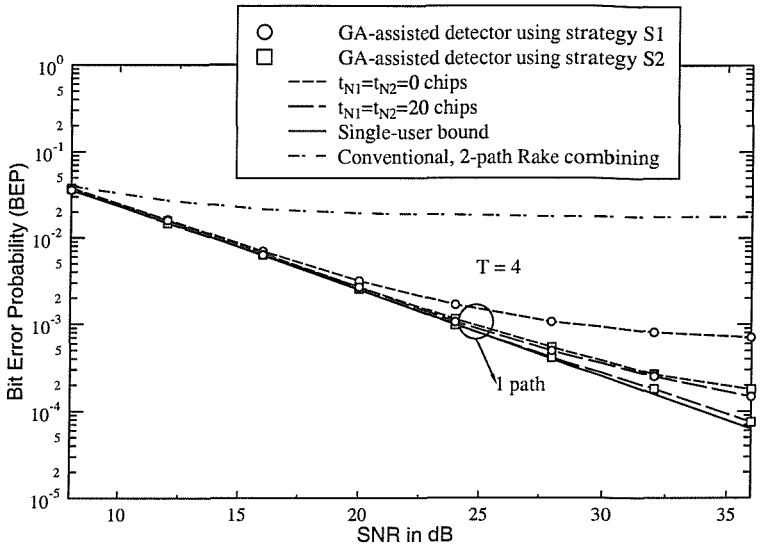

Figure 6.11: The **desired bits'** error probability performance for the GA-assisted multiuser detector over Rayleigh fading channels employing the EEB detection strategies S1 and S2 with a population size of $P = 30$ using random signature sequences of length 31 and supporting $K = 10$ users with various truncated window sizes. The GA configuration and the simulation parameters used are listed in Table 6.2 and Table 6.1, respectively.

lower number of correlation metric evaluation compared to the optimum multiuser detector using a brute-force approach. Furthermore, both the EEBs and the desired bits are detected by the same GAs, resulting in potential complexity savings.

CHAPTER 7

Conclusions and Discussion

This concluding chapter summarises the results that were presented in this dissertation, and our suggestions for further work are outlined.

7.1 Summary and Conclusions

This dissertation is concerned with the application of GAs in CDMA multiuser detection, in order to circumvent the complexity problem that arises when employing an optimum multiuser detector.

A basic overview of GAs employed as optimisation tools was presented in Chapter 2. The terms and definitions that are associated with GAs were introduced. In order to justify the employment of GAs, an example was provided, which showed how a GA performed a search for the optimum solution. From the example, we observed that the GA identifies high-fitness individuals and exploits similarities amongst the individuals. Based on this concept, the notion of schema was introduced by Holland [29], which can be used in predicting the behaviour of GAs over the course of the evolution. This led to the derivation of the schema theorem, as formulated by Holland [29]. Since its introduction in the 1970s, numerous variants of GAs have been developed, each of which was found to be suited for solving specific problems. Hence the general concensus is that GAs should not be treated as off-the-shelf optimisation algorithms that are expected to solve every problem efficiently. Some of the more popular operations and strategies that constituted a

GA were highlighted, which were subsequently investigated, in order to determine their usefulness in the context of our multiuser detection problem.

We commenced our study of GA-assisted CDMA multiuser detectors by first considering a symbol-synchronous CDMA system supporting K users over an AWGN channel as well as a non-dispersive Rayleigh fading channel. Having established the mathematical notations that were adopted in the dissertation, we proceeded to derive the correlation metric of Equation (3.23) as formulated by Verdu [1] for the optimum multiuser detector. It can be seen that for attaining the optimum BEP performance, every possible K-bit combination must be tested, in order to find the combination that maximises the correlation metric. Hence the optimum multiuser detector has a computational complexity that is exponentially proportional to the number of users to be detected. Thus its implementation becomes impractical, when there is a high number of users. Hence the GA-assisted multiuser detector was proposed, in order to circumvent this complexity problem. According to our results obtained in Section 3.5, we demonstrated that the type of GA operations and strategies invoked can have a significant impact on the convergence rate and hence also on the resulting BEP and on the complexity of the detector. Upon comparing our proposed schemes to other similar GA-assisted multiuser detectors proposed for example by Juntti *et al.* [65], Wang *et al.* [66] and Ergün *et al.* [67,68], we can see the reasons why they have concluded that GAs are not particularly promising for implementation in CDMA multiuser detectors. However, we have made no claims concerning the optimality of our adopted GA configuration, which was invoked in our GA-assisted multiuser detector, since we have only investigated a fraction of the potentially suitable GA implementations. Based on our adopted GA configuration characterised in Table 3.9, we can see that the GA-assisted multiuser detector is capable of achieving a near-optimum BEP performance over both AWGN channels as well as over non-dispersive Rayleigh fading channels with the assistance of perfect CIR coefficient estimation. This can be achieved at a significantly lower computational complexity than that required by the optimum multiuser detector.

We have demonstrated that the GA-assisted multiuser detector is capable of achieving the near-optimum BEP performance up to a certain channel SNR value with the aid of the perfect knowledge of the users' CIR coefficients. In reality, these CIR coefficients must be estimated at the receiver. Conventional CIR estimation schemes requires the transmission of known pilot symbols from each user, in order to assist the CIR estimator at the receiver in acquiring the users' CIR coefficients. However, pilot-symbol based estimation will reduce the throughput and bandwidth efficiency of the system. Furthermore, a training period is required for adaptive

filter-based CIR estimation, such as the Kalman filter [18], in order to acquire and update the filter tap weights. We noticed that the correlation metric of Equation (3.23) requires that the users' CIR coefficients be known. However, by treating these CIR coefficients as unknown variables, we can employ GAs also for jointly estimating the CIR coefficients as well as the transmitted bits simultaneously for all users by optimising the correlation metric given by Equation (4.6). In the context of joint CIR estimation and symbol detection solely by the GAs, the search space became continuous, having an infinite number of possible points, simply because the fading attenuation and phase trajectories are continuous. Hence, the GA configuration that was adopted previously had to be modified. Specifically, the mutation operation and the mating pool size had to be adapted since the number of quantities to be determined was doubled. Through simulation, we have determined the value of the maximum mutation size λ_{max} as well as the mating pool size T that were capable of offering an acceptable CIR estimation performance, having an MSE as low as 0.001 in conjunction with known data bits. Having determined the GA parameters, the BEP performance of the joint GA-assisted multiuser CIR estimator and symbol detector was evaluated by simulations. It was shown that the BEP performance was limited due to the imperfect CIR estimation. However, the same phenomenon is also expereinced in a single-user scenario employing a matched filter having the same channel estimation MSE. Since the CIR estimation can be conducted without explicit training sequences or decision feedback, our proposed detector is capable of offering a potentially higher throughput and a shorter detection delay, than that of explicitly trained CDMA multiuser detectors.

It is well-known that diversity techniques can be used for mitigating the hostile effects of the transmission channel, in order to attain a BEP performance improvement. A symbol-synchronous CDMA system in conjunction with multiple receiving antennas was investigated in Chapter 5. By assuming that the antennas are placed at a distance higher than half the signals' wavelength, every user's signal received at each antenna is uncorrelated, which gives rise to an independent correlation metric at each antenna. From an optimisation point of view, the associated multiple correlation metrics resulted in a decision conflict, since a particular bit sequence may optimise one correlation metric but not the others. GAs can resolve this conflict by invoking the Pareto optimality approach, in order to assist the search for the optimum solution. The Pareto optimality approach is accomplished by identifying the non-dominated individuals in a population by considering the figure of merit from each antenna independently. The corresponding individuals are then placed in the mating pool. This approach is compared to the traditional way of selecting

individuals for the mating pool, which contains all non-identical individuals. Simulation results have shown that the Pareto optimality approach performed consistently better in terms of a lower BEP, than the traditional approach. Furthermore, a substantial performance gain was achieved, when antenna diversity was invoked compared to no diversity, without incurring additional computational complexity at the multiuser detector.

Finally, we applied the GA-assisted multiuser detector in an asynchronous CDMA system in Chapter 6. In order to reduce the computational complexity involved in detecting the entire bit sequence of all the users, a truncated observation window was invoked, such that the window encompasses at most one complete bit duration of each user. The EEBs were then tentatively detected according to two different strategies. Firstly, the EEBS can be tentatively estimated based on the hard decisions of the matched filter outputs. The GA-assisted multiuser detector then proceeded to search for the desired bits sequence that optimised the correlation metric. Since the estimated EEBs were corrupted by the interference inflicted by other users, the EBEP was high and this limited the overall performance of the GA-assisted multiuser detector. In our second approach, the EEBs and the desired bits were estimated by the GA-assisted multiuser detector simultaneously. As a result, the EEBs benefited from a lower bit error probability and the overall performance of the detector approached the optimum performance.

7.2 Suggestions for Future Work

We have demonstrated in this dissertation that GAs can be applied to CDMA multiuser detection schemes, which are capable of offering near-optimum performance at a reduced computational complexity compared to the conventional optimum multiuser detector. However, as we have mentioned in Chapter 2, the GAs that we have studied in this dissertation constitute a fraction of the entire GA-based optimisation literature. Hence other GA configurations may exist that can solve the optimisation problem associated with multiuser detection more efficiently. As we have seen, the specific values of certain GA parameters, such as the population size P, mating pool size T and the probability of mutation p_m may significantly affect the convergence rate and hence the achievable BEP under different conditions. An important aspect, which was not investigated in this dissertation, is the adaptation of these parameters according to the conditions. For example, the probability of mutation can be changed adaptively according to the number of users. Furthermore, by exploiting the different BEP criteria for different users and services, the

population size P and the number of generations Y can be adaptively adjusted, such that once the BEP criteria of certain users are met, they can be removed from the optimisation process. This will subsequently reduce the number of decision variables so that the population size can be reduced further, thereby reducing the computational complexity imposed.

In this dissertation, we have only considered a BPSK modulation based transmission schemes. While this type of modulation method is easy to implement and requires less complex receivers, it suffers from a low spectral efficiency. On the other hand, a CDMA system employing M-ary modulation, where $M > 2$ exhibits better spectral efficiency and hence it is capable of achieving a higher transmission rate within the same transmission bandwidth, while using the same spreading factor as BPSK modulation [100]. However, due to the intricate signal constellation associated with M-ary modulation, the complexity of the detector will increase. In the context of the optimum multiuser detector, the computational complexity of an M-ary modulation scheme is on the order of M^K. Hence, if for example we consider Quadrature Phase Shift Keying (QPSK) modulation, the computational complexity of the optimum multiuser detector supporting K users will be on the order of 4^K. This figure is 'astronomical' even for a system supporting $K = 10$ users. We have seen that the GA-assisted multiuser detector is capable of significantly reducing the computational complexity and yet deliver a near-optimum performance in conjunction with BPSK modulation. Hence, if the GA-assisted multiuser detector is used in an M-ary modulation scheme, the complexity reduction is likely to be more significant.

The properties of the GAs render them capable of solving optimisation problems having continuous decision variables. We have seen that the GA-assisted CIR coefficient estimator can achieve an estimation MSE of as low as 0.001 in a time-variant fading channel. Following this concept, the GA can also be invoked in order to obtain the soft decisions associated with the transmitted bits. These soft decisions can then be transferred to a channel codec, such as a Turbo Trellis Coded Modulation (TTCM) scheme or a Bit-Interleaved Coded Modulation (BICM) scheme [101], in order to achieve a further performance gain.

APPENDIX A

Glossary

2G	Second Generation
3G	Third Generation
AWGN	Additive White Gaussian Noise
BEP	Bit Error Probability
BPSK	Binary Phase Shift Keying
C-GA/MSD	Cascaded-Genetic Algorithm/Multi-Stage Detector
CDMA	Code Division Multiple Access
CIR	Channel Impulse Response
DBEP	Desired Bit Error Probability
DS	Direct Sequence
E-GA/MSD	Embedded-Genetic Algorithm/Multi-Stage Detector

EBEP	EEB Error Probability
EEB	End Edge Bit
EM	Expectation Maximisation
EP	Evolutionary Programming
ES	Evolutionary Strategy
FIR	Finite Impulse Response
GA	Genetic Algorithm
IS-95	Interim Standards 95
ITU	International Telecommunication Union
LLF	Log-Likelihood Function
LMMSE	Linear Minimum Mean Squared Error
LMS	Least Mean Square
MAI	Multiple Access Interference
MAP	Maximum *a posteriori* Probability
ML	Maximum Likelihood
MMSE	Minimum Mean Squared Error
MMSE-BLE	Minimum Mean Squared Error Block Linear Equalizer
MMSE-BDFE	Minimum Mean Squared Error Block Decision Feedback Equalizer

MSD	Multi-Stage Detector
MSE	Mean Squared Error
PDF	Probability Density Function
PIC	Parallel Interference Cancellation
QPSK	Quadrature Phase Shift Keying
SEB	Start Edge Bit
SIC	Successive Interference Cancellation
SNR	Signal-to-Noise Ratio
SS	Spread Spectrum
UMTS	Universal Mobile Telecommunications System
UTRA	UMTS Terrestrial Radio Access
W-CDMA	Wideband CDMA
ZF-BLE	Zero-Forcing Block Linear Equalizer
ZF-BDFE	Zero-Forcing Block Decision Feedback Equalizer

APPENDIX B

List of Symbols

$a_k(t)$	kth user's signature sequence.
$\boldsymbol{a}$	Signature sequence vector.
$\alpha_k(t)$	Rayleigh distributed amplitude.
$\hat{b}_k^{(m)}$	Detected mth data bit of the kth user at the receiver.
$b_k^{(m)}$	mth data bit of the kth user.
$\boldsymbol{b}$	Data bit vector.
$\boldsymbol{C}$	CIR coeffcients diagonal matrix.
$\delta(H)$	Defining length of schema H.
Δ	Mutation size for real-valued variables.
$\Gamma_\tau(t)$	Rectangular pulse of unity amplitude from $0 \leq t < \tau$ and zero otherwise.

$h_k(t)$	Complex lowpass channel impulse response associated with the kth user's signal.
H	Schema notation.
K	Number of users in the system.
$\Lambda(\boldsymbol{X})$	Objective function where $\boldsymbol{X}$ is a vector containing the decision variables to be optimised.
λ_{max}	Maximum mutation size for real-valued variables.
L	Number of multipaths
L_d	Number of diversity antennas
$m(H, y)$	Number of instances corresponding to the schema H at the yth generation.
M	Number of data bits transmitted in a packet.
$n(t)$	Zero-mean complex additive white Gaussian noise with independent real and imaginary components, each having a double-sided power spectral density of $N_0/2$ W/Hz.
$\boldsymbol{n}$	Gaussian noise vector.
N_c	Spreading factor, or the number of chips in one data bit duration T_b.
$o(H)$	Order to schema H.
$\Omega(\boldsymbol{b})$	Correlation metric.
p_i	Probability of selection corresponding to the ith individual.
p_m	Probability of mutation.

$p_s(H)$	Probability of survival of schema H.
$\phi_k(t)$	Channel phase uniformly distributed between $[0, 2\pi)$.
P	Population size.
$r(t)$	Received signal.
ρ_{lk}	Cross-correlation of the lth user's and the kth user's signature sequence.
$\boldsymbol{R}$	User signature sequence cross-correlation matrix.
$\hat{s}_k(t)$	Equivalent lowpass representation of the kth user transmitted CDMA signal.
$s_k(t)$	Channel impaired signal of the kth user.
$\tau_{k,l}$	Random delay corresponding to user k over the lth path.
τ_{N1}, τ_{N2}	Observation window boundary
T	Mating pool size.
T_b	Data bit duration.
T_c	Chip duration.
ξ_k	kth user's signal energy per bit.
$\boldsymbol{\xi}$	Signal energy per bit diagonal matrix.
z_l	Matched filter output associated with the lth user.
$\boldsymbol{Z}$	Matched filter output vector.

Bibliography

[1] S. Verdú, "Minimum probability of error for asynchronous gaussian multiple-access channel," *IEEE Transactions on Communications*, vol. 32, pp. 85–96, January 1986.

[2] A. Viterbi, *CDMA: Principles of Spread Spectrum Communication.* Reading MA, USA: Addison-Wesley, June 1995. ISBN 0201633744.

[3] R. Prasad, *CDMA for Wireless Personal Communications.* London: Artech House, May 1996. ISBN 0890065713.

[4] S. Glisic and B. Vucetic, *Spread Spectrum CDMA Systems for Wireless Communications.* London, UK: Artech House, April 1997. ISBN 0890068585.

[5] T. Ojanperä and R. Prasad, *Wideband CDMA for Third Generation Mobile Communications.* London, UK: Artech House, 1998.

[6] L. Miller and J. Lee, *CDMA Systems Engineering Handbook.* London, UK: Artech House, 1998.

[7] R. Price and E. Green Jr., "A communication technique for multipath channels," *Proceedings of the IRE*, vol. 46, pp. 555–570, March 1958.

[8] M. Saquib, R. Yates, and A. Ganti, "Power control for an asynchronous multi-rate decorrelator," *IEEE Transactions on Communications*, vol. 48, pp. 804–812, May 2000.

[9] J.-T. Chen, C. Papadias, and G. Foschini, "Dynamic signature assignment for direct-sequence cdma systems," *IEEE Communications Letters*, vol. 4, pp. 181–183, June 2000.

[10] C. Lee and R. Steele, "Effects of Soft and Softer Handoffs on CDMA System Capacity," *IEEE Transactions on Vehicular Technology*, vol. 47, pp. 830–841, August 1998.

[11] S. Moshavi, "Multi-user detection for DS-CDMA communications," *IEEE Communications Magazine*, vol. 34, pp. 124–136, October 1996.

[12] E. Kuan, *Burst-by-burst Adaptive Multiuser Detection CDMATechniques.* PhD thesis, University of Southampton, UK, 1999.

[13] R. Lupas and S. Verdú, "Linear multiuser detectors for synchronous code divison multiple access channels," *IEEE Transactions on Information Theory*, vol. 35, pp. 123–136, January 1989.

[14] R. Lupas and S. Verdú, "Near-far resistance of multiuser detectors in asynchronous channels," *IEEE Transactions on Communications*, vol. 38, pp. 509–519, April 1990.

[15] H. Liu and Z. Siveski, "Differentially coherent decorrelating detector for cdma single-path time-varying Rayleigh fading channels," *IEEE Transactions on Communications*, vol. 47, pp. 590–597, April 1999.

[16] A. Duel-Hallen, "A family of multiuser decision-feedback detectors for synchronous code-division multiple access channel," *IEEE Transactions on Communications*, vol. 43, pp. 421–434, February/March/April 1995.

[17] U. Madhow and M. Honig, "MMSE interference suppression for direct-sequence spread-spectrum CDMA," *IEEE Transactions on Communications*, vol. 42, pp. 3178–3188, December 1994.

[18] T. Lim, L. Rasmussen, and H. Sugimoto, "An asynchronous multiuser CDMA detector based on the kalman filter," *IEEE Journal on Selected Areas in Communications*, vol. 16, pp. 1711–1722, December 1998.

[19] A. Klein and P. Baier, "Linear unbiased data estimation in mobile radio sytems applying CDMA," *IEEE Journal on Selected Areas in Communications*, vol. 11, pp. 1058–1066, September 1993.

[20] A. Klein, G. Kaleh, and P. Baier, "Zero forcing and minimum mean square error equalization for multiuser detection in code division multiple access channels," *IEEE Transactions on Vehicular Technology*, vol. 45, pp. 276–287, May 1996.

[21] P. Jung and J. Blanz, "Joint detection with coherent receiver antenna diversity in CDMA mobile radio systems," *IEEE Transactions on Vehicular Technology*, vol. 44, pp. 76–88, February 1995.

[22] S. Verdú, *Multiuser Detection.* Cambridge, UK: Cambridge University Press, 1998.

[23] P. Patel and J. Holtzman, "Analysis of a simple successive interference cancellation scheme in a DS/CDMA system," *IEEE Journal on Selected Areas in Communications*, vol. 12, pp. 796–807, June 1994.

[24] M. Varanasi and B. Aazhang, "Multistage detection in asynchronous code-division multiple-access communications," *IEEE Transactions on Communications*, vol. 38, pp. 509–519, April 1990.

[25] T.-B. Oon, R. Steele, and Y. Li, "Performance of an adaptive successive serial-parallel CDMA cancellation scheme in flat Rayleigh fading channels," in *Proceedings of the IEEE Vehicular Technology Conference (VTC)*, (Phoenix, USA), pp. 193–197, 4–7 May 1997.

[26] L. Rasmussen, T. Lim, and T. Aulin, "Breadth-first maximum likelihood detection in multiuser CDMA," *IEEE Transactions on Communications*, vol. 45, pp. 1176–1178, October 1997.

[27] L. Wei, L. Rasmussen, and R. Wyrwas, "Near optimum tree-search detection schemes for bit-synchronous multiuser CDMA systems over Gaussian and two-path Rayleigh-fading channels," *IEEE Transactions on Communications*, vol. 45, pp. 691–700, June 1997.

[28] M. Nasiri-Kenari, R. Sylvester, and C. Rushforth, "Efficient soft-in-soft-out multiuser detector for synchronous CDMA with error-control coding," *IEEE Transactions on Vehicular Technology*, vol. 47, pp. 947–953, August 1998.

[29] J. Holland, *Adaptation in Natural and Artificial Systems.* Ann Arbor, Michigan: University of Michigan Press, 1975.

[30] X. Wang and H. V. Poor, "Adaptive joint multiuser detection and channel estimation in multipath fading CDMA," *Wireless Networks*, vol. 4, pp. 453–470, June 1998.

[31] D. E. Goldberg, *Genetic Algorithms in Search, Optimization, and Machine Learning.* Reading, Massachusetts: Addison-Wesley, 1989.

[32] K. Yen and L. Hanzo, "Genetic algorithm assisted joint multiuser symbol detection and fading channel estimation for synchronous cdma systems." Accepted for publication in IEEE Journal on Selected Areas in Communications.

[33] K. Yen and L. Hanzo, "Antenna-diversity-assisted genetic algorithm-based multiuser detection schemes for synchronous cdma systems." To appear in the Proceedings of the IEEE Vehicular Technology Conference (VTC) 2001, Spring conference.

[34] K. Yen and L. Hanzo, "Genetic algorithm assisted multiuser detection in asynchronous cdma communications." To appear in the IEEE Communications Conference (ICC) 2001.

[35] S. S. Rao, *Optimization : Theory and Applications.* New Delhi: Wiley Eastern, 1978.

[36] T. Bäck, U. Hammel, and H.-P. Schwefel, "Evolutionary computation: Comments on the history and current state," *IEEE Transactions on Evolutionary Computation*, vol. 1, pp. 3–17, April 1997.

[37] C. Darwin, *On the Origin of Species.* London: John Murray, 1859.

[38] I. Rechenberg, "Cybernetic solution path of an experimental problem," tech. rep., Ministry of Aviation, Royal Aircraft Establishment, U.K., 1965.

[39] H.-P. Schwefel, *Evolutionsstrategie und numerische Optimierung.* PhD thesis, Technische Universität Berlin, 1975.

[40] L. J. Fogel, A. J. Owens, and M. J. Walsh, *Artificial Intelligence through Simulated Evolution.* New York: John Wiley, 1966.

[41] M. Mitchell, *An Introduction to Genetic Algorithms.* Cambridge, Massachusetts: MIT Press, 1996.

[42] K. S. Tang, K. F. Man, S. Kwong, and Q. He, "Genetic algorithms and their applications," *IEEE Signal Processing Magazine*, vol. 13, pp. 22–37, November 1996.

[43] D. Whitley, "A genetic algorithm tutorial," *Statistics and Computing*, vol. 4, pp. 65–85, June 1994.

[44] S. Forrest, "Genetic algorithms: Principles of natural selection applied to computation," *Science*, vol. 261, pp. 872–878, August 1993.

[45] H. Mühlenbein, *Foundations of Genetic Algorithms*, ch. Evolution in time and space – The Parallel Genetic Algorithm, pp. 316–337. California, USA: G. Rawlins, ed., Morgan Kaufmann, 1991.

[46] J. J. Grefenstette and J. E. Baker, "How genetic algorithms work: A critical look at implicit parallelism," in *Proceedings of the Third International Conference on Genetic Algorithms* (J. D. Schaffer, ed.), (California, USA), pp. 20–27, Morgan Kaufmann, 1989.

[47] B. L. Miller and D. E. Goldberg, "Genetic algorithms, selection schemes, and the varying effects of noise," *Evolutionary Computation*, vol. 4, pp. 113–131, Summer 1996.

[48] G. Harik, E. Cantú-Paz, D. E. Goldberg, and B. L. Miller, "The gambler's ruin problem, genetic algorithms, and the sizing of populations," in *Proceedings of the 1997 IEEE Conference on Evolutionary Computation* (T. Bäck, ed.), (New York), pp. 7–12, IEEE Press, 1997.

[49] M. D. Vose and G. E. Liepins, "Punctuated equilibria in genetic search," *Complex Systems*, vol. 5, pp. 31–44, January/February 1991.

[50] A. E. Nix and M. D. Vose, "Modeling genetic algorithms with Markov chains," *Annals of Mathematics and Artificial Intelligence*, vol. 5, pp. 79–88, January/February/March 1992.

[51] M. D. Vose, *Foundations of Genetic Algorithms 2*, ch. Modeling Simple Genetic Algorithms, pp. 63–73. California, USA: L. D. Whitley, ed., Morgan Kaufmann, 1993.

[52] A. H. Wright, *Foundations of Genetic Algorithms*, ch. Genetic Algorithms for Real Parameter Optimization, pp. 205–218. California, USA: G. Rawlins, ed., Morgan Kaufmann, 1991.

[53] C. Z. Janikow and Z. Michalewicz, "An experimental comparison of binary and floating point representations in genetic algorithms," in *Proceedings of the Fourth International Conference on Genetic Algorithms* (R. K. Belew and L. B. Booker, eds.), (California, USA), pp. 31–36, Morgan Kaufmann, 1991.

[54] R. Tanese, *Distributed Genetic Algorithms for Function Optimization.* PhD thesis, University of Michigan, 1989.

[55] J. E. Baker, "Adaptive selection methods for genetic algorithms," in *Proceedings of the First International Conference on Genetic Algorithms and Their Applications* (J. J. Grefenstette, ed.), (New Jersey, USA), pp. 101–111, Lawrence Erlbaum Associates, 1985.

[56] T. Blickle and L. Thiele, "A comparison of selection schemes used in evolutionary algorithms," *Evolutionary Computation*, vol. 4, pp. 361–394, Winter 1996.

[57] D. E. Goldberg and K. Deb, *Foundations of Genetic Algorithms*, ch. A Comparative Analysis of Selection Schemes Used in Genetic Algorithms, pp. 69–93. California, USA: G. Rawlins, ed., Morgan Kaufmann, 1991.

[58] L. J. Eshelman and J. D. Schaffer, "Preventing premature convergence in genetic algorithms by preventing incest," in *Proceedings of the Fourth International Conference on Genetic Algorithms* (R. K. Belew and L. B. Booker, eds.), (California, USA), pp. 115–122, Morgan Kaufmann, 1991.

[59] G. Syswerda, "Uniform crossover in genetic algorithms," in *Proceedings of the Third International Conference on Genetic Algorithms* (J. D. Schaffer, ed.), (California, USA), pp. 2–9, Morgan Kaufmann, 1989.

[60] W. Spears and K. De Jong, *Foundations of Genetic Algorithms*, ch. An Analysis of Multi-Point Crossover, pp. 301–315. California, USA: G. Rawlins, ed., Morgan Kaufmann, 1991.

[61] J. D. Schaffer, R. A. Caruana, L. J. Eshelman, and R. Das, "A study of control parameters affecting online performance of genetic algorithms for function

optimization," in *Proceedings of the Third International Conference on Genetic Algorithms* (J. D. Schaffer, ed.), (California, USA), pp. 51–60, Morgan Kaufmann, 1989.

[62] J. J. Grefenstette, "Optimization of control parameters for genetic algorithms," *IEEE Transactions on Systems, Man and Cybernetics*, vol. SMC-16, pp. 122–128, January 1986.

[63] T. Bäck, "Optimal mutation rates in genetic search," in *Proceedings of the Fifth International Conference on Genetic Algorithms* (S. Forrest, ed.), (California, USA), pp. 2–8, Morgan Kaufmann, 1993.

[64] T. Bäck, "Self adaptation in genetic algorithms," in *Proceedings of the First European Conference on Artificial Life* (F. J. Varela and P. Bourgine, eds.), (Massachusetts, USA), pp. 263–271, MIT Press, 1992.

[65] M. J. Juntti, T. Schlösser, and J. O. Lilleberg, "Genetic algorithms for multiuser detection in synchronous CDMA," in *IEEE International Symposium on Information Theory - ISIT'97*, (Ulm, Germany), p. 492, 1997.

[66] X. F. Wang, W. S. Lu, and A. Antoniou, "A genetic algorithm-based multiuser detector for multiple-access communications," in *IEEE International Symposium on Circuits and System - ISCAS'98*, (Monterey, California, USA), pp. 534–537, 1998.

[67] C. Ergün and K. Hacioglu, "Application of a genetic algorithm to multistage detection in CDMA systems," in *Proceedings of the 9th Mediterranean Electrotechnical Conference - MELECON'98*, (Tel-Aviv, Israel), pp. 846–850, 1998.

[68] C. Ergün and K. Hacioglu, "Multiuser detection using a genetic algorithm in CDMA communications systems," *IEEE Transactions on Communications*, vol. 48, pp. 1374–1383, August 2000.

[69] S. Abedi, *Genetic Multiuser Detection for Code Division Multiple Access Systems*. PhD thesis, University of Surrey, 2000.

[70] S. Abedi and R. Tafazolli, "Genetic multiuser receiver for code division multiple access communications," *Electronics Letters*, vol. 36, pp. 1957–1958, November 2000.

[71] M. Pursley, "Performance evaluation for phase-coded spread-spectrum multiple-access communication-part I: System analysis," *IEEE Transactions on Communications*, vol. COM-25, pp. 795–799, August 1977.

[72] R. Morrow Jr., "Bit-to-bit error dependence in slotted DS/SSMA packet systems with random signature sequences," *IEEE Transactions on Communications*, vol. 37, pp. 1052–1061, October 1989.

[73] J. Holtzman, "A simple, accurate method to calculate spread-spectrum multiple-access error probabilities," *IEEE Transactions on Communications*, vol. 40, pp. 461–464, March 1992.

[74] M. K. Varanasi and B. Aazhang, "Near-optimum detection in synchronous code-division multiple-access systems," *IEEE Transactions on Communications*, vol. 39, pp. 725–736, May 1991.

[75] J. Proakis, *Digital Communications*. New York, USA: McGraw-Hill, 3rd ed., 1995.

[76] S. Chen, A. K. Samingan, B. Mulgrew, and L. Hanzo, "Adaptive minimum-ber linear multi-user detection for ds-cdma signals in multipath channels." Accepted for publication in IEEE Transactions on Signal Processing.

[77] J. Cavers, "An analysis of pilot symbol assisted modulation for rayleigh fading channels," *IEEE Transactions on Vehicular Technology*, vol. 40, pp. 686–693, November 1991.

[78] Z. Xie, C. Rushforth, R. Short, and T. Moon, "Joint signal detection and parameter estimation in multiuser communications," *IEEE Transactions on Communications*, vol. 41, pp. 1208–1216, August 1993.

[79] U. Fawer and B. Aazhang, "Multiuser receiver for code division multiple access communications over multipath channels," *IEEE Transactions on Communications*, vol. 43, pp. 1556–1565, February–April 1995.

[80] T. Kawahara and T. Matsumoto, "Joint decorrelating multiuser detection and channel estimation in asynchronous cdma mobile communications channels," *IEEE Transactions on Vehicular Technology*, vol. 44, pp. 506–515, August 1995.

[81] S. Chen and Y. Wu, "Maximum likelihood joint channel and data estimation using genetic algorithms," *IEEE Transactions on Signal Processing*, vol. 46, pp. 1469–1473, May 1998.

[82] Z. Zvonar and M. Stojanovic, "Performance of antenna diversity multiuser receivers in CDMA channels with imperfect fading estimation," *Wireless Personal Communications*, vol. 3, no. 1-2, pp. 91–110, 1996.

[83] D. N. Kalofonos, M. Stojanovic, and J. G. Proakis, "Analysis of the impact of channel estimation errors on the performance of a MC-CDMA system in a Rayleigh fading channel," in *IEEE Global Telecommunications Conference*, vol. 4, (Phoenix, Arizona, USA), pp. 213–217, November 1997.

[84] M. J. Omidi, P. G. Gulak, and S. Pasupathy, "Parallel structures for joint channel estimation and data detection over fading channels," *IEEE Journal of Selected Areas in Communications*, vol. 16, pp. 1616–1629, December 1998.

[85] M. Stojanovic and Z. Zvonar, "Performance of multiuser detection with adaptive channel estimation," *IEEE Transactions on Communications*, vol. 47, pp. 1129–1132, August 1999.

[86] P. Schramm, "Differentially coherent demodulation for differential bpsk in spread spectrum systems," *IEEE Transactions on Vehicular Technology*, vol. 48, pp. 1650–1656, September 1999.

[87] M. Juntti, *Multiuser Demodulation for DS-CDMA Systems in Fading Channels*. PhD thesis, University of Oulu, 1997.

[88] A. Klein, B. Steiner, and A. Steil, "Known and novel diversity approaches as powerful means to enhance the performance of cellular mobile radio systems," *IEEE Journal on Selected Areas in Communications*, vol. 14, pp. 1784–1795, December 1996.

[89] P. Diáz and R. Agustí, "The use of coding and diversity combining for mitigating fading effects in a DS/CDMA system," *IEEE Transactions on Vehicular Technology*, vol. 47, pp. 95–102, February 1998.

[90] A. Naguib and A. Paulraj, "Performance of wireless CDMA with m-ary orthogonal modulation and cell site antenna arrays," *IEEE Journal on Selected Areas in Communications*, vol. 14, pp. 1770–1783, December 1996.

[91] P. van Rooyen, R. Kohno, and I. Oppermann, "DS-CDMA performance with maximum ratio combining and antenna arrays," *Wireless Networks*, vol. 4, pp. 479–488, June 1998.

[92] N. Srinivas and K. Deb, "Multiobjective optimization using nondominated sorting in genetic algorithms," *Evolutionary Computation*, vol. 2, pp. 221–248, Autumn 1994.

[93] E. Zitzler and L. Thiele, "Multiobjective evolutionary algorithms : A comparative case study and the strength Pareto approach," *IEEE Transactions on Evolutionary Computation*, vol. 3, pp. 257–271, November 1999.

[94] J. Panicker and S. Kumar, "Effect of system imperfections on BER performance of a CDMA receiver with multipath diversity combining," *IEEE Transactions on Vehicular Technology*, vol. 45, pp. 622–630, November 1996.

[95] F.-C. Zheng and S. K. Barton, "Near-far resistent detection of CDMA signals via isolation bit insertion," *IEEE Transactions on Communications*, vol. 43, pp. 1313–1317, February/March/April 1995.

[96] Z. Xie, R. Short, and C. Rushforth, "Family of suboptimum detectors for coherent multiuser communications," *IEEE Journal on Selected Areas in Communications*, vol. 8, pp. 683–690, May 1990.

[97] S. S. H. Wijayasuriya, G. H. Norton, and J. P. McGeehan, "A sliding window decorrelating receiver for multiuser DS-CDMA mobile radio networks," *IEEE Transactions on Vehicular Technology*, vol. 45, pp. 503–521, August 1996.

[98] M. J. Juntti and B. Aazhang, "Finite memory-length linear multiuser detection for asynchronous CDMA communications," *IEEE Transactions on Communications*, vol. 45, pp. 611–622, May 1997.

[99] J. Shen and Z. Ding, "Edge decision assisted decorrelators asynchronous CDMA channels," *IEEE Transactions on Communications*, vol. 47, pp. 438–445, March 1999.

[100] F. M. Ozluturk, S. Tantaratana, and A. W. Lam, "Performances of DS/SSMA communications with MPSK signalling and complex signature sequences," *IEEE Transactions on Communications*, vol. 43, pp. 1127–1133, February/March/April 1995.

[101] S. X. Ng, T. H. Liew, L.-L. Yang, and L. Hanzo, "Comparative study of TCM, TTCM, BICM and BICM-ID schemes." Submitted to IEEE VTC 2001 Spring.

Author Index

H

J

K

L

M

N

O

X

Z

Index

T

W